Lamb, Christopher Anthony (2011) *Investigation of GLUT4 sorting into the insulin responsive compartment: a role for ubiquitination and deubiquitination.* PhD
http://theses.gla.ac.uk/2380/

Copyright and moral rights for this thesis are retained by the author

A copy can be downloaded for personal non-commercial research or study, without prior permission or charge

This thesis cannot be reproduced or quoted extensively from without first obtaining permission in writing from the Author

The content must not be changed in any way or sold commercially in any format or medium without the formal permission of the Author

When referring to this work, full bibliographic details including the author, title, awarding institution and date of the thesis must be given.

Glasgow Theses Service
http://theses.gla.ac.uk/
theses@gla.ac.uk

Investigation of GLUT4 sorting into the insulin responsive compartment: A role for ubiquitination and deubiquitination

A thesis submitted to the
COLLEGE OF MEDICAL, VETERINARY AND LIFE SCIENCES

For the degree of
DOCTOR OF PHILOSOPHY

By Christopher A Lamb

Institute of Molecular, Cell and Systems Biology
College of Medical, Veterinary and Life Sciences
University of Glasgow

November 2010

© Christopher A Lamb 2010

Abstract

GLUT4 is the insulin-regulated glucose transporter found in muscle and adipose tissue. On insulin stimulation, GLUT4 translocates from a slowly recycling storage compartment (GLUT4 storage vesicles or GSVs) to the plasma membrane. This allows glucose to enter cells by diffusion down its concentration gradient, clearing glucose from the plasma. This response is defective in the disease states of insulin resistance and type 2 diabetes. The aim of this study is to understand how GLUT4 enters GSVs, which will hopefully extend our knowledge of insulin responsive tissues.

Previous studies from our lab, expressing GLUT4 in yeast, have shown that GLUT4 is subject to the same nitrogen- and ubiquitin-dependent trafficking as the yeast amino acid permease Gap1p. In my thesis I have extended these studies into 3T3-L1 adipocytes, and shown that GLUT4 is ubiquitinated in this insulin responsive cell line. A ubiquitin resistant version of GLUT4 (HA-GLUT4 7K/R) has an impaired ability to enter GSVs and does not translocate in response to insulin. However GLUT4 mutants with single ubiquitination sites outwith the large intracellular loop are ubiquitinated and traffic in an identical manner to wild type GLUT4, addressing concerns that mutation of the large intracellular loop of GLUT4 in HA-GLUT4 7K/R affects its trafficking.

The GGA family of clathrin adaptor proteins have previously been implicated in sorting of newly synthesised GLUT4 into GSVs. Our lab has shown previously that the two yeast Ggas are required for ubiquitin dependent trafficking of GLUT4 in yeast, as is the case for Gap1p. I have gone on to show that the ubiquitin binding function of the GGA3 GAT domain is, at least partially, required for an *in vitro* interaction between GLUT4 and the VHS-GAT domains of GGA3. When expressed in adipocytes, a ubiquitin binding deficient mutant of myc-GGA3 reduces the proportion of GLUT4 loaded into a subcellular fraction enriched in GSVs, suggesting that GLUT4 ubiquitination is one of the signals for GGA dependent sorting into GSVs.

As ubiquitination is usually thought of as a signal to direct lysosomal degradation, and only 0.1 % of total GLUT4 is ubiquitinated at any one time, there may be a role for a deubiquitination step in ubiquitin dependent GLUT4 traffic. Work by our collaborator (Nai-Wen Chi, UCSD) has demonstrated that

the GSV cargo IRAP and its binding partner tankyrase-1 are required for normal insulin responsive GLUT4 traffic. An interaction between tankyrase and the deubiquitinase (DUB) USP25 has been demonstrated by yeast two hybrid analysis, and this DUB contains a putative tankyrase binding motif. USP25 may therefore be recruited to GSVs by IRAP, with tankyrase acting as a scaffold. I demonstrated that GST-USP25 binds tankyrase-1 from an adipocyte lysate, and that a version of the enzyme with a mutation in the putative tankyrase binding motif (GST-USP25 R1049A) does not. I also used siRNA to deplete USP25 from 3T3-L1 adipocytes, and found that this results in a reduction of GLUT4 levels in these cells. A concomitant reduction in the fold change of insulin-stimulated glucose transport into these cells suggests that GLUT4 is not sequestered in GSVs, but is rather directed to the lysosome.

In summary, my data show that ubiquitination of GLUT4 is required for the transporter to be loaded into its insulin responsive compartment (GSVs). I also began to characterise the role of the ubiquitin binding GAT domain of GGA3 and the deubiquitinase USP25 in GLUT4 traffic, opening up two further avenues for research into the insulin regulated trafficking of GLUT4.

Table of contents

List of tables

List of figures

Acknowledgements

First of all I'd like to thank my supervisor Dr. Nia Bryant for all the constructive criticism, advice and support over the last few years, especially running those gels when I was getting a bit overwhelmed and letting me stop doing iodixanol gradients…! THANK YOU.

A big thank you to Dr Rebecca McCann (aka Wee Becky, Beckster etc) for getting the ball rolling on the GLUT4-ubiquitin project, and answering my repeated questions in the early days. Most importantly, thank you for the box of index cards with solution and media recipes – the importance of which cannot be underestimated.

Thank you to Dr Scott Shanks (aka Dr Scotch Eggs) for being a generally awesome benchmate (and neighbour), and providing a sounding board and source of all yeast and PCR knowledge. Also thanks to Dr Chris Macdonald (aka The Curly One/Zebra) for the regular cloning advice, pub sessions and the template for a low-stress write-up. This is probably the time to apologise for all the buffers I stole, sorry about that…

Thanks to the rest of the current Bryant group, especially Iain for being a competent (ahem) "minion", and those who have gone on to better things – Tom, Lindsay (COG), and Maz. You've all helped in big or small ways. Also to the rest of lab 241, especially the 3T3-L1/GLUT4 crew (holla!), thanks for the help, advice and general banter (especially during long sessions in the virus room of cell culture eh Andy?) over the last few years. Also thank you to Professor Frances Brosky's group at UCSF for making my visit there enjoyable.

Thanks to all my other friends up in Glasgow for the good times over the last few years, especially those going through a PhD at the same time. It's good to know I wasn't alone. Also to the Sunday night Cooper's pub quiz team and all the people I met through GUSWPC for keeping me active, healthy and occasionally inebriated during my time at Glasgow.

Finally a massive thank you to Mum and Dad (Linda and John) for the constant encouragement, advice, love and support.

Declaration

I declare that the work presented in this thesis has been carried out by myself unless otherwise stated. It is entirely of my own composition and has not been submitted, in whole or in part, for any other degree. Permission has been granted by the publisher for any reproduced figures.

Christopher Anthony Lamb

November 2010

Abbreviations

~	approximately
ADP	adenosine diphosphate
ALP	alkaline phosphatise
A	amps
AP	adaptor protein/assembly polypeptide complex
APNE	*N*-acetyl-DL-phenylalanine ß-naphthyl ester
AS160	Akt substrate of 160 kilodaltons
ARF	ADP ribosylation factor
ATP	adenosine triphosphate
b	DNA base pair
BSA	bovine serum albumin
°C	degrees Celsius
cDNA	complementary DNA
CEN	centromeric
cfu	colony forming unit
Ci	curie
CPS	carboxypeptidase S
CPY	carboxypeptidase Y
C-terminal	carboxy terminal
$CuSO_4$	copper sulphate
ddH_2O	double distilled water
DMEM	Dulbecco's modified Eagle's medium
DMF	dimethyl formamide
DMSO	dimethyl sulphoxide
DNA	deoxyribonucleic acid
DNTP	deoxynucleotide triphosphate
DUB	deubiquitinating enzyme
E1	ubiquitin activating enzyme
E2	ubiquitin conjugating enzyme
E3	ubiquitin ligase
E. coli	*Escherichia coli*
ECL	enhanced chemiluminescence
EDTA	ethylenediamine tetraacetic acid
ER	endoplasmic reticulum

FCS	foetal calf serum
FM4-64	N-(3-triethylammoniumpropyl)-4-(p-diethylaminophenyl-hexatrienyl)pyridiumdibromide
5-FOA	5-fluoroorotic acid
g	gram
xg	multiple of gravitational force
GAE	γ adaptin ear
GAT	GGA and TOM1
GFP	*Aequorea victoria* green fluorescent protein
GGA	Golgi localised, γ adaptin ear containing, ARF binding protein
GLUT	glucose transporter
GST	glutathione-S-transferase
GSV	GLUT4 storage vesicle
GUV	giant unilamellar vesicle
H_2O_2	hydrogen peroxide
HA	influenza haemagglutinin epitope tag
HCl	hydrochloric acid
HDM	high density microsome
HEPES	2[4(2-Hydroxyethyl)-1-piperazine]ethanesulphonic acid
HES	HEPES, sucrose, EDTA
HRP	horseradish peroxidise
Ig	immunoglobulin isotype
IPTG	isopropyl-ß-D-thiogalactopyranoside
IRAP	insulin responsive aminopeptidase
IRS	insulin receptor substrate
IRV	insulin responsive vesicle
JAMM	JAB1, MPN/MOV34 metalloenzymes
k	kilo (prefix)
KCl	potassium chloride
k_d	dissociation constant
K_2HPO_4	dipotassium hydrogen orthophosphate
KH_2PO_4	potassium dihydrogen orthophosphate
KOAc	potassium acetate
KOH	potassium hydroxide
l	litre
LDM	low density microsome
LiOAC	lithium acetate

LSB	Laemmli's sample buffer
µ	micro (prefix)
m	milli (prefix)
M	molar
$MgSO_4$	magnesium sulphate
MHCII	major histocompatability complex class II molecule
min	minute
MVB	multivesicular body
n	nano (prefix)
N-terminal	Amino-terminal
NaCl	sodium chloride
Na_2HPO_4	disodium hydrogen orthophosphate
NaH_2PO_4	sodiun dihydrogen orthophosphate
NaOH	sodium hydroxide
NCS	newborn calf serum
NEM	N-ethyl maleimide
NH_4Cl	ammonium chloride
NSF	N-ethyl maleimide sensitive factor
OD_{600}	optical density at 600 nm
ORF	open reading frame
OTU	otubain
p	pico (prefix)
PAGE	polyacrylamide gel elecrophoresis
PBS	phosphate buffered saline
PBS-T	0.1 % Tween-20 in phosphate buffered saline
PCR	polymerase chain reaction
PI	phosphatidylinositol
PIPES	1,4-piperazinediethanesulphonic acid
PKB	protein kinase B/Akt
PKC	protein kinase C
RNA	ribonucleic acid
RS	retention sequence
S. cerevisiae	*Saccharomyces cerevisiae*; Baker's yeast
SD	yeast synthetic dextrose media
SDM	site directed mutagenesis
SDS	sodium dodecyl sulphate
SH2	Src-homology 2

SIM	SUMO interacting motif
siRNA	short interfering RNA
SNARE	soluble NSF attachment protein receptor
SUMO	small ubiquitin like modifier
TAE	tris-acetic acid-EDTA
TE	tris-EDTA
TEMED	N,N,N',N',-tetramethyl ethylene diamine
TfR	transferrin receptor
TGN	*trans*-Golgi network
Tris	2-amino-2(hydroxymethyl)-1,3-propanediol
Ub	ubiquitin
UBA	ubiquitin associated domain
Ubc	ubiquitin conjugating enzyme
UBL	ubiquitin like
UBX	ubiquitin regulatory X
UCH	Ubiquitin C-terminal hydrolase
UIM	ubiquitin interacting motif
USP	ubiquitin specific protease
UTR	untranslated region
VAMP	vesicle associated membrane protein
VHS	Vps27, Hrs, STAM
VPS	vacuolar protein sorting
v/v	units per unit volume
w/v	units weight per unit volume
Wnt	Wingless/Int protein
YPD	yeast extract, peptone, dextrose
YT	yeast extract, tryptone, NaCl

Chapter 1 – Introduction

1.1 Compartmentalisation of eukaryotic cells

One of the defining features of eukaryotic cells is the presence of internal membrane bound organelles, such as the nucleus, mitochondria and an endomembrane system (Figure 1.1) (Vellai and Vida, 1999;Dacks and Field, 2007). These characteristics allow the compartmentalisation of reactions in specialised organelles. For example, lysosomes are the site of hydrolysis of proteins and phagocytosed particles, peroxisomes are the location of peroxide breakdown, secretory protein synthesis occurs at the endoplasmic reticulum, and so on.

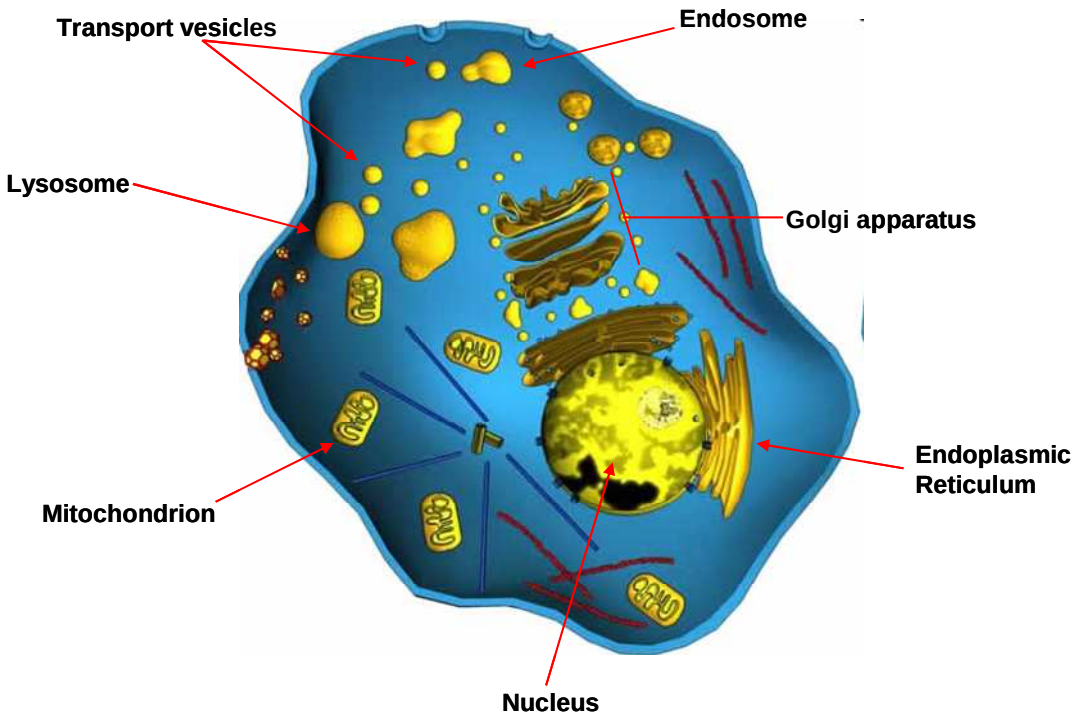

Figure 1.1 Organelles within a mammalian cell.

Reproduced with permission from http://www.abcam.com/index.html?pageconfig=resource&rid=16

A problem with this system is that molecules may need to move from one compartment to another to carry out their function. As an example, secreted proteins are synthesised in the endoplasmic reticulum, modified in the Golgi membranes and must then reach the plasma membrane. Additionally, many cells need to move molecules from one compartment to another in response to external stimuli. Examples of this include mast cell degranulation in response to stimulation with specific antigen (Lawson *et al.*, 1978), secretion of hormones, such as insulin secretion in response to raised plasma glucose (Eliasson *et al.*, 2008), and synaptic vesicle exocytosis (Martin, 1997).

Therefore, mechanisms must be in place to permit the movement of proteins from one compartment to another, allowing molecules to move to the correct site to carry out their function while still maintaining organellar identity.

1.1.1 Vesicle traffic

One of the main routes by which proteins can move from one compartment to another is through the formation of coated vesicles (Kirchhausen, 2000). The formation of coated vesicles is required to collect molecules destined for another compartment together, helping to maintain organelle identity throughout the life of a cell. There are three main coat protein families found in mammalian and yeast cells. COPI (coatomer protein I) consists of a complex with seven subunits which appears to be involved in retrograde traffic from the Golgi to the endoplasmic reticulum and through the Golgi cisternae (Kirchhausen, 2000). GTP-bound ArfI is responsible for recruiting COPI complexes to membranes (Serafini *et al.*, 1991). The γ subunit of the COPI complex is responsible for cargo recognition, recognising cytosolic motifs such as the dilysine (KKXX) (Harter *et al.*, 1996).

COPII coated vesicles are required for anterograde traffic from the endoplasmic reticulum to the Golgi (Kirchhausen, 2000). The GTPase Sec12p recruits Sar1p to the membrane (Barlowe *et al.*, 1993;Barlowe and Schekman, 1993) and this forms the basis for a complex forming which includes the cargo recognition module of Sec23/24p and the Sec13/Sec31p coat (Barlowe *et al.*, 1994).

Clathrin coats are the third main family of vesicle coat complexes and are distributed throughout various intracellular transport processes. Clathrin coats consist of heavy and light chains, with three heavy chains forming a three legged structure (“triskelion”) and these recruit the light chain (Brodsky *et al.*, 2001). However clathrin coats do not interact with vesicle cargos directly – they rely on adaptor molecules to facilitate interaction (Knuehl *et al.*, 2006).

The role of clathrin adaptors is to link the cytosolic domains of vesicle cargos and sorting receptors (via specific sorting motifs as described in section 1.1.3) with clathrin coats (Robinson, 2004). Several protein families fulfil this role – these include Dab2 (Mishra *et al.*, 2002), the GGAs (Golgi localised, γ-adaptin ear containing, ARF-binding proteins) (Pelham, 2004;Robinson, 2004) and the AP

(adaptor protein/assembly polypeptide) complexes 1-4 (Robinson, 2004). AP1 and 2 were the first adaptors characterised (Keen, 1987;Robinson, 2004). GGAs are discussed more extensively in section 1.2.2.

1.1.2 SNARE proteins

To allow transport vesicles to reach their target compartment, a mechanism for selective targeting of said compartments is required. This selectivity is conferred in part by a family of proteins called SNAREs (soluble, *N*-ethyl maleimide sensitive factor attachment receptor proteins) (McNew *et al.*, 2000). SNAREs are often termed the "minimal machinery for membrane fusion" as purified SNARE proteins reconstituted in liposomes can induce liposome fusion *in vitro* (Weber et al., 1998).

In general, SNAREs have a single transmembrane domain, a highly conserved 60-70 amino acid SNARE motif and an N terminal peptide of variable length and structure (Jahn and Scheller, 2006). Fusion occurs when four SNARE motifs align in parallel and interact to form an energetically favourable core complex (Sutton *et al.*, 1998). The four SNARE motifs are generally contributed by two or three Q SNAREs (with a central glutamine residue) and one R SNARE (with a central arginine residue) (Fasshauer *et al.*, 1998). The four SNARE motifs zipper together, pulling vesicle and target membranes together and contributing to fusion of the membranes. All participating SNAREs subsequently exist as a complex on the target membrane (the *cis*-complex). The *cis*-complex is disassembled in an ATP-dependent manner (Sollner *et al.*, 1993), which allows the SNAREs to be recycled for further rounds of fusion (Jahn and Scheller, 2006).

SNARE proteins associate with specific membranes within the cell where they catalyse particular fusion reactions. For example, syntaxin-4 is a plasma membrane SNARE, whereas VAMP2 is associated with secretory vesicles, such as those involved in neurotransmitter release (Hong, 2005). This means that specific SNARE complexes can form between these membranes to facilitate membrane fusion (McNew *et al.*, 2000).

1.1.3 Intrinsic protein signals

Proteins themselves may contain intrinsic signals that direct their trafficking from one compartment to another, due to recognition by coat protein components or their adaptors (as discussed in 1.1.1). Two well characterised intrinsic sorting motifs are acidic dileucine motifs, usually conforming to the sequence DXXLL, and tyrosine based motifs (YXXΦ, where Φ is a bulky hydrophobic residue). The acidic dileucine motif is found in proteins which are sorted from the *trans*-Golgi network (TGN) into the endosomal system, including the two mannose-6-phosphate receptors (Chen *et al.*, 1997;Tortorella *et al.*, 2007;Braulke and Bonifacino, 2009) and sortilin (Shiba *et al.*, 2002). The motif is bound by the VHS domain of GGA proteins (Nielsen *et al.*, 2001;Shiba *et al.*, 2002). YXXΦ motifs are also found in proteins which traffic along the lysosomal pathway, including LAMP-1 (Honing *et al.*, 1996;Braulke and Bonifacino, 2009), with the modification being bound by the AP-1 and 2 adaptor complexes (Honing *et al.*, 1996). YXXΦ motifs are required for Golgi exit and entry into the endosomal system.

1.1.4 Sorting via post-translational modification

Post translational protein modifications are those which occur once a polypeptide chain has been produced, and can include protein conjugation to carbohydrates, lipids, functional groups such as phosphates, and other proteins. One well characterized modification required for protein sorting is the mannose-6-phosphate modification found on soluble proteins directed to the endosomal system and eventually the lysosome, such as cathepsin D (Hida *et al.*, 2007).

This modification allows binding of the lysosomal hydrolases to one of the two mannose-6-phosphate receptors (MPR); the cation-dependent MPR and the cation independent MPR (Ghosh *et al.*, 2003;Braulke and Bonifacino, 2009). These two receptors then direct sorting of the hydrolases in a manner dependent on the receptor cytosolic targeting motifs, as described in 1.1.3.

1.1.5 Ubiquitin as a post translational modification.

Ubiquitin is a 76 amino acid polypeptide, highly conserved throughout eukaryotes (Goldstein *et al.*, 1975;Ciechanover, 2005). Proteins can be modified at free amino groups (usually lysine residues, but occasionally the N-terminal residue of a protein (Coulombe *et al.*, 2004), serine, cysteine or threonine (Ishikura *et al.*, 2010)) by the addition of ubiquitin moieties which, depending on the type of modification, can result in degradation at the proteasome for soluble proteins, or for membrane proteins trafficking through the endosomal system, leading ultimately to lysosomal degradation (Hicke and Dunn, 2003;Piper and Luzio, 2007).

Ubiquitin's proteolysis-stimulating activity was initially identified as APF-1 (ATP-dependent proteolysis factor 1), an 8.5 kD protein component of reticulocyte lysate required for proteolysis, which could be conjugated reversibly to protein substrates (Ciechanover, 2005). Later studies confirmed that APF-1 was ubiquitin (Wilkinson *et al.*, 1980). Ubiquitin is conjugated to proteins through the action of three different enzymes. E1 (ubiquitin activating) enzymes activate and form a high energy thioester bond with ubiquitin. E2 (ubiquitin conjugating) enzymes receive ubiquitin from E1 via a transthiolation reaction. Then the E2 and E3 (ubiquitin ligase) enzymes work together to transfer ubiquitin to a lysine side chain (Ciechanover, 2005). The E3 enzymes are the most numerous of the three groups and give each reaction its substrate specificity, often providing a platform for E2 and substrate to bind (Pickart, 2001).

The proteolysis-activating activity of ubiquitin was initially associated with the proteasome, a large 26 S multienzyme complex consisting of a 19 S regulatory particle and 20 S core particle which degrades substrates modified with a polyubiquitin chain linked through lysine 48 of ubiquitin (K48 linked polyubiquitin) (Ciechanover, 2005). However, as discussed in the next section, more recent work has identified that other ubiquitin modifications exist and these have various roles.

1.1.6 Other ubiquitin modifications.

Addition of a single ubiquitin moiety (monoubiquitination), often at multiple lysine residues, has been shown to be involved in endocytosis and protein trafficking (Haglund *et al.*, 2003;Urbe, 2005). Ubiquitin itself contains seven lysine residues (at positions 6, 11, 27, 29, 33, 48 and 63) (Pickart and Fushman, 2004), and polymeric chains at all of these residues have been reported *in vivo* (Peng *et al.*, 2003). K63 linked polyubiquitin has been implicated in vesicle trafficking (discussed further in the next section) and regulation of signalling cascades, by forming a scaffold on which signalling intermediates may assemble (Kanayama *et al.*, 2004). The BRCA1/BARD1 ubiquitin ligase complex assembles K6 polyubiquitin chains *in vitro* (Wu-Baer *et al.*, 2003) and the BRCA1 subunit can be autoubiquitinated with these chains (Wu-Baer *et al.*, 2003). For the purposes of this study, the role of monoubiquitination and K63 linked polyubiquitin in protein traffic will be considered further in the next section.

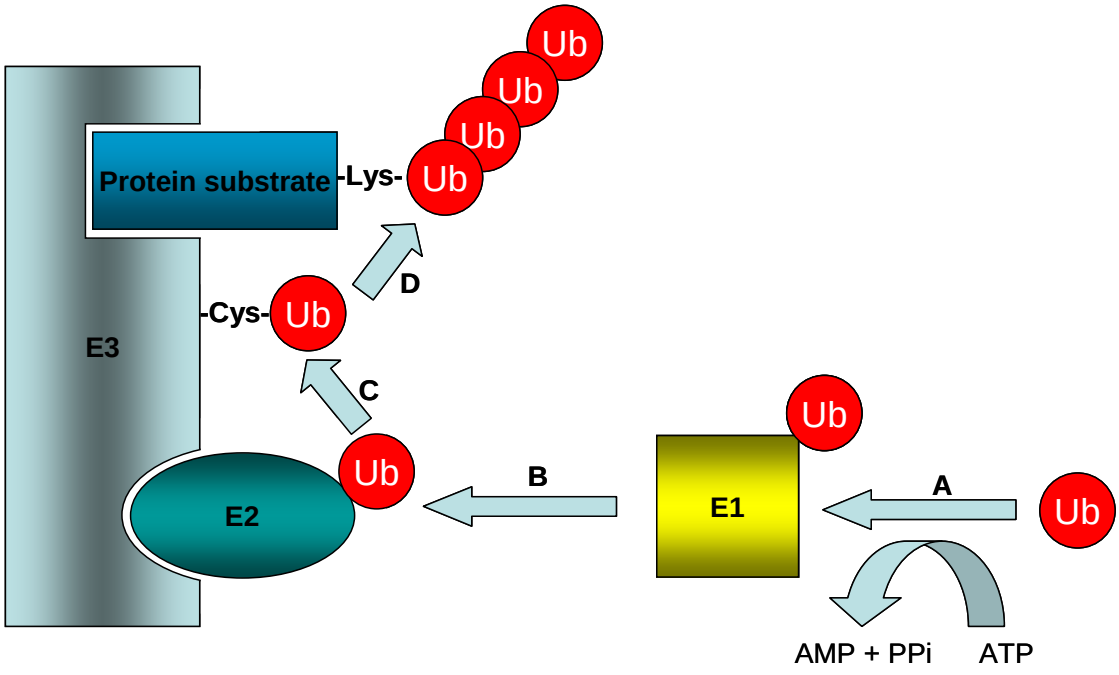

Figure 1.2 Ubiquitin conjugation to target proteins.

A. Free ubiquitin is activated by formation of a high energy thioester bond with an E1 enzyme. B. A transthiolation reaction passes ubiquitin to the E2 enzyme. C. The E2 and E3 enzymes work together, via a thiol-ester intermediate on the E3 ligase to D. Transfer ubiquitin to protein substrates.

1.2 Ubiquitination regulates protein traffic

It is now becoming widely accepted that many plasma membrane receptors and channels are internalised on the basis of monoubiquitin or K63 linked polyubiquitin modifications (Urbe, 2005). Examples in mammalian cells include MHCII β chain in dendritic cells (Shin *et al.*, 2006), aquaporin 2 in Madin-Darby canine kidney cells (Kamsteeg *et al.*, 2006) and the neurotrophin receptor TrkA (Geetha *et al.*, 2005;Wooten and Geetha, 2006). The protein is ubiquitinated, internalised and either trafficked to the lysosome for degradation, or in the case of some proteins they may be recycled back to the cell surface (Shenoy, 2007;Berthouze *et al.*, 2009;Mukai *et al.*, 2010) (discussed further in section 1.3).

In *Saccharomyces cerevisiae* (yeast) and mammalian cells the role of ubiquitin in membrane protein traffic has been extensively studied, and it appears that the modification plays a role in more than internalisation of membrane proteins. A particularly well studied example is the general amino acid permease Gap1p. This twelve-transmembrane domain channel protein is regulated in response to nitrogen availability (Roberg *et al.*, 1997;Magasanik and Kaiser, 2002). On preferential nitrogen sources such as glutamate Gap1p is trafficked directly to the proteolytically active endosomal system (Roberg *et al.*, 1997). However on poor nitrogen sources Gap1p is directed to the plasma membrane to increase amino acid uptake into the cell (Roberg *et al.*, 1997) (Figure 1.3).

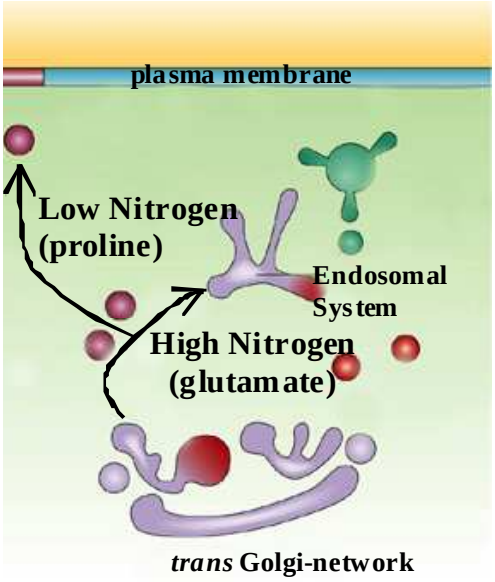

Figure 1.3 Gap1p traffic in *S. Cerevisiae*

On rich nitrogen sources, for example glutamate, Gap1p is sorted to the endosomes to be degraded at the vacuole. On poor nitrogen sources such as proline, where amino acid uptake is required, Gap1p is directed to the plasma membrane. Adapted with permission from Macmillan Publishers Ltd from Bryant *et al*., copyright (2002)

Work over the last decade has elucidated the role ubiquitin plays in this process, and one study (Risinger and Kaiser, 2008) has identified that different ubiquitin modifications on Gap1p give rise to different trafficking events. Monoubiquitination, which is dependent on a ubiquitin ligase complex containing the E3 ligase Rsp5p and the adaptor proteins Bul1p/2p, causes internalisation of Gap1p from the plasma membrane (Helliwell *et al.*, 2001;Soetens *et al.*, 2001;Risinger and Kaiser, 2008). However, polyubiquitination is required for the direct sorting of Gap1p from the TGN to the vacuole in favourable nitrogen conditions (Risinger and Kaiser, 2008). In summary, the studies on yeast Gap1p showed that i) an external stimulus can alter the trafficking of a membrane protein in yeast and ii) the ubiquitination status of a membrane protein at the TGN can target its trafficking into the endosomal system.

1.2.1 ESCRTs and multivesicular body sorting.

The ultimate fate of ubiquitinated membrane proteins is entry into the intralumenal vesicles (ILVs) of multivesicular bodies (MVBs), which subsequently fuse with lysosomes (Piper and Luzio, 2007). The contents of the MVB are degraded by lysosomal hydrolases on fusion of the MVB with the limiting

membrane of the lysosome (Hicke and Dunn, 2003;Woodman and Futter, 2008) (Figure 1.4).

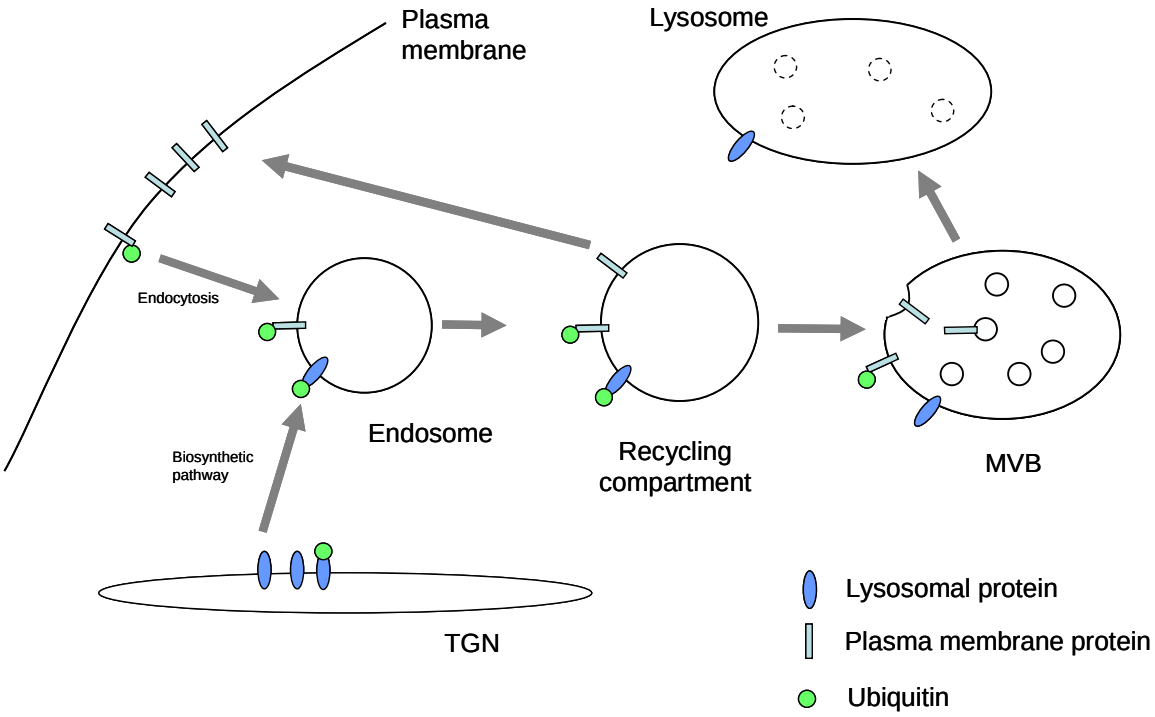

Figure 1.4 Membrane protein trafficking to multivesicular bodies.

Ubiquitinated plasma membrane receptors and channels, and biosynthetic cargoes destined for the lysosome, are trafficked via the endosomal system to the limiting membrane of multivesicular bodies (MVBs) where they may be internalised into intralumenal vesicles. Rescue and recycling of ubiquitinated proteins can occur at the recycling endosome.

In yeast, multivesicular bodies were originally identified as a "pre-vacuolar compartment" which becomes enlarged when a subset of yeast *VPS* (vacuolar protein sorting) genes are mutated – the so called "class E" mutants (Raymond *et al.*, 1992;Piper *et al.*, 1995;Woodman and Futter, 2008). The yeast class E Vps proteins represent the ESCRT proteins (Endosomal Sorting Complex Required for Transport), which have orthologues in mammalian cells. In the following discussion the yeast orthologues are only named when the nomenclature differs from the mammalian orthologue.

There are currently thought to be four ESCRT complexes. ESCRT-0 is a complex of Hrs (hepatocyte growth factor regulated tyrosine kinase) and STAM (signal transducing adaptor molecule) (Vps27 and Hse1 in yeast, respectively) (Urbe, 2005;Williams and Urbe, 2007). Both ESCRT-0 components can bind ubiquitin, through the UIM (ubiquitin interacting motif) found on STAM and the unusual

ubiquitin binding VHS (Vps27, Hrs, STAM) domain of Hrs (Ren and Hurley, 2010). This results in clustering of ubiquitinated cargoes into microdomains (Bilodeau *et al.*, 2002;Williams and Urbe, 2007), aided by ESCRT-0 binding to clathrin (Raiborg *et al.*, 2006).

ESCRT-I in mammals is a trimeric complex consisting of VPS23/TSG101, VPS28 and one of four VPS37 isoforms, with the addition of Mvb12 in yeast (Raiborg and Stenmark, 2009). ESCRTII is a tetramer with two subunits of VPS25 and single subunits of VPS36 and VPS22 (Williams and Urbe, 2007;Wollert *et al.*, 2009). Both complexes have a relatively low affinity for ubiquitin and are thought to function only when cargo has been pre-clustered by the ESCRT-0 complex (Raiborg and Stenmark, 2009).

After passing from ESCRT-0 to II, ubiquitinated cargos are received by ESCRT-III. ESCRT-III is composed of a number of highly charged subunits referred to as CHMPs (charged multivesicular body proteins) in mammals (Vps2,4,20,24 and 32 in yeast), several of which are capable of forming polymeric structures (Williams and Urbe, 2007;Raiborg and Stenmark, 2009). This complex seems to be required for membrane deformation and the final budding of ILVs.

A recent study using recombinant ESCRT components to reconstitute intralumenal vesicle budding into giant unilamellar vesicles (GUVs) has identified the roles of the four ESCRT complexes in ILV budding (Wollert and Hurley, 2010). ESCRT-0 clusters the model cargoes of GFP/CFP fused to the C-terminus of ubiquitin in microdomains. ESCRT-I and II are involved in formation of membrane buds, localising to bud necks and confining cargoes to the buds. ESCRT-I and II finally recruit ESCRT-III components and cause scission of the bud necks, resulting in ILV formation (Wollert and Hurley, 2010). This study provides compelling evidence of the mechanism underlying ILV formation.

1.2.2 GGA proteins sort ubiquitinated substrates

The GGA (Golgi localised, gamma adaptin ear containing, Arf binding) family of clathrin adaptor proteins was discovered simultaneously by three groups in 2000 (Dell'Angelica *et al.*, 2000;Hirst *et al.*, 2000;Boman *et al.*, 2000). There are two family members in yeast (Gga1/2p) and three in humans (GGA1-3) (Dell'Angelica *et al.*, 2000;Hirst *et al.*, 2000;Boman *et al.*, 2000). GGAs contain four domains:

the VHS domain which binds acidic dileucine sorting motifs, the GAT (GGA and TOM1) domain which interacts with both Arf and ubiquitin, a clathrin binding hinge region and a gamma adaptin ear like domain which interacts with accessory proteins (Mattera *et al.*, 2004;Pelham, 2004).

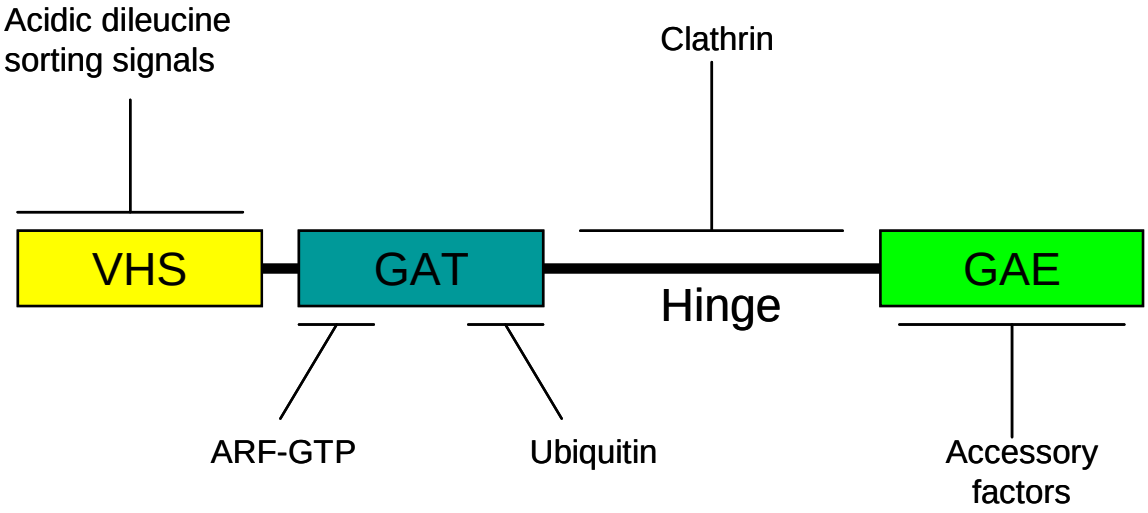

Figure 1.5 Domain structure of a typical GGA protein.
Interacting partners for each domain are indicated.

Structural studies have identified that the GAT domain of GGA3 contains two ubiquitin binding sites (Scott *et al.*, 2004;Bilodeau *et al.*, 2004;Kawasaki *et al.*, 2005) and *in vitro* binding of ubiquitin to the GAT domain can be significantly reduced by mutation of single residues (E250 and D284) in both sites (Kawasaki *et al.*, 2005). In yeast, a study has shown that *gga*Δ cells mislocalise Gap1p to the plasma membrane under poor nitrogen conditions, and this sorting defect is maintained on deletion of the ubiquitin-binding portions of the GAT domain, despite normal Gap1p ubiquitination (Scott *et al.*, 2004). This highlights the importance of the ubiquitin-GAT interaction in sorting yeast membrane proteins into the vacuolar degradation pathway.

In mammalian cells the story is less clear cut. GGA3 has been shown to have a role in sorting of ubiquitinated EGF receptor (Puertollano and Bonifacino, 2004). The EGF receptor is normally ubiquitinated on ligand stimulation at the plasma membrane, resulting in its internalisation and trafficking to the endosomal system (Stang *et al.*, 2000). If GGA3 is depleted via siRNA, the EGF receptor accumulates in an aberrant early endosomal compartment along with the cation-independent mannose 6 phosphate receptor (CIMPR) (Puertollano and Bonifacino, 2004).

Most studies on mammalian GGA dependent sorting have tended to focus on the VHS and GAT domains in combination (Li and Kandror, 2005;Kakhlon *et al.*, 2006), or on the role of the VHS domain which sorts acidic dileucine motifs (Hirst *et al.*, 2007;Doray *et al.*, 2008). However one study has highlighted that the GGA3 VHS-GAT domains in combination can bind ubiquitin and that GGA3 interacts with TSG101 (Puertollano and Bonifacino, 2004). TSG101 forms part of ESCRT I, so potentially GGAs perform a similar function to the ESCRT-0 complex as discussed in 1.2.1. A recent study (Kang *et al.*, 2010) has linked the GGA3 dependent lysosomal sorting of beta-site APP cleaving enzyme 1 (BACE-1) to BACE-1 ubiquitination; mutation of the BACE-1 dileucine motif did not affect sorting, whereas mutation of its ubiquitination site at K501 prevented lysosomal sorting (Kang *et al.*, 2010), as did expression of a full length GGA3 mutant which was impaired in its ability to bind ubiquitin (Kang *et al.*, 2010).

Indeed it remains unclear whether mammalian GGAs are functionally redundant as those of yeast are. One study has suggested that GGA1 and 3 are capable of binding to the same intracellular membranes, as depletion of GGA1 resulted in increased membrane accumulation of GGA3 and vice versa (Hirst *et al.*, 2009). Also, specific depletion of GGA2 results in the defective sorting of the lysosomal hydrolase cathepsin D, without altering the localisation of the classical GGA cargos of the mannose-6-phosphate receptors or GGA1 and 3 (Hida *et al.*, 2007). *In vitro* studies have shown that GGA1 and 3 have a considerably higher affinity for ubiquitin than GGA2 (Shiba *et al.*, 2004) indicating that GGA2 may have a different role to the odd-numbered GGAs. The situation is further complicated by the fact that GGAs can themselves be ubiquitinated (Shiba *et al.*, 2004); in the case of GGA3 ubiquitination, this can act as a signal for trafficking of the lysosomal protein LAPTM5 to the lysosome (Pak *et al.*, 2006).

1.3 Deubiquitinating enzymes (DUBs)

Deubiquitinating enzymes or DUBs are responsible for the cleavage of ubiquitin from substrate proteins, and thus counteract the activity of the E1-3 enzyme cascade. There are approximately 79 DUBs encoded by the human genome; these fall into five families – the ubiquitin C-terminal hydrolases (UCH), ubiquitin specific proteases (USPs), Josephins, Otubains (OTU) and JAB1/MPN/MOV34 metalloenzymes (JAMM) (Komander *et al.*, 2009;Reyes-Turcu *et al.*, 2009). UCH,

USP, Josephin and OTU enzymes are cysteine proteases whereas the JAMM family are zinc metalloproteases (Komander *et al.*, 2009;Reyes-Turcu *et al.*, 2009).

DUBs play three key roles in ubiquitin metabolism – they cleave precursors to release free ubiquitin, remove ubiquitin from substrate proteins and trim polyubiquitin chains. Although these three activities have wide ranging effects on many subcellular processes, including regulation of signalling cascades (Sun, 2010), endoplasmic reticulum associated degradation (ERAD) (Hassink *et al.*, 2009) and remodelling of chromatin structure (Zhu *et al.*, 2007) the most pertinent role of DUBs for this study is the role they play in determining the fate of membrane proteins.

1.3.1 Role of DUBs in endocytic and endosomal traffic.

As discussed in 1.2, ubiquitination is crucial for directing trafficking of membrane proteins, routing them from the plasma membrane to degradative compartments, or from the TGN to the endosomal system (Hicke and Dunn, 2003). Cleavage of ubiquitin modifications from target proteins can therefore modify their fate. I will now consider several examples of how DUBs modulate the ubiquitination status of membrane proteins and alter their trafficking properties.

In mammalian cells, multiple studies have identified that ubiquitination of plasma membrane receptors and channel proteins results in their internalisation (Geetha *et al.*, 2005;Kamsteeg *et al.*, 2006;Shin *et al.*, 2006;Wooten and Geetha, 2006). Members of the G-protein coupled receptor family (seven transmembrane receptors) are internalised on the basis of their ubiquitination and the levels of their signalling downregulated accordingly (Shenoy, 2007). One well characterised example of the role of DUBs in this process concerns the ß2-adrenergic receptor (ß2-AR). The receptor is deubiquitinated by two redundant DUBs, USP33 and USP20 (Berthouze *et al.*, 2009). Simultaneous depletion of both proteins by siRNA dramatically increases lysosmal trafficking of ß2-AR and therefore its degradation (Berthouze *et al.*, 2009). The recycling of the receptor to the cell surface is also reduced under these conditions which reduces downstream signalling as measured by accumulation of cyclic AMP – these phenotypes are also observed in cells co-expressing catalytically inactive forms

of USP33 and USP20 (Berthouze *et al.*, 2009). So in this case the DUBs are rescuing the receptor from degradation.

Doa4p (degradation of alpha 4) is a yeast DUB which has been shown to interact with components of the yeast ESCRT machinery, specifically the ESCRT-III component Snf7, which along with its interacting partner Bro1 causes recruitment of the DUB to endosomes and multivesicular bodies. It was initially thought that Doa4p's main role was to maintain free ubiquitin levels, which seemed plausible given that deletion of *DOA4* caused a reduction in ubiquitin levels in stationary phase yeast (Swaminathan *et al.*, 1999) and that depletion could be compensated by blocking trafficking to the MVB (Swaminathan *et al.*, 1999). Secondly, a Δ*doa4* strain exhibited defective ubiquitin dependent sorting to the vacuole and this can be compensated by overexpression of ubiquitin (Losko *et al.*, 2001).

However, more recent work has suggested that Doa4p may play a more direct role in MVB sorting than merely maintaining the pool of free ubiquitin. It appears that the massive overexpression of ubiquitin used in earlier studies resulted in bypassing of key components of the ESCRT machinery, and on more moderate expression of ubiquitin the trafficking of Gap1p is found to be defective in a Δ*doa4* strain, localising to the plasma membrane even under conditions of optimal nitrogen supply (Nikko and Andre, 2007). The same study also looked at the effect of *DOA4* deletion on sorting of carboxypeptidase S (CPS), a biosynthetic cargo which traffics to the vacuole constitutively (Odorizzi *et al.*, 1998). If Doa4p is absent or a catalytically inactive version of the DUB is expressed CPS is localised to the vacuolar membrane and cannot enter the lumen of the vacuole (Nikko and Andre, 2007). This suggests that the deubiquitination activity of Doa4p is required for entry of cargo proteins into the ILVs of MVBs, and thus entry into the vacuolar lumen.

In mammals, the ESCRT-0 complex binds two DUBs, AMSH (McCullough *et al.*, 2004) and UBPY (Kato *et al.*, 2000). AMSH is a JAMM family DUB which can process K63 linked polyubiquitin chains and deubiquitinate the epidermal growth factor receptor (EGFR) *in vitro* (McCullough *et al.*, 2004). AMSH depletion results in an increased rate of EGFR degradation (McCullough *et al.*, 2004), indicating that EGFR is stabilised by AMSH activity.

The second DUB, UBPY (also called USP8), has significant sequence similarity to yeast Doa4p (Clague and Urbe, 2006). The role of UBPY in endocytosis is less clear, as recent work has shown that depletion of the DUB severely impairs degradation of EGF-R and the Met tyrosine kinase receptor (Clague and Urbe, 2006;Row *et al.*, 2006;Alwan and van Leeuwen, 2007). Unlike AMSH, UBPY can cleave K48 and K63 linked polyubiquitin equally well. siRNA mediated depletion of UPBY results in the formation of aberrant, enlarged endosomes and multivesicular bodies (Row *et al.*, 2006). UBPY may deubiquitinate cytosolic as well as membrane bound proteins – the current hypothesis is that UBPY may deubiquitinate and thus stabilise components of the ESCRT machinery; this has been readily demonstrated for STAM, which is destabilised on knockdown of UBPY, concordant with a redistribution of Hrs from a cytosolic and perinuclear distribution to solely perinuclear structures (Row *et al.*, 2006). In the fruit fly *Drosophila melanogaster* (*Drosophila*) UBPY has been shown to play a role in the trafficking of the Wingless (Wg; a *Drosophila* Wnt orthologue) receptor Frizzled (Mukai *et al.*, 2010). UBPY knockdown flies show abnormal wing development due to decreased Wnt signalling during development, caused by increased ubiquitination (and thus degradation) of the Frizzled receptor (Mukai *et al.*, 2010).

1.4 GLUT4 and Type 2 diabetes.

1.4.1 Glucose homeostasis and Type 2 Diabetes

The activities of the hormone insulin allow clearance of glucose from the bloodstream following a meal. Raised postprandial plasma glucose causes insulin to be released from the pancreatic β cells into the circulation, altering the activity of insulin responsive tissues such as adipose, muscle and the liver (Figure 1.6). This results in clearance of plasma glucose.

The dysregulation of the insulin response is known as diabetes mellitus, or more generally diabetes. In Type 1 diabetes, the form of the disease responsible for about 5 % of cases (source: World Health Organisation (WHO)), the immune system raises an autoimmune response against the β cells of the pancreas. This

destroys the cells, preventing insulin secretion and thus clearance of plasma glucose (Zimmet *et al.*, 2001).

Type 2 diabetes, by far the most common form of the disease, responsible for approximately 95 % of cases (WHO estimate), has a different aetiology. Type 2 diabetes is the pathogenic progression of a state known as insulin resistance, where insulin becomes less effective at stimulating adipose and muscle, preventing clearance of plasma glucose (Saltiel and Kahn, 2001;Zimmet *et al.*, 2001). Type 2 diabetes tends to present at around 40 years of age after a prolonged period of insulin resistance, and has been linked to a sedentary lifestyle and high carbohydrate diet in at least 80 % of cases (Venables and Jeukendrup, 2009). Type 2 diabetes is one component of the so-called metabolic syndrome, with other components including hyperinsulinaemia, visceral obesity, dyslipidaemia and hypertension (Zimmet *et al.*, 2001).

Both types of diabetes result in complications with the circulatory system, including retinopathy, neuropathy, and cardiovascular disease. According to recent estimates there are approximately 220 million diabetics worldwide (Zimmet *et al.*, 2001) and fatalities due to diabetic complications may reach 2.2 million by 2030 (WHO estimate), with most of these cases being due to type 2 diabetes. Therefore to better to understand type 2 diabetes, it is vital to understand the biology of insulin responsive tissues.

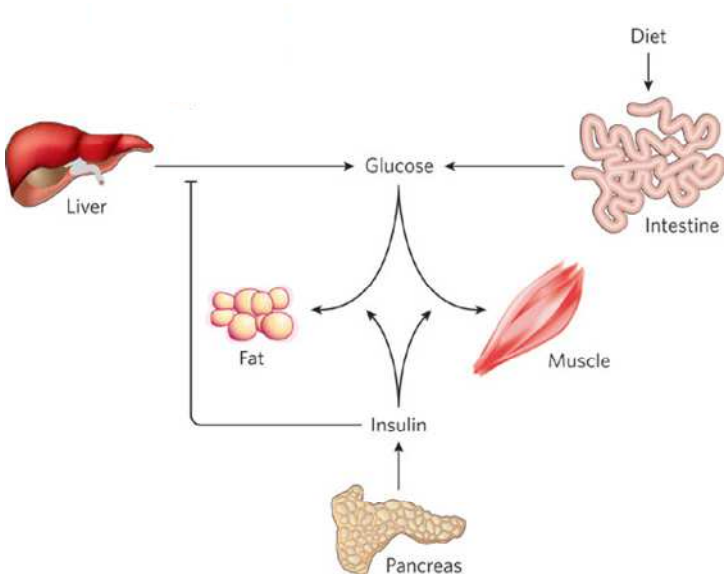

Figure 1.6 Regulation of glucose homeostasis by insulin.

Adapted with permission from Macmillan Publishers Ltd from Rosen and Spiegelman, copyright (2006)

1.4.2 GLUT4

One of the major actions of insulin is to increase the amount of the facilitative glucose transporter GLUT4 present at the cell surface of fat and muscle cells (Figure 1.7) and it is this response which is defective in Type 2 diabetes and insulin resistance (Saltiel and Kahn, 2001;Lin and Sun, 2010). GLUT4 presence at the plasma membrane of muscle and adipose allows glucose to enter the cells by diffusion down its concentration gradient. GLUT4 is a twelve-transmembrane domain channel protein, part of a larger family of thirteen facilitative sugar transporters including GLUT1-12 and the H^+ coupled myo-inositol transporter H-MIT (Wood and Trayhurn, 2003).

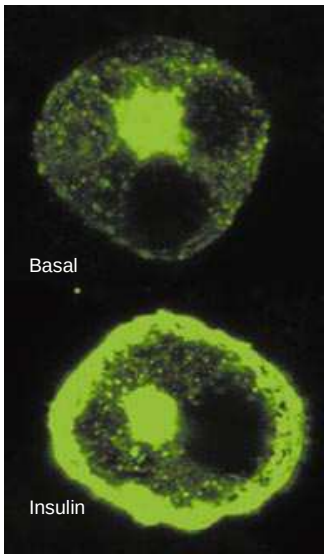

Figure 1.7 Insulin stimulates translocation of GLUT4 from intracellular stores to the cell surface.

3T3-L1 adipocytes expressing GLUT4 with a C-terminal GFP tag were treated with 100 nM insulin (lower panel) or not (upper panel) for 15 minutes and total GLUT4 detected by immunofluorescence. Adapted with permission from Macmillan Publishers Ltd from Saltiel and Kahn, copyright (2001).

The insulin stimulated glucose transport activity in muscle and adipose was initially identified by two groups in 1980. One study used a subcellular fractionation approach and a cell free reconstitution of rat adipose glucose uptake activity to show that a glucose transport activity moved from the intracellular compartments of the plasma membrane to the cell surface on insulin stimulation (Suzuki and Kono, 1980). The second study used the glucose transport inhibitor cytochalasin B inhibit glucose transport in rat adipocytes, and

found that insulin stimulation increased the amount of cytochalasin B sensitive glucose transport activity on these cells (Cushman and Wardzala, 1980). This transport activity was associated with a channel protein in screens of cDNA libraries of insulin responsive tissues, identifying a transporter in rat adipose which shared some sequence similarity with the rat brain and liver glucose transporter. The identity of this transporter as the insulin regulated glucose transporter was confirmed using the monoclonal antibody 1F8 (Birnbaum, 1989;James *et al.*, 1989;Fukumoto *et al.*, 1989).

1.4.3 GLUT4 traffic in insulin responsive cells

The trafficking itinerary of GLUT4 is complex with several key questions remaining unresolved; however a picture of the process is beginning to emerge and I will discuss the findings underlying this model.

The trafficking pathway occupied by cargoes such as the transferrin receptor (TfR) is known as the constitutive recycling pathway, and involves proteins cycling between the endosomes and the plasma membrane. About 40 % of total cellular GLUT4 is found in this cycle under basal conditions, as demonstrated by endosome ablation analysis using HRP conjugated transferrin (Livingstone *et al.*, 1996). The remainder of GLUT4 occupies a second cycle between the TGN and the endosomes. This has been observed in several studies. Shewan *et al.* (2003) demonstrated that GLUT4 cycles between the endosomes and a perinuclear compartment, which represented a subdomain of the TGN enriched in the SNARE proteins syntaxin 6 and 16. Karylowski and colleagues (2004) showed that in the basal state an HA-GLUT4-GFP reporter cycles between endosomes and the perinuclear compartment without transiting the cell surface.

Two models have been proposed to explain the mobilisation of GLUT4 in response to insulin. The first model, termed dynamic exchange, suggests that most GLUT4 molecules occupy a constitutive recycling pathway between the cell surface and endosomal system, similar to that seen for TfR. On insulin stimulation, the increase in plasma membrane GLUT4 is caused by an increase in the exocytic rate constant, and decrease in the endocytic rate constant, of GLUT4, with a net increase in the number of GLUT4 molecules at the plasma membrane (Karylowski *et al.*, 2004;Martin *et al.*, 2006).

The second model, known as static retention, suggests that GLUT4 is retained in an essentially static storage compartment in basal conditions, analogous to the secretory vesicles found in neurons. On insulin stimulation GLUT4 discharged from this storage compartment into the cell surface recycling pathway, raising GLUT4 levels at the plasma membrane without any effect on exocytosis or endocytosis rates (Govers *et al.*, 2004;Coster *et al.*, 2004). More recent work seems to suggest that both these mechanisms play a role in GLUT4 exocytosis in response to insulin, and that previous studies had biased the recycling kinetics of GLUT4 in their systems due to the cell culture conditions used; if 3T3-L1 adipocytes are replated after transfection, there is an increase in the proportion of GLUT4 in the in the basal cycling pool, from 20% to almost 80 % (Muretta *et al.*, 2008).

Three key trafficking motifs have been identified within GLUT4 : an N-terminal FQQI motif (Verhey *et al.*, 1995)and dileucine (Verhey and Birnbaum, 1994) and TELEY motifs, both close to the C terminus (Shewan *et al.*, 2000). Each motif appears to have its own role in the intracellular retention of GLUT4, and one study has investigated the role of all these motifs in retention in particular compartments (Blot and McGraw, 2008). Mutation of the phenylalanine residue in the FQQI motif to tyrosine results in an accumulation of HA-GLUT4-GFP in a perinuclear compartment thought to represent the Stx16 positive compartment, whereas mutation of the same residue to alanine resulted in a decrease in basal retention of HA-GLUT4-GFP (Blot and McGraw, 2008). This result relates to an earlier study, which implicates the FQQI motif in the AS160 (Akt substrate of 160 kilodaltons, a Rab GAP) dependent intracellular retention of GLUT4 (Capilla *et al.*, 2007). Mutation of the TELEY motif to TALAY resulted in a decreased basal retention, which was additive to that of the AQQI mutation, suggesting that these two motifs regulate different aspects of the basal retention mechanism (Blot and McGraw, 2008). Mutation of the dileucine motif to dialanine results in a reduction in the rate of return of surface HA-GLUT4-GFP to basal levels (Blot and McGraw, 2008).

The model proposed by the authors of this study is that GLUT4 traffic is centred on the recycling endosome (Figure 1.8). GLUT4 is internalised from the plasma membrane in a manner dependent on the dileucine motif, with a small number of GLUT4 molecules reaching the cell surface under basal conditions via the constitutive recycling pathway (Verhey *et al.*, 1995;Blot and McGraw, 2008). In

basal conditions GLUT4 is retained intracellularly by slowly cycling between the endosomes and two specialised "storage compartments" – one being the Stx16 positive region of the TGN (Shewan *et al.*, 2003) which retains GLUT4 in an AS160 dependent manner via the FQQI motif and does not undergo insulin responsive translocation, and a second vesicular pool which retains GLUT4 via the TELEY motif and translocates in response to insulin, (Blot and McGraw, 2008). The latter vesicular pool represents the insulin responsive compartment which has previously been named GLUT4 storage vesicles (GSVs) (Bryant *et al.*, 2002).

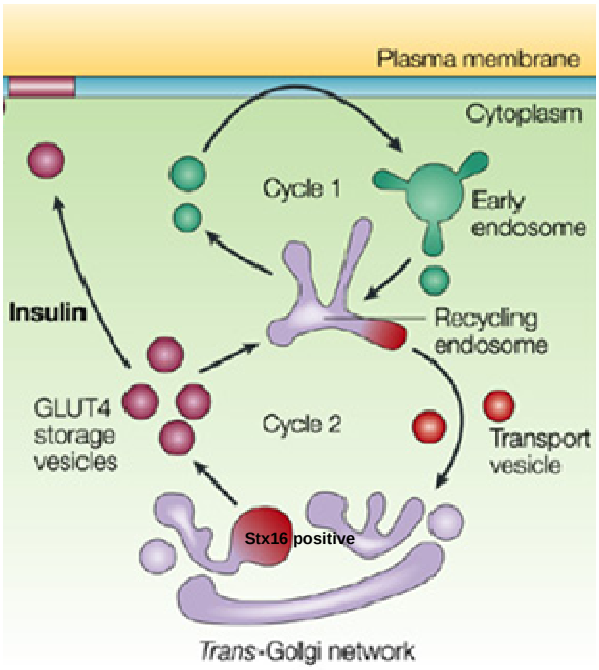

Figure 1.8 A model of GLUT4 traffic in insulin responsive cells.

GLUT4 occupies two linked cycles in insulin responsive tissues. Cycle 1 is the constitutive, rapid recycling pathway between the recycling endosome and the plasma membrane. Cycle 2 is between the TGN and endosomes, and includes the slowly recycling, highly insulin responsive GLUT4 storage vesicles. Reproduced with permission from Macmillan Publishers Ltd from Bryant *et al.*, copyright (2002)

1.4.4 GLUT4 Storage vesicles

The population of subcellular compartments which represent GSVs have been defined as a subset of the low-density microsomal (LDM) fraction of adipocytes which lack the transmembrane protein cellugyrin (Kupriyanova *et al.*, 2002;Jedrychowski *et al.*, 2010). Cellugyrin was initially identified as a component of GLUT4 vesicles in 3T3-L1 adipocytes (Kupriyanova and Kandror,

2000). However, use of a monoclonal antibody raised against cellugyrin showed that cellugyrin containing vesicles only contained about 40-50 % of total cellular GLUT4, with the remaining GLUT4 in other compartments (Kupriyanova and Kandror, 2000) – this figure is reminiscent of the relative amount of GLUT4 in the endosomal system compared to specialised compartments in earlier studies (Livingstone *et al.*, 1996). Also, the cellugyrin negative vesicles were shown to be much more insulin responsive than cellugyrin positive ones (Kupriyanova and Kandror, 2000) and this result was confirmed using a GLUT4 specific monoclonal antibody (Kupriyanova *et al.*, 2002). These data collectively suggest that cellugyrin negative vesicles from the LDM fraction of 3T3-L1 adipocytes represent insulin responsive GSVs.

GSVs have several well-characterised protein components including the SNARE protein VAMP2 (vesicle associated membrane protein 2) (Cain *et al.*, 1992;Martin *et al.*, 1996), sortilin (Lin *et al.*, 1997), the insulin responsive aminopeptidase IRAP (Ross *et al.*, 1996;1997) and LRP1 (low density liposome receptor related protein 1) (Jedrychowski *et al.*, 2010).

Several of these proteins are required for formation of GSVs from donor membranes. The sorting receptor sortilin was characterised as a 110 kD component of GSVs (Lin *et al.*, 1997;Morris *et al.*, 1998). Sortilin has been shown to be essential and sufficient for formation of GSVs in 3T3-L1 cells. Sortilin is induced 2 days after adipocyte differentiation and this event coincides with formation of functional GSVs (Shi and Kandror, 2005). siRNA mediated depletion of sortilin reduced formation of GSVs in an *in vitro* budding assay, and consequently reduced insulin stimulated glucose transport (Shi and Kandror, 2005). Expression of epitope tagged GLUT4 in the absence of sortilin in undifferentiated 3T3-L1 cells results in rapid degradation of the transporter; however co-expression of GLUT4 and sortilin resulted in formation of functional GSVs in the undifferentiated cell line (Shi and Kandror, 2005).

The lumenal domains of IRAP and GLUT4 can interact with that of sortilin as demonstrated by cross-linking and yeast two-hybrid analysis (Shi and Kandror, 2007). The GLUT4-IRAP interaction appears essential for recruitment of IRAP into GSVs (Shi *et al.*, 2008). Also, co-expression of sortilin and GLUT4 in undifferentiated 3T3-L1 cells results in formation of an insulin-responsive compartment in these cells; this requires the lumenal interactions of sortilin, as

a sortilin mutant with a truncated lumenal domain can only partially reconstitute the insulin responsive compartment (Shi and Kandror, 2005;Shi *et al.*, 2008)

LRP1 is another GSV cargo which was identified in a recent proteomic analysis of immunoisolated cellugyrin-negative GSVs (Jedrychowski *et al.*, 2010). It interacts with GLUT4, IRAP and sortilin, and depletion of LRP1 results in the depletion of all three proteins (Jedrychowski *et al.*, 2010).

Two major questions remain unanswered concerning the regulated trafficking of GLUT4; firstly, what is the signal that causes GSVs to translocate in response to insulin; and secondly, how is GLUT4 loaded into the insulin responsive GSVs? There is a reasonable amount of evidence that has gone some way to answering the first of these questions. It appears that the insulin signalling cascade results in phosphorylation of AS160 (Akt substrate of 160 kilodaltons – a RabGAP protein) by Akt/protein kinase B (Sano *et al.*, 2003). This phosphorylation event results in fusion of GSVs with the plasma membrane, in a manner dependent on the amino terminal FQQI motif of GLUT4 (Capilla *et al.*, 2007). LRP1, a GSV protein, can also recruit AS160 on its cytosolic domain, possibly providing a link from GSVs to the insulin signalling pathway (Jedrychowski *et al.*, 2010).

The overall aim of this thesis is to address the second question, contributing to the data discussed in this section and section 1.4.3 to better understand how GLUT4 enters the insulin responsive compartment.

1.5 A role for ubiquitin in the trafficking of GLUT4?

In recent years work in our laboratory has been focused on testing the hypothesis that GLUT4 is modified with ubiquitin and that this modification is essential for insulin-responsive trafficking of the transporter. In this section I will discuss data that support this hypothesis.

1.5.1 Ubiquitin-like proteins regulate GLUT4 traffic.

Functional cloning approaches in Chinese hamster ovary cells have identified a putative regulator of GLUT4 trafficking, which colocalises with GLUT4 at GSVs. This regulator was termed TUG (tether, containing UBX domain, for GLUT4)

(Bogan *et al.*, 2003). TUG contains two ubiquitin like domains. The first of these is a C-terminal UBX (ubiquitin regulatory X) domain, which is involved in interaction with the p79/VCP ATPase, a generic molecular motor (Bogan *et al.*, 2003;Tettamanzi *et al.*, 2006). The long splice variant of TUG appears to be able to sequester GLUT4 within the cell in a manner dependent on this UBX domain (Bogan *et al.*, 2003). The second is an N-terminal ubiquitin-like (UBL) domain. The structure of this domain has been solved using NMR spectroscopy (Tettamanzi *et al.*, 2006). The data from this study suggest that TUG does not participate in protein conjugation as ubiquitin does as it lacks the key diglycine motifs and acceptor lysine residues to do so. However a region of the molecular surface with high electrostatic potential and backbone mobility has characteristics of a region involved in protein-protein interactions, which is typical behaviour for UBL domain containing proteins which often function as adaptor molecules (Tettamanzi *et al.*, 2006).

TUG has also been shown to be essential for insulin-responsive GLUT4 trafficking (Yu *et al.*, 2007) since RNAi mediated TUG depletion, or expression of a dominant negative TUG fragment, enhances glucose uptake by both basal and insulin stimulated 3T3-L1 adipocytes, and that this appears to be achieved by disrupting formation of the perinuclear GLUT4 compartment (Yu *et al.*, 2007). Additionally, this study indicates that TUG is capable of interacting with the large cytosolic loop of GLUT4. In the context of this thesis, the studies on TUG collectively suggest that a molecule with a high degree of structural similarity to, and the potential to interact with, ubiquitin has an important role in the insulin sensitivity of GLUT4.

It has previously been demonstrated that GLUT4 is modified by addition of small ubiquitin-like modifier 1 (SUMO1) at lysine residues (Lalioti *et al.*, 2002), and that overexpression of the SUMO conjugating enzyme mUbc9 increases levels of GLUT4 in cultured skeletal muscle cells which consequently increases glucose transport rates (Giorgino *et al.*, 2000;Liu *et al.*, 2007), while mUbc9 depletion has the opposite effect (Liu *et al.*, 2007). It is conceivable therefore that SUMOlation and, possibly, ubiquitin modifications are involved in regulating GLUT4 trafficking and glucose uptake in response to insulin. Indeed, SUMOlation itself can act as a tag for ubiquitination, directing E3 ubiquitin ligases to target proteins in certain cases. For example, in *Schizosaccharomyces pombe* (fission

yeast) the ubiquitin ligase complex Slx5-Slx8 is recruited to substrates by its ability to bind SUMO polymers (Mullen and Brill, 2008;Geoffroy and Hay, 2009).

1.5.2 Evidence from yeast.

Unpublished data from the expression of hGLUT4 in *S. cerevisiae* has shown that hGLUT4 is subject to the same nitrogen dependent trafficking as Gap1p (McCann R.K., 2007). On rich nitrogen sources, hGLUT4 is directed constitutively to the proteolytically active endosomal system, and on poor nitrogen sources the transporter is stabilised (McCann R.K., 2007) in an similar fashion to Gap1p (Roberg *et al.*, 1997), indicating that it is trafficked away from the proteolytically-active endosomal system. However a ubiquitin-resistant mutant of hGLUT4 (GLUT4-7K/R) cannot be directed to the vacuole on rich nitrogen sources, and deletion of both yeast *GGA* genes recapitulates this phenotype (Lamb *et al.*, 2010). By both co-immunoprecipitation and using a GST pull-down approach, GLUT4 has been shown to be ubiquitinated in yeast (Lamb *et al.*, 2010). These findings suggest that GLUT4 is subjected to ubiquitin-dependent trafficking to the vacuole in yeast, in a manner similar to Gap1p.

1.5.3 Evidence from 3T3-L1 adipocytes

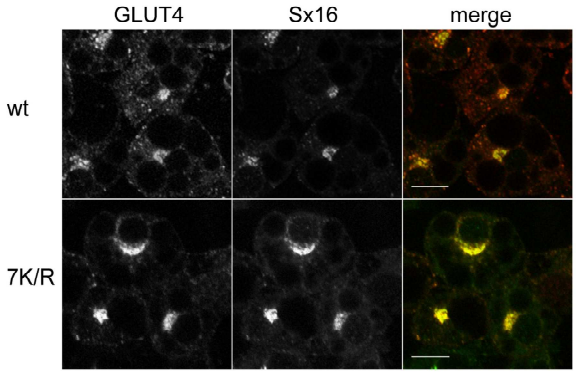

Figure 1.9 A ubiquitin-resistant version of GLUT4 cannot exit the syntaxin 16 positive subdomain of the TGN in 3T3-L1 adipocytes.

3T3-L1 adipocytes expressing HA-GLUT4 (wt) or HA-GLUT4 7K/R (7K/R) were stained for the HA epitope (GLUT4) and syntaxin 16 (Sx16) as a marker of the TGN. Image used by permission of Dr. R. McCann.

Although the yeast studies provide evidence that ubiquitination of GLUT4 alters its trafficking, the analyses had to be extended to a more physiologically relevant mammalian cell line to draw any firm conclusions about the role of GLUT4 ubiquitination *in vivo*. 3T3-L1 adipocytes are a well established model system for studying the insulin responsive phenotype (Mackall *et al.*, 1976). HA-GLUT4 7K/R cannot exit the Stx16 positive region of the TGN and is excluded from cytosolic puncta thought to represent GSVs (McCann R.K., 2007) (Figure 1.9), and initial data suggested that HA-GLUT4 7K/R cannot translocate in response to insulin, unlike its wild type counterpart (McCann R.K., 2007). However, the translocation data can only be taken as preliminary as the retroviral HA-GLUT4 7K/R construct used in these studies expressed the mutant protein at much lower levels than the wild type HA-GLUT4 (Shewan *et al.*, 2000) construct. These data suggest that GLUT4 ubiquitination is involved in GLUT4 entering the insulin responsive compartment.

1.5.4 GGA proteins regulate GLUT4 entry into GSVs

Two key studies have implicated the GGA family of clathrin adaptor proteins in GLUT4 sorting into GSVs from the TGN, and they both rely on expressing a dominant negative fragment of GGA (VHS-GAT) which contains the cargo binding domains and the Arf binding site required for membrane association, but none of the effector domains. This GGA fragment was generated from GGA2 and is proposed to have dominant negative activity against all three mammalian GGAs (Li and Kandror, 2005).

The first study from 2004 (Watson *et al.*) demonstrated that expression of VHS-GAT resulted in reduced insulin stimulated GLUT4 translocation as assessed by confocal microscopy, and that the *in vitro* budding of GLUT4 containing vesicles is inhibited by the presence of VHS-GAT. The second study (Li and Kandror, 2005) demonstrated that GLUT4 colocalises with GGA2 in a perinuclear compartment, likely the TGN. This study also showed that VHS-GAT expressing cells cannot rapidly re-form the GSV compartment after stimulation with insulin, and that GLUT4 is loaded less effectively into the GSV enriched supernatant (produced from centrifugation of a 3T3-L1 adipocyte lysate at 16 000 xg for 20 minutes) in VHS-GAT expressing cells.

One further finding of Li and Kandror (2005) is that GSVs can interact with GGA adaptors *in vitro*. Although components of GSVs have been shown to have a requirement for dileucine sorting motifs interacting with the VHS domains of GGAs, notably IRAP (Hou *et al.*, 2006) and sortilin (Nielsen *et al.*, 2001;Shiba *et al.*, 2002), there is no published evidence for GLUT4 interacting directly with GGAs. Although GLUT4 does contain a dileucine motif at residues 489 and 490 (Verhey and Birnbaum, 1994;Shewan *et al.*, 2000) there seems to be little requirement for this motif in trafficking from the TGN to the GSVs; the motif appears to have a more important role in internalising the transporter (Verhey *et al.*, 1995;Sandoval *et al.*, 2000;Blot and McGraw, 2008).

As the internalisation step is apparently not GGA dependent, there is a possibility that the GAT domain plays a role in GLUT4 traffic by interacting with ubiquitin moieties on GLUT4, as has been observed for yeast Gap1p (Scott *et al.*, 2004;Bilodeau *et al.*, 2004). This is certainly not excluded by the two studies which implicate the GGAs in sorting of GLUT4 (Watson *et al.*, 2004;Li and Kandror, 2005) as they make use of a dominant negative VHS-GAT construct which would disrupt interactions with both cargo binding domains of endogenous GGAs.

1.6 Is GLUT4 deubiquitination required for its insulin responsive traffic?

So far evidence has been presented which supports the hypothesis that ubiquitination of GLUT4 is required for its loading into GSVs. However, there is a potential flaw in the reasoning behind this hypothesis. Ubiquitination of membrane proteins is canonically thought of as being a modification required for trafficking of proteins to the lysosome/vacuole compartment and their subsequent destruction by vacuolar hydrolases. Also work from our laboratory has demonstrated that only 0.1 % of total GLUT4 is ubiquitinated in the cell at any one time (Lamb *et al.*, 2010) which suggests the modification is a transient one. There is therefore a potential requirement for a deubiquitination step in the post – TGN trafficking of GLUT4, to prevent its delivery to the lysosome, and to direct the transporter to GSVs. As discussed in 1.3.1, DUBs can rescue their substrates from lysosomal degradation; could this be the case for GLUT4? And if so, how are DUB(s) recruited to GSVs?

1.6.1 IRAP and Tankyrase

As has previously been stated in section 1.4.4, GLUT4 shares GSVs with a number of other proteins and one of these is the insulin responsive aminopeptidase IRAP, also known as vp165 and gp160. Although widely expressed, IRAP was characterized as a component of GSVs (Ross *et al.*, 1996) and found to have an identical trafficking itinerary to GLUT4 in adipocytes (Ross *et al.*, 1997). Subsequently IRAP has been localized to vesicles in neurons, where it colocalises with GLUT4 (Fernando *et al.*, 2007;2008) and in cells of the immune system, where it plays a role in antigen presentation (Saveanu *et al.*, 2009) which suggests the peptidase has broader roles in vesicle traffic than previously thought.

In undifferentiated 3T3-L1 cells, IRAP is found primarily at the plasma membrane (Ross *et al.*, 1998) but on differentiation it is sequestered in an intracellular compartment, resulting in an approximately 8-fold increase in plasma membrane localized IRAP on insulin stimulation (Ross *et al.*, 1998). As with GLUT4, the trafficking of IRAP is defective in adipocytes from Type 2 diabetics. Less IRAP is found in the low density microsomal fraction (LDM) which contains GSVs, and insulin stimulated translocation of IRAP is severely impaired (Maianu *et al.*, 2001). An IRAP knockout mouse line does exist and these animals exhibit normal glucose tolerance, despite having decreased tissue levels of GLUT4 and insulin responsive glucose uptake (Keller *et al.*, 2002). These data indicate a role for IRAP in maintaining GLUT4 stability.

Work in 3T3-L1 adipocytes has demonstrated that IRAP depletion using siRNA impairs the insulin stimulated translocation of GLUT4; however the reverse is not true (Yeh *et al.*, 2007;Jordens *et al.*, 2010). IRAP interacts with a poly-ADP ribose polymerase (PARP) known as tankyrase 1 (Chi and Lodish, 2000;Sbodio and Chi, 2002). Tankyrase 1 was initially identified as a protein with *in vitro* PARP activity localised to telomeres (Smith *et al.*, 1998). It contains a C terminal catalytic domain, a sterile alpha motif (SAM) and a series of N-terminal ankyrin (ANK) repeats (Figure 1.10), and has a closely related homologue, tankyrase 2 (Kaminker *et al.*, 2001). The ANK repeats contain the IRAP interaction domain, binding an RXXPDG motif within IRAP conserved in other tankyrase interacting

partners such as NuMa and TRAF1 which are involved in DNA replication (Chi and Lodish, 2000;Sbodio and Chi, 2002). The domain of tankyrase 1 required for this interaction is the C-terminal region of the ANK repeat domain, named subdomain V (Chi and Lodish, 2000).

In tankyrase depleted 3T3-L1 adipocytes, both GLUT4 and IRAP are redirected to denser membrane compartments and fail to translocate normally in response to insulin (Yeh *et al.*, 2007). Taken together these data suggest that IRAP may provide a "handle" on GSVs to which proteins regulating GLUT4 traffic, such as tankyrase 1, can associate. Tankyrase 1 itself, with its capacity for protein-protein interactions (via the ANK domains (Seimiya and Smith, 2002)) and oligomerisation (via the sterile alpha motif (Sbodio *et al.*, 2002)) could potentially act as a scaffolding molecule, recruiting various factors to GSVs.

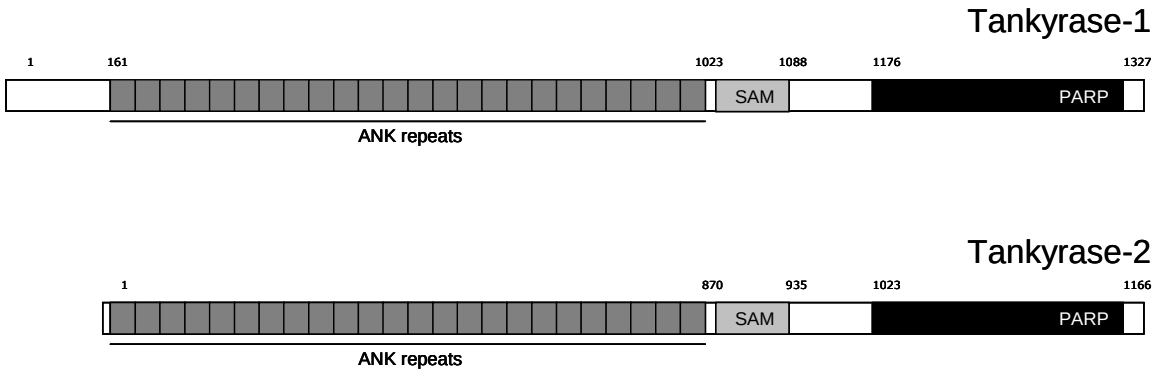

Figure 1.10 Schematic of tankyrase-1 and 2.

Ankyrin repeat domains (ANK), sterile alpha motif (SAM) and catalytic poly-ADP ribose polymerase (PARP) domains are indicated.

1.6.2 USP25: a candidate GLUT4 DUB

From the data discussed in section 1.6.1 it would appear that IRAP and tankyrase form part of a complex that can regulate GLUT4 entry into GSVs (Chi and Lodish, 2000;Yeh *et al.*, 2007). A link between these data and the hypothesis that GLUT4 deubiquitination is required for entry into GSVs is provided by data from the laboratory of Nai-Wen Chi (UCSD). The deubiquitinase USP25 has been shown to interact with tankyrase in a yeast two hybrid screen, and contain a putative tankyrase binding motif (RTPADG) near the C-terminus (Sbodio and Chi, 2002). Co-immunoprecipitation experiments have also demonstrated that tankyrase and USP25 interact *in vivo* (N-W Chi, unpublished).

The *USP25* gene was originally isolated as a locus within the short arm of chromosome 21 which was duplicated in Down's syndrome patients (Valero *et al.*, 1999). The gene has three different protein products (Valero *et al.*, 2001). USP25a is the ubiquitously expressed 1055 amino acid isoform. USP25b is also broadly expressed at much lower levels than USP25a, but is not found in murine tissues. USP25m is the largest isoform at 1087 amino acids, and restricted to striated muscle in both mice and humans (Valero *et al.*, 2001;Bosch-Comas *et al.*, 2006).

USP25m has been shown to play a role in protein turnover in muscle. The isoforms of USP25 expressed in muscle can interact readily with filamin-C, ACTA1 and MyBPC1 as demonstrated by yeast two hybrid analysis, *in vitro* pull-down assays and co-immunoprecipitation experiments (Bosch-Comas *et al.*, 2006). In fact, this study identifies MyBPC1 as a specific substrate of USP25; MyBPC1 is deubiquitinated and stabilised in HEK293 cells on overexpression of USP25 (Bosch-Comas *et al.*, 2006).

Several studies have shed light on the regulation of USP25 activity and its molecular architecture. USP25 contains several key structural domains as shown in Figure 1.11. It contains three N terminal ubiquitin binding motifs (a single UBA and two UIM), a SUMO interacting motif (SIM), catalytic domains (USP1/2) and a long C-terminal coiled-coil region which appears to be required for catalysis (Meulmeester *et al.*, 2008;Denuc *et al.*, 2009).

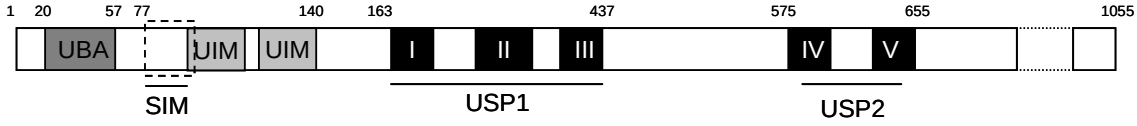

Figure 1.11 Schematic of USP25a.

Key structural and catalytic domains are highlighted.

USP25 can itself be post-translationally modified. Meulmeester *et al.* (2008) demonstrated using mutagenic and mass spectrometry analyses that USP25 can be SUMOlated on two sites (lysines 99 and 141) within its two UIMs. SUMOlation appears to have an inhibitory effect on USP25 activity (Meulmeester *et al.*, 2008)– the authors speculate that this is due to the SUMO moieties blocking access of ubiquitin to the UIMs and thus preventing access of ubiquitinated substrates.

USP25 can also be ubiquitinated, and auto-deubiquitinate, as reported by a second study (Denuc *et al.*, 2009). The authors identified K99 as the site of ubiquitination using mass spectrometry. Mutation of this residue did not greatly reduce *in vitro* DUB activity of USP25. The authors suggest that as K99 SUMOlation is known to be an inactivating modification, mutation of K99 would be expected to result in an over-active form of USP25. As this is not the case, it can be inferred that ubiquitination of USP25 at K99 is an activating mutation (Denuc *et al.*, 2009). Denuc *et al*. went on to present a model building on that of Meulmeester *et al* (2008) whereby SUMOlated USP25 is held in an inactive conformation by the interaction of the SUMO moiety at K99 with the SUMO interacting motif (SIM), and the K141 SUMO blocking access to the UIMs and thus preventing access of ubiquitinated substrates. On ubiquitination at K99, ubiquitinated substrates are able to interact with the UIMs, resulting in efficient ubiquitin chain hydrolysis.

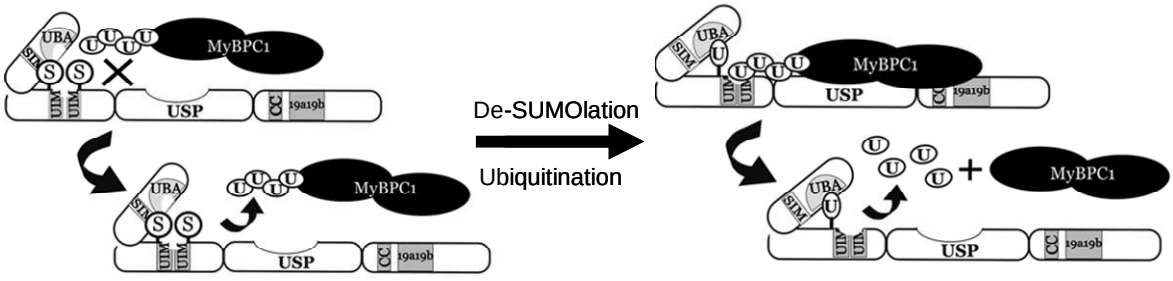

Figure 1.12 Model for USP25 regulation by SUMOlation and ubiquitination.

SUMOlation prevents access of ubiquitinated substrates (left panel) whereas ubiquitination allows their access to UIMs and thus efficient ubiquitin chain hydrolysis. Adapted from Denuc *et al*. (2009)

Finally, USP25 has recently been shown to interact with SYK (spleen tyrosine kinase) in HEK 293 cells (Cholay *et al.*, 2010). The interaction is dependent on the C terminal SH2 domain of SYK and a C-terminal region of USP25 between residues 726 and 944, as demonstrated by yeast-2-hybrid analysis and co-immunoprecipitation experiments (Cholay *et al.*, 2010). SYK is capable of phosphorylating USP25 at a tyrosine residue, possibly at residue Y740 as predicted by bioinformatic analyses (Cholay *et al.*, 2010). This phosphorylation of USP25 results in its downregulation; overexpression of SYK results in a decrease in USP25 cellular levels, which can be countered by addition of the kinase inhibitor piceatannol (Cholay *et al.*, 2010).

From these data, it is clear that USP25 activity and abundance can be modulated by several different factors. Taken together with the data on the interaction of tankyrase with USP25 (Sbodio and Chi, 2002), it is tempting to speculate that regulated USP25 DUB activity is required to deubiquitinate GLUT4 and prevent its lysosomal degradation.

1.6.3 3T3-L1 adipocyte data versus knockout mice: a confusing picture.

The story is complicated somewhat by the phenotypes observed in tankyrase deficient mice. As discussed in section 1.6.1, IRAP knockout mice have less GLUT4 than wild type littermates, and reduced insulin stimulated glucose uptake, despite apparently normal glucose tolerance (Keller *et al.*, 2002).

However a recent study (Yeh *et al.*, 2009) demonstrated that tankyrase 1 knockout mice have reduced perirenal and epididymal adipose deposits, and 43% of normal plasma leptin levels which indicated an overall loss of adiposity consistent with their increased lipid utilisation; they also exhibit hyperinsulinaemia and a decrease in plasma glucose (Yeh *et al.*, 2009). The tankyrase knockout mice appear to have increased expression of GLUT4 which can account for this phenotype, and they exhibit an increased fold change in glucose transport in response to insulin (Yeh *et al.*, 2009). A second study shows that adipocytes isolated from mice deficient in tankyrase 1 or 2 both exhibit glucose uptake rates similar to wild type littermates (Chiang *et al.*, 2008).

This does not support the hypothesis that IRAP and tankyrase form a platform for USP25 recruitment, as a reduction in cellular GLUT4 and altered insulin stimulated glucose uptake would be expected in tankyrase deficient mice if this were the case, as observed for IRAP knockouts (Keller *et al.*, 2002). There is therefore still some confusion in the literature as to the roles that the two tankyrases play in GLUT4 traffic.

1.7 A model for ubiquitin dependent loading of GLUT4 into GSVs.

From the data presented so far we can present a model for the ubiquitin dependent loading of GLUT4 into GSVs (Figure 1.13). Newly synthesized GLUT4 at the TGN is ubiquitinated by an as yet unidentified ligase. Ubiquitinated GLUT4 can then exit the TGN in a GGA dependent manner, reaching GSVs. On entry into GSVs GLUT4 is deubiquitinated by a complex containing IRAP, tankyrase and USP25. GLUT4 is thus rescued from lysosomal degradation and can respond to insulin.

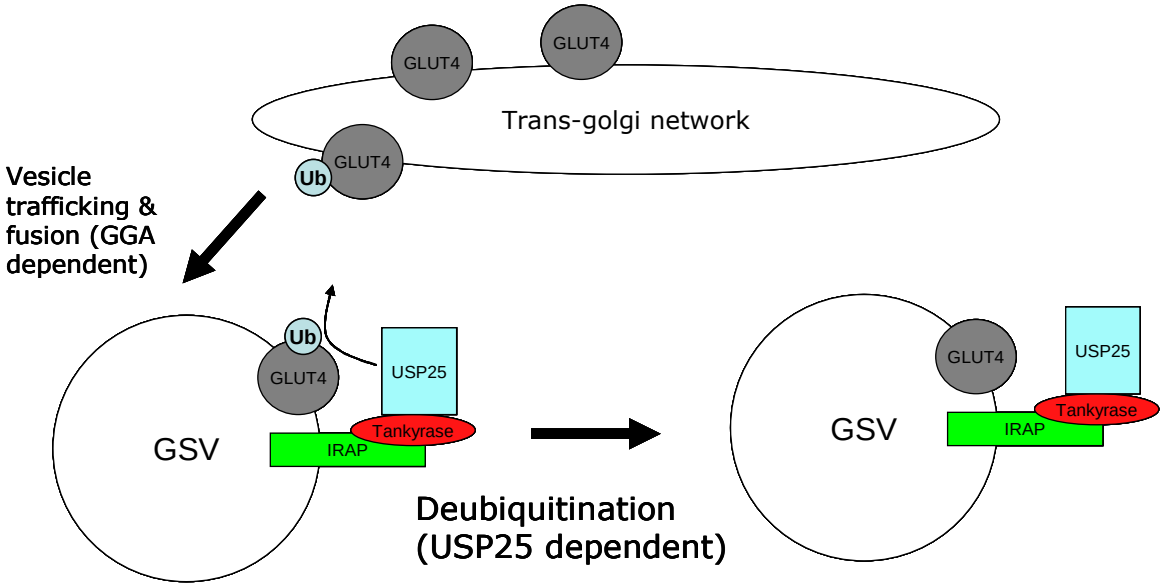

Figure 1.13 A model for ubiquitin dependent GLUT4 loading into GSVs.

1.8 Aims of the project

The aim of this study was to test the hypothesis that ubiquitination of GLUT4 is required for the GGA dependent sorting step from the TGN into GSVs; subsequent GLUT4 deubiquitination by USP25 then stabilises GLUT4 and prevents its trafficking to the lysosome. This hypothesis was tested using *S. cerevisiae* and the insulin responsive 3T3-L1 adipocyte cell line as model systems.

Chapter 2 - Materials & Methods

2.1 Materials.

2.1.1 Reagents, enzymes and media components.

All chemicals were from Sigma-Aldrich (Poole, Dorset, UK), VWR (Poole, Dorset, UK) or Fisher Scientific (Leicester, UK). DNA restriction endonucleases and *Pfu*® polymerase were from Promega (Southampton, UK). T4 DNA ligase was from New England Biolabs (Hitchin, UK). Platinum *Pfx*® polymerase and dNTPs were from Invitrogen (Paisley, UK). Fast Start High Fidelity polymerase was from Roche diagnostics (Burgess Hill, West Sussex, UK). Broad range protein markers were from Biorad (Hertfordshire, UK). Bacterial and yeast media components were from either Melford Laboratories Ltd (Suffolk, UK), Difco laboratories Inc (Appleton Woods Laboratory Equipment and Consumables, Birmingham, UK) or Formedium (Hunstanton, Norfolk, UK). Mammalian cell culture media components were from Invitrogen (Paisley, UK). Mirus TransIT TKO® transfection reagent was from Geneflow Ltd (Fradley, Staffordshire, UK). [^{3}H]2-deoxyglucose solution was from Perkin Elmer (Cambridge, UK).

2.1.2 Bacterial and yeast strains

The bacterial and yeast strains used in this study are listed in Table 2.6 and Table 2.7. Plasmids were maintained and propagated in XL-1 Blue (Stratagene) or TOP10 (Invitrogen) *E. coli*. Recombinant proteins were expressed in BL-21 (DE3) cells (Invitrogen). The parent strain of BHNY1 (YNL297C) was purchased from the Invitrogen Yeast GFP clone collection (Huh *et al.*, 2003).

2.2 Yeast cell culture

Yeast strains were grown non-selectively in YPD (1 %(w/v) yeast extract (Formedium), 2 %(w/v) D-glucose, 2 %(w/v) peptone), and selectively in synthetic dextrose (SD) medium (0.67 % (w/v) yeast nitrogen base without amino acids, 2 % (w/v) glucose supplemented with appropriate amino acids). To give a solid medium, 2 % (w/v) agar was added to the above mixtures prior to autoclaving.

2.2.1 Preparation of yeast competent cells

Transformation competent yeast were prepared according to the lithium acetate method as described by Ito *et al.*, (1983). Routinely a 50 ml culture of the appropriate yeast strain was grown to an OD_{600} of 0.5 to 1. Cells were harvested in a bench top centrifuge for 2 minutes at 640 xg. The cells were resuspended in 10 ml LiTE-Sorb (0.1 M LiOAc, 10 mM Tris-HCl (pH 7.6), 1.2 M sorbitol) and re-pelleted. The cell pellet was resuspended in 1 ml LiTE-Sorb and incubated at 30 °C with shaking for 1 hour. The cell suspension was incubated on ice for at least half an hour, and was subsequently transformed with the desired plasmid or stored at –80 °C with an equal volume of 40 % (v/v) glycerol/0.5 % (w/v) NaCl solution.

2.2.2 Yeast transformation

Approximately 10 ng plasmid DNA and 100 µl 70 % PEG-3350 was added to a 100 µl aliquot of competent cells and mixed by inversion. The mixture was incubated with shaking at 30 °C for 45 minutes, and cells were heat shocked at 42 °C for 20 minutes. Cells were pelleted in a bench top microfuge at approximately 6000 xg for 2 minutes, resuspended in 200 µl sterile H_20 and plated onto selective media. Plates were kept at 30 °C for 2 to 4 days until colonies appeared.

2.2.3 Preparation of yeast cell lysates for SDS-PAGE and immunoblot.

To analyse the protein composition of yeast cells by SDS-PAGE or immunoblot analysis, 5 OD_{600} units of each culture was harvested, resuspended in 50 µl TWIRL buffer (5 % SDS, 8 M urea, 10 % glycerol, 500 µM Tris-HCl pH 6.8, 0.2% bromophenol blue) and heated at 65 °C for 10 minutes. 15 µl (1.5 OD_{600} units) of each sample was resolved by SDS-PAGE and immunoblotted for the desired proteins.

2.2.4 Plasmid rescue from yeast

Cultures were grown to stationary phase in 10 ml of selective media. 5 OD_{600} equivalents of yeast cells were harvested in a microcentrifuge at 669 xg for 2 minutes. The cell pellet was resuspended in 0.5 ml buffer S (100 mM K_2HPO_4 pH7.2, 10 mM EDTA, 50 mM ß-mercaptoethanol, 50 µg/ml yeast lytic enzyme (prepared in 50 mM Tris-HCl pH 7.7, 1 mM EDTA, 50 % (v/v) glycerol) and incubated at 37 °C for 30 minutes. The resulting spheroplasts were lysed by resuspended and briefly vortexed in 100 µl lysis buffer (25 mM Tris HCl pH 7.5, 25 mM EDTA, 2.5% SDS), with subsequent heating at 65 °C for 30 minutes. 166 µl 3 M potassium acetate was added to the mixture followed by a 10 minute incubation on ice and centrifugation for ten minutes at 14 000 xg. The resulting supernatant was transferred to a Promega Wizard® Plus SV miniprep column, and DNA isolated from the supernatant by following the manufacturer's instructions. The purified DNA was transformed into competent XL-1 Blue *E. coli*. A selection of transformants was picked and plasmid identity was verified using DNA sequencing (University of Dundee).

2.2.5 APNE assay.

To screen yeast strains for Pep4p activity the APNE assay was used (Wolf and Fink, 1975).The strains under test were patched onto YPD agar and grown overnight at 30 °C. The next day, 8 ml of reaction mixture (RxM; 0.2 M Tris-HCl pH 7.4, 0.8 mg/ml Fast Garnet GBC salt, 0.2 mg/ml N-acetyl-phenylalanine-ß-naphthyl-ester (APNE)) was overlaid onto the plates with the yeast patches. The RxM was allowed to solidify and colour changes observed over several minutes; red indicated wild type cells, white *pep4* mutants.

2.3 Mammalian cell culture techniques

2.3.1 Cell culture of 3T3-L1 murine fibroblasts and adipocytes

3T3-L1 fibroblasts were cultured in Dulbecco's modified Eagle's medium (DMEM) supplemented with 10 % (v/v) newborn calf serum (NCS). Fibroblasts were maintained as sub-confluent cultures at 37 °C in a 10 % CO_2 humidified incubator. The fibroblasts were grown to confluency and maintained for up to three days before induction of differentiation by addition of DMEM supplemented with 10 % (v/v) foetal calf serum (FCS), 0.25 µM dexamethosone, 0.5 mM 3-isobutyl-1-methylxanthine and 1 µg/ml insulin. After 3 days, the differentiation mixture was replaced with DMEM containing 10 % (v/v) FCS and 1 µg/ml insulin. Adipocytes were re-fed with medium containing 10 % (v/v) FCS at 2 to 3 day intervals and used for experiments between 8 and 12 days post differentiation.

2.3.2 RNA oligonucleotide synthesis

All RNA oligonucleotides used in this study were synthesised by Qiagen (Crawley, West Sussex) and are detailed in Table 2.4.

2.3.3 Transfection of 3T3-L1 adipocytes with siRNA oligonucleotides.

At day 6 and 7 post-differentiation, 3T3-L1 adipocytes were incubated with 50 nM siRNA oligonucleotides (detailed in Table 2.4) complexed with TransIT-TKO® transfection reagent (Mirus, Madison, WI) using an adapted version of the manufacturer's protocol. For a 24 well plate, 6 µl TransIT-TKO® reagent and 1.25 µl of 20 mM stock siRNA solution was combined in 100 µl of serum-free DMEM. After 20 minutes, this mixture was added drop wise to a single well of a 24 well plate. This process was scaled up for larger culture dishes. The siRNA treated adipocytes were then used for experiments on day 8 post differentiation.

2.3.4 Retroviral infection of 3T3-L1 fibroblasts

Fibroblasts were seeded to give approximately 40 % confluency. The next day, 2ml of viral supernatant (produced as in 1.3.6) was combined with 2ml DMEM + 10 % FCS, and 10 µg/ml polybrene. This mixture was used to replace the fibroblast growth medium, and the cells were left to grow for 12 hours at 37 °C. Cells were subsequently maintained in DMEM + 10 % FBS with 2.5 µg/ml puromycin which selected for cells harbouring retrovirus. On confluency the cells were differentiated as in 1.3.1 without drug selection, and then maintained in DMEM + 10% FBS with 2.5 mg/ml puromycin until required for experiments.

2.3.5 Cell culture of Plat-E cells

Plat-E cells were cultured in DMEM supplemented with 10 % (v/v) FCS, 1 µg/ml puromycin and 10 µg/ml blasticidine. Cells were maintained as subconfluent cultures at 37 °C in a humidified 5 % CO_2 incubator.

2.3.6 Preparation of retrovirus using Plat-E cells.

Cells were seeded at a density of 5 x 10^6 cells per 10 cm dish, with one dish per virus being produced, in DMEM + 10 % FCS. On the following day, the cells were transfected with the appropriate retroviral constructs using Lipofectamine™ 2000 reagent. Following transfection, the cells were maintained in DMEM + 10 % FBS for 48 hours at 37 °C, and subsequently switched to 32 °C overnight to induce virus particle production. The viral supernatant was harvested from the plates, clarified by a 5 minute centrifugation at 500 xg and stored at -80 °C until required.

2.4 DNA manipulation

Standard DNA manipulation procedures were used throughout the study (Sambrook *et al.*, 1989).

2.4.1 Plasmid DNA purification

Promega Wizard® Plus SV miniprep kits were routinely used to isolate DNA from small bacterial cultures (< 10 ml). For larger preparations (> 50 ml) Qiagen® Plasmid Maxi kits were used.

2.4.2 DNA oligonucleotide synthesis

DNA oligonucleotides were synthesised by Yorkshire Biosciences Ltd (Heslington, York, UK) or VHbio Ltd (Gateshead, UK) and diluted in sterile double distilled water to a final concentration of 50 pmol/µl before use.

2.4.3 Polymerase Chain Reaction

The high fidelity Platinum *Pfx*® polymerase (Invitrogen) was routinely used to PCR amplify desired DNA sequences.

A typical PCR mixture consisted of:

10 mM dNTPs	5 µl
50 mM $MgSO_4$	3 µl
10x *Pfx* buffer	5 µl
Enhancer solution	5 µl
ddH_20	28 µl
Forward primer (50 pmol/µl stock)	1 µl
Reverse primer (50 pmol/µl stock)	1 µl
Plasmid DNA	1 µl
Pfx DNA polymerase	1 µl

And the conditions normally used were:

1. 95 °C	1 minute
2. 94 °C	90 seconds
3. 56 °C	1 minute

4. 68 °C	1 minute/kb
5. 68 °C	10 minutes
6. 4 °C	Final hold

Steps 2 to 4 were repeated 30 times during the course of the PCR.

For amplification of larger templates and GC rich sequences the FastStart High Fidelity PCR system (Roche) was used. The mixture in this case consisted of:

10 mM dNTPs	1 µl
10x Reaction buffer	5 µl
DMSO	1-5 µl (2-10 %)
Forward primer (50 pmol/µl stock)	4 µl
Reverse primer (50 pmol/µl stock)	4 µl
Template DNA	1 µl
2.5 U FastStart High Fidelity enzyme	0.5 µl
ddH_20	to 50 µl

For templates of less than 3 kb, a reaction profile essentially the same as that for *Pfx* was utilised. For longer templates the following was used:

1. 94 °C	2 minutes
2. 94 °C	30 seconds
3. 52 °C	30 seconds
4. 68 °C	1 minute/kb
5. 94 °C	30 seconds
6. 52 °C	30 seconds
7. 68 °C	1 min/kb (+ additional 20 seconds per cycle number)
8. 68 °C	7 minutes
9. 4 °C	Final hold

Steps 2-4 were repeated ten times during the course of the reaction, followed by 25 cycles of steps 5-7.

Electrophoresis was used to resolve DNA fragments generated by PCR through 0.8 % (w/v) agarose in tris-acetate (TAE) buffer (40 mM Tris-acetate, 1 mM EDTA). DNA fragments were extracted from agarose gels using the QIAquick® gel extraction kit (Qiagen).

2.4.4 Site Directed Mutagenesis.

Site directed mutagenesis (SDM) of DNA sequences was performed using *Pfu*® polymerase (Promega) according to the Stratagene QuikChange® method. Synthetic oligonucleotides, detailed in Table 2.5, were used to exchange one amino acid residue for another with the mutagenic codon at the approximate centre of the oligonucleotide. A typical recipe for a SDM reaction was as follows:

Purified template plasmid	50 ng
Forward primer	125 ng
Reverse primer	125 ng
10x *Pfu* buffer	5 µl
10 mM dNTPs	1 µl
Pfu polymerase	1 µl
ddH20	to 50 µl

Typical reaction conditions for SDM were:

1. 95 °C	1 minute
2. 95 °C	50 seconds
3. 60 °C	50 seconds
4. 68 °C	16 minutes
5. 68 °C	7 minutes
6. 4 °C	Final hold

Steps 2 to 4 were repeated 18 times during the course of the reaction.

On completion of the reaction, the mixture was treated with 1 µl (10 units) *Dpn*I for 1 hour at 37 °C, to digest methylated template plasmid. 5 µl of the resultant mixture was transformed into competent XL-1 Blue *E. coli*, and transformants selected for on solid 2x YT (1.6 % tryptone, 1 % yeast extract, 0.5 % NaCl) + 2 % agar supplemented with 100 µg/ml ampicillin. Several of the resultant colonies were picked, grown up in 10 ml of 2YT + 100 µg/ml ampicillin and plasmid purified. Mutations were verified by DNA sequencing (Sequencing service, University of Dundee).

2.4.5 Plasmid construction

To generate a construct encoding a ubiquitin binding deficient version of the GST-Dsk2p UBA protein to act as a negative control in pull-down experiments, I took advantage of the published crystal structure of Dsk2p in complex with ubiquitin (Ohno *et al.*, 2005), which identified the residues M342 and F344 (numbering relative to the full length protein) as essential for ubiquitin binding. pGEX-*DSK2*$_{UBA}$ (Raasi *et al.*, 2005) was subject to site directed mutagenesis using primer pair 352 and 353 (Table 2.5) to generate pCAL1, encoding GST-Dsk2p UBA M342R F344A (GST-UBA$_{mut}$). This work was carried out in collaboration with Dr. Rebecca McCann.

pHAGLUT4 URA3 (pCAL4) was constructed by amplification of the *HA-GLUT4* open reading frame from pRM55 (constructed by Dr Rebecca McCann) using oligonucleotides 1 and 2 (Table 2.5). This generated a product containing the GLUT4 ORF, with internal HA tag between residues 63 and 64, flanked by sequences homologous to the 3' end of the *CUP1* promoter and the 5' end of the *PHO8 3' UTR*. The product was used to repair a gapped pNB701 (Struthers *et al.*, 2009), which encodes the ORF of RS-ALP (Piper *et al.*, 1997) under the control of the copper responsive *CUP1* promoter (Winge *et al.*, 1985;Mascorro-Gallardo *et al.*, 1996) and the *3'UTR* of *PHO8*.

pGEX-GGA3 VHS-GAT$_{mut}$ (pCAL6) was constructed by site directed mutagenesis of pGEX-GGA3 VHS-GAT (a gift from Juan Bonifacino, (Dell'Angelica *et al*, 2000)). This was achieved by sequential site directed mutagenesis using primer pairs 457/458 (E250N mutation) and 459/460 (D284G mutation), sequences detailed in Table 2.5.

pCAL10 was constructed by amplification of the GGA3 short isoform mRNA from the IMAGE clone 4814878 in pBluescriptR (a gift from Professor Margaret S. Robinson) using oligos 489 and 511 (Table 2.5) to introduce a 5' myc tag and *EcoR*I site, and a 3' *Sal*1 site. This approximately 2 kb fragment was subcloned into pCR2.1. The myc-GGA3 fragment was excised from pCAL10 using *EcoR*I and *Sal*I and ligated into simultaneously digested pBABE puro (Morgenstern and Land, 1990),a gift from Professor David James, to generate pCAL11. Mutation of the myc-GGA3 GAT domain was carried out in an identical fashion to that for pGEX-GGA3 VHS-GAT, generating pCAL12.

pCAL13 was constructed by site directed mutagenesis of pGEX-USP25 (Meulmeester *et al.*, 2008) using primer pair 559 and 560 to mutate the arginine at position 1049 within the putative tankyrase binding motif of USP25 (Sbodio and Chi, 2002) to alanine.

2.5 Protein methods

2.5.1 Elecrophoretic separation of proteins

The separation of proteins by electrophoresis was carried out with discontinuous polyacrylamide gels (SDS-PAGE) following the basic method outlined by Laemmli (1970). Proteins were separated on gels composed of a stacking layer (5 % (v/v) acrylamide in stacking buffer (0.25 M Tris-HCl (pH 6.8), 0.2 % (w/v) SDS) and a separating layer (normally 10% acrylamide in separating buffer; 0.75 M Tris-HCl (pH 8.8), 0.2 % (w/v) SDS). A 30 % (v/v) acrylamide-bisacrylamide mixture (37.5:1 ratio, Severn Biotech Ltd, Worcestershire) was used to make the gels. The tris-glycine electrophoresis buffer used contained 25 mM Tris-HCl, 250 mM glycine, 0.1 % (w/v) SDS). Resolved proteins were visualised on gels by agitating the gels in Coomassie Brilliant Blue solution (0.25 g Coomassie Brilliant Blue R250 in methanol: H_20: glacial acetic acid (4.5:4.5:1 v/v/v)) for 30 minutes, followed by overnight agitation in destain solution (5 % (v/v) methanol, 10 % (v/v) glacial acetic acid) to give clearly visible bands.

2.5.2 Transfer of proteins to nitrocellulose membranes

A Bio-Rad Trans-Blot® SD cell was used to transfer proteins from polyacrylamide gels onto nitrocellulose membranes (Protran, 0.45 µm pore). Gels and membranes were sandwiched between 6 pieces of Whatman 3M filter paper soaked in semi dry transfer buffer (50 mM Tris-HCl, 40 mM glycine, .037% (w/v) SDS, 10% methanol. The assembly was subject to a constant 180 mA current for between 35 minutes (one gel) to one hour (three gels).

2.5.3 Immunoblot analysis

After protein transfer, unfilled sites on the nitrocellulose membrane were blocked using 5 % (w/v) non-fat dried milk in PBST (0.1 % (v/v) Tween-20 in PBS) or TBST (0.1 % (v/v) Tween-20 in TBST (0.1 % (v/v) Tween-20 in Tris-HCl buffered saline (TBS – 0.5 M NaCl, 10 mM Tris-HCl pH 7.6) according to the conditions required for each primary antibody. The membranes were exposed to primary antibody for 2 hours at room temperature or at 4 °C overnight with agitation. Primary antibodies were diluted as described in Table 2.1 in 1 % (w/v) non-fat dried milk in PBST/TBST, except anti-FAS which was diluted in 5 % (w/v) non-fat dried milk in PBST.

The membrane was subsequently washed six times with PBST/TBST for five minutes each. The membranes were exposed to secondary antibody at the concentrations described in Table 2.2 in 5 % (w/v) non-fat dried milk in PBST/TBST for between 1 and 2 hours at room temperature, with agitation. A further six 5-minute washes in PBST/TBST were carried out and protein bands visualized using enhanced chemiluminescence (ECL).

2.5.4 Antibodies

Primary and secondary antibodies used in the study are detailed in Table 2.1 and Table 2.2 respectively. Polyclonal antisera against USP25 was generated by Eurogentec (Liege, Belgium) using an 87 day protocol. Briefly, two New Zealand white rabbits were immunised with 100 µg recombinant USP25 (generated as in 2.5.6) at days 0, 14, 28 and 56 of the protocol. Serum was collected from the

rabbits before the first immunisation (pre immune), and on days 38, 66 and 87 subsequently. The sera were stored at -80 °C until use.

2.5.5 Quantification of immunoblots.

Immunoblots were scanned using Photoshop® (Adobe) and immunoreactive bands measured using ImageJ software (National institutes of Health, USA). The integrated density of each band was measured and a background reading for an equally sized area of the image subtracted to give a numeric value for the band intensity.

2.5.6 GST fusion protein preparation

For pGEX-*DSK2*$_{UBA}$ and pGEX-*GGA3 VHS-GAT* based constructs, 10 ml of 2YT + 100 µg/ml ampicillin was inoculated with *E. coli* BL-21 (DE-3) cells harbouring a plasmid encoding the appropriate GST fusion protein and incubated at 37 °C overnight with shaking. The 10ml culture was inoculated into 400 ml Terrific Broth (1.2 % (w/v) tryptone, 2.4 % (w/v) yeast extract, 0.4 % (w/v) glycerol, 0.05 M K_2HPO_4, 0.016 M KH_2PO_4) and grown until OD_{600} = 0.6. Protein expression was induced with 1mM IPTG and the cells were incubated for a further 4 hours at 37 °C with shaking. The cells were harvested by centrifugation and resuspended in 19.5 ml phosphate buffered saline (PBS; 140 mM NaCl, 3 mM KCl, 1.5 mM KH2PO4, 8 mM Na_2HPO_4). The cells were treated with lysozyme (1 mg/ml) on ice for 30 minutes and subsequently sonicated for five 30 second bursts with 30 second iced pauses. The lysate was spun at 17640 xg at 4 °C to remove insoluble components. The lysate was incubated with 1ml of a 50 % glutathione-Sepharose bead slurry with rotation for 1 hour. The beads were washed three times with cold PBS to remove non-specifically bound proteins, and stored at 4 °C in PBS supplemented with EDTA free protease inhibitor cocktail (Roche) (containing leupeptin, α2 macroglobulin, pefabloc SC, pepstatin, PMSF, chymostatin, E-64, bestatin, trypsin inhibitor) at a bead:buffer ratio of 1:1.

For pGEX-*USP25* and derivatives a similar protocol was used with several modifications. Proteins were purified from 2 litres of culture rather than 400 ml, and cells were lysed using a Microfluidizer M-110P cell disruptor set at

10,000 psi. After binding of the fusion protein to the beads, they were washed three times with PBS + 1 % (v/v) Triton-X, three times with PBS + 0.5M NaCl and three times with PBS alone. Thrombin cleavage of GST-USP25, releasing USP25 from the beads, was performed by incubating the beads in thrombin cleavage buffer (50 mM Tris-HCl pH 8.0, 150 mM NaCl, 2.5 mM $CaCl_2$) containing 0.04 units of thrombin per µl sample with rotation at room temperature for 2 hours.

2.5.7 GST fusion protein concentration estimation

20 µl of a 50 % (v/v) glutathione Sepharose bead suspension was pipetted into a microfuge tube, spun at 500 xg for 1 minute and the supernatant removed. GST fusion protein was eluted from the beads by adding 400 µl 2 × LSB (4 % (w/v) SDS, 100 mM Tris-HCl pH6.8, 20 % (v/v) glycerol, 0.04 % (w/v) bromopbenol blue, 10 % (v/v) ß-mercaptoethanol), (i.e. a 1 in 40 dilution of the beads) and heating at 37 °C for 30 minutes. 20 µl of sample was run on a 10% SDS-PAGE gel with standard amounts of BSA (0.4, 1, 2 and 3 µg). After staining with Coomassie and subsequent destaining, protein concentration on the beads could be estimated visually.

2.6 GST fusion protein pull-down with yeast lysate

400 ml cultures of the appropriate yeast transformants (expressing wt HA-GLUT4) were grown to mid log phase – approximately 0.5 OD_{600} of cells/ml of culture. Cells were collected by centrifugation and the pellets resuspended in 40 ml YPD-Sorb (1.2 M sorbitol, 0.5 % yeast nitrogen base (Formedium), 1% D-glucose, 1% peptone). Cells were converted to spheroplasts by treatment with 120 µl ß mercaptoethanol and 400 µl 50 mg/ml yeast lytic enzyme in yeast lytic enzyme buffer (50 mM Tris pH 7.7, 1 mM EDTA, 50% glycerol) and incubation for 1 hour at 30 °C. Spheroplasts were collected by centrifugation for 5 minutes at 1000 xg. The spheroplasts were resuspended in 250 µl lysis buffer (200 mM sorbitol, 100 mM KOAc, 1% Triton-X, 50 mM KCl, 20 mM PIPES pH 6.8, 1 mM N-ethyl maleimide (NEM)) supplemented with EDTA free protease inhibitor cocktail (Roche) and agitated for one hour to lyse spheroplasts.

Samples were subsequently centrifuged at 14000 xg for 15 minutes at 4°C to pellet insoluble material. Lysates were equalized for protein concentration by the BCA assay (Thermo Fisher Scientific, Cramlington) if required to approximately 10 mg/ml. Approximately 200 µl of the diluted lysate was added to 20 µg of glutathione-Sepharose beads with appropriate GST fusion proteins bound. The beads were incubated with the fusion proteins with gentle agitation for 2 hours at 4 °C. The beads were washed three times with lysis buffer, drained and bound proteins eluted in 40 µl 2x LSB for 15 minutes at 65 °C. 20 µl of each sample was run out on a 10% SDS-PAGE gel alongside 2.5% of input lysate for each yeast transformant, followed by immunoblotting with antibodies against specific proteins.

2.7 GST fusion protein pull-down with 3T3-L1 adipocyte lysate.

Adipocytes were starved of serum using serum-free DMEM for at least two hours prior to starting the procedure. Two 10 cm plates were used per reaction condition. Following treatment cells were kept on ice and washed three times with ice cold PBS. Cells were scraped in 250 µl lysis buffer (50 mM Sodium HEPES, 150 mM NaCl, 5 mM EDTA, 1 mM NEM, 1 % Triton X-100, EDTA free protease inhibitor cocktail (Roche)) and homogenised using a syringe and needle (10 x 25 G, 2 x 26 G). The homogenates were clarified by a 10 minute centrifugation at 500 xg and 4 °C. The clarified homogenate was agitated at 4 °C for a further hour to disrupt membranes, then centrifuged at 14 000 xg and 4 °C for 15 minutes to pellet insoluble material. If required, protein concentrations were equalized by using the Bradford assay. An aliquot of lysate was retained and mixed with 2 X LSB (whole cell lysate). The remaining lysate was divided between the appropriate immobilized GST fusion proteins, with approximately 200 µl lysate per 20 µl bead suspension. The bead/lysate mix was mixed gently at 4 °C for 2 hours to allow binding of proteins. The beads were washed three times with lysis buffer and bound proteins eluted by addition of 2 x LSB with 10% beta-mercaptoethanol.

2.8 Indirect immunofluorescence with 3T3-L1 adipocytes.

Cells were grown on sterilised coverslips in a 24 well plate. Cells were starved of serum using serum-free DMEM for two hours prior to starting the procedure, and insulin stimulated (100 nM insulin for 15 minutes, 37 °C). For surface epitope staining, cells were washed twice with PBS then cross-linked with 200 µl 3 % (v/v) paraformaldehyde (PFA) for 30 minutes, washed twice with PBS then washed twice with 20 mM glycine (GLY) in PBS to quench free aldehyde groups. The coverslips were then incubated with 200 µl blocking solution (2 % (w/v) BSA/20 mM glycine in PBS (BSA/GLY)) for 20 minutes. To incubate the cells with the primary antibody, the coverslips were placed cell side down onto a 40 µl drop of primary antibody preparation (dissolved in BSA-GLY) on parafilm for 45 minutes, then washed four times with BSA/GLY. Fluorophore conjugated secondary antibody in BSA/GLY was applied to the cells in a similar manner for 30 minutes, then washed as previously. The cells were returned to a 24 well plate, washed twice with PBS and surface bound antibodies fixed using 3 % (v/v) PFA for 30 minutes. The coverslips were washed twice with PBS and the PFA quenched with GLY as previously. The cells were blocked and permeablised using 200 µl 20 mM glycine, 2 % (w/v) BSA and 0.1 % (w/v) saponin in PBS (BSA/GLY/SAP) for twenty minutes. The coverslips were incubated with primary antibody preparation in BSA/GLY/SAP for 45 minutes, washed in BSA/GLY/SAP, incubated with secondary antibody for 30 minutes and given four further BSA/GLY/SAP washes. The coverslips were washed finally in PBS, dried and mounted onto slides using Immumount (Thermo). The mounted coverslips were analysed using a 63 x oil immersion objective lens fitted to a Zeiss LSM Pascal Exciter confocal fluorescence microscope, and images overlaid using LSM software (Zeiss).

2.9 [^{3}H]2-Deoxyglucose uptake assays

For these experiments cells were grown in 12 well plates. After differentiation (as in 2.3.1) cells were serum starved for at least two hours. Each twelve well plate was maintained at 37 °C and washed four times with Krebs Ringer Phosphate (KRP; 128 mM NaCl, 4.7 mM KCl, 5 mM NaH_2PO_4, 1.25 mM $MgSO_4$, 1.25

mM $CaCl_2$, pH7.4). The wells of each plate were treated as follows for 30 minutes at 37 °C:

- 3 wells 475 µl KRP (Basal)
- 3 wells 475 µl KRP + 1 µM insulin (Insulin)
- 3 wells 475 µl KRP + 5 µM cytochalasin B (Basal CytoB)
- 3 wells 475 µl KRP + 1 µM insulin + 5 µM cytochalasin B (Insulin CytoB)

After the 30 minute incubation, 25 µl of [^{3}H]2-deoxyglucose solution in KRP was added to the wells such that the final deoxyglucose concentration was 50 µM with 0.25 µCi per well. Transport was allowed to proceed for 5 minutes after which time the contents of the wells was removed and the plates washed three times by immersion in ice cold PBS. Cells were air dried for 1 hour at room temperature and solubilised in 1 ml 1 % Triton X-100 for 2 hours. Solubilised cells were transferred into scintillation vials containing 5 ml scintillation fluid, and radioactivity associated with the cells measured using liquid scintillation spectrophotometry. When results of these experiments are expressed as fold change of glucose uptake from basal cells, the calculation is:

Fold change = (Insulin – Insulin CytoB)/(Basal – Basal CytoB)

2.10 Isolation of low density microsomes from 3T3-L1 adipocytes.

2 x 10 cm^2 plates of confluent adipocytes were washed twice with cold PBS and once with HES buffer (20 mM HEPES, 225 mM sucrose, 1 mM EDTA, pH 7.4) plus protease inhibitors (Roche) (HES+I). The cells were subsequently scraped on ice in 1 ml HES+I and homogenised using a syringe and needle. All further centrifugation steps were carried out at 4 °C. The homogenate was centrifuged at 500 xg for ten minutes in a chilled microcentrifuge (Beckman Coulter). The supernatant was removed and centrifuged in a TLA-100 rotor at 5113 xg for twelve minutes to remove the plasma membrane, mitochondria and nuclei. The supernatant was again centrifuged at 8795 xg for seventeen minutes to remove high density microsomes (HDM). The final step involved centrifugation of the supernatant at 88760 xg for 75 minutes. The resulting supernatant was removed

and the pellet resuspended in 0.4 ml HES+I to give the low density microsome fraction (LDM).

2.11 Iodixanol gradient analysis of LDMs from 3T3-L1 adipocytes.

LDMs were isolated as in 2.10 from 2 x 10cm² plates of adipocytes expressing HA-GLUT4. This fraction was resuspended in iodixanol and HES+I to a final iodixanol concentration of 14 % (v/v). The resulting mixture was transferred to Quickseal® polyallomer tubes (Beckman Coulter), sealed within the tubes and briefly vortexed to mix the sample. The samples were transferred to a near vertical rotor (TLN-100) (Beckman-Coulter) and centrifuged at 295,000 xg at 4 °C for 1 hour. Fractions of approximately 300 µl were collected from the bottom of the gradient. 150 µl of each fraction was removed and mixed with 4 x Laemmli's sample buffer (200mM Tris-HCl, 8 % (w/)v SDS, 0.4 % (w/v) bromophenol blue, 40 % (v/v) glycerol, 10 % (v/v) ß-mercaptoethanol) and heated at 65 °C for ten minutes. The fractions were subjected to SDS-PAGE on 10 % (v/v) gels to allow detection of HA-GLUT4 by immunoblot analysis using the HA-11 antibody (Covance).

2.12 Enrichment of GSVs using subcellular fractionation

To produce a cellular fraction enriched in GLUT4 GSVs from differentiated 3T3-L1 adipocytes a method similar to that published by Li *et al*. (2005) was used. Briefly, 2 10 cm plates per condition under test were scraped in 500 µl PBS, homogenised using 12 strokes of a syringe and needle (10 x 25 G, 2 x 26 G) and centrifuged at 500 xg and 4 °C for 10 minutes to pellet insoluble material. The supernatant of this step was subjected to further centrifugation at 16 000 xg for 20 minutes. The pellets and supernatants from this step were collected and PBS added to both to equalise protein concentrations to approximately 2 mg/ml. In the case of the HA-GLUT4 constructs, approximately 20 µg of supernatant and 5 µg pellet fractions were routinely run on the gels (due to the higher concentrations of HA-GLUT4 in the pellet fraction).

Antigen	Working dilution	Description	Reference/ Source
A. v. GFP	1:1000 (IB)	Mouse monoclonal antibody (JL-8) raised against *Aequorea victoria* Green Fluorescent Protein (GFP).	Living colors®
FAS	1:200 (IB)	Mouse monoclonal antibody against residues 9-202 of human fatty acid synthase.	BD biosciences.
GAPDH	1:30,000 (IB)	Mouse monoclonal antibody (clone 6C5) against GAPDH.	Ambion®
GLUT4	1:1000 (IB)	Rabbit polyclonal antibody against C-terminal 14 amino acids of GLUT4.	(Brant *et al.*, 1992)
GLUT4	1:1000 (IB)	Rabbit polyclonal antibody against C-terminal 14 amino acids of GLUT4.	Synaptic Systems.
HA	1:1000 (IB) 1:200 (IF)	Mouse monoclonal antibody (clone 16B12) against an epitope from the human influenza haemagglutinin protein (YPYDVPDYA).	Covance Research products
IRAP	1:2000 (IB)	Mouse monoclonal antibody against IRAP	Gift from Professor Paul Pilch
IRS-1	1:1000 (IB)	Rabbit polyclonal antibody raised against the C-terminal 14 amino acids of rat liver IRS-1 (YASINFQKQPEDRQ)	Upstate (New York)
Myc	1:1000 (IB) 1:500 (IF)	Rabbit polyclonal antibody raised against the myc epitope (EQKLISEEDL) conjugated to KLH.	Abcam
Stx-4	1:3000 (IB)	Rabbit polyclonal antiserum raised against the cytosolic domain of rat syntaxin-4	Synaptic Systems
Tankyrase 1/2	1:300 (IB)	Rabbit polyclonal IgG raised against amino acids 745-1094 of Tankyrase -1 of human origin	Santa Cruz biotechnology (California)
Ubiquitin	1:1000 (IB)	Mouse monoclonal antibody (clone P4D1) raised against denatured bovine ubiquitin.	Covance Research products
USP25	1:4000 (IB)	Rabbit polyclonal antibody raised against GST-USP25	(Bosch-Comas *et al.*, 2006)
Vti1p	1:30,000 (IB)	Rabbit polyclonal antibody raised against Vti1p	Generated by Eurogentec.

Table 2.1 Primary antibodies used in this study.

IB = immunoblotting, IF = Immunofluorescence.

	Working dilution	Description	Reference/ Source
Anti Rabbit-HRP	1:5000 (IB)	HRP conjugated whole IgG from donkey.	GE Healthcare
Anti Mouse-HRP	1:2000 (IB)	HRP conjugated whole IgG from sheep.	GE Healthcare
Anti Mouse–Cy3	1:200 (IF)	Cy3 conjugated anti-mouse IgG from goat.	Jackson Immunoresearch (Stratech)
Anti Mouse-DyLight488	1:200 (IF)	DyLight488 conjugated anti-mouse IgG from goat.	Jackson Immunoresearch (Stratech)
Anti Rabbit-AlexaFluor 488	1:400 (IF)	AlexaFluor 488 conjugated anti-rabbit IgG, from goat.	Living Colours (Invitrogen)

Table 2.2 Secondary antibodies used in this study.

IB = immunoblotting, IF = immunofluorescence

Number	Plasmid	Description	Reference
1	pPLO2010	*pep4-ΔH3* allele in pRS306. Constructed by first subcloning a 4.6kb *Sac*I-*Sal*I fragment containing the *PEP4* gene into pRS306, then removing the 1.3-kbp *Hin*dIII fragment contained within the *Sac*I-*Sal*I insert, generating the *ΔH3* allele.	(Nothwehr *et al.*, 1995)
13	pNB701	Yeast expression plasmid (CEN, URA3) encoding Pho8p from the *CUP1* promoter	(Struthers *et al.*, 2009)
169	pBABE puro	Retroviral expression vector, AmpR, puro	(Morgenstern and Land, 1990) gift from Professor David James
321	pRM4	Retroviral expression vector encoding HA-tagged GLUT4 7K/R	Constructed by Dr R. McCann
358	pHA-GLUT4	Retroviral expression vector encoding HA-tagged GLUT4	(Shewan *et al.*, 2000)
359	pGEX-$DSK2_{UBA}$	*E. coli* expression vector encoding the UBA domain of *S. cerevisiae* Dsk2p (residues 328-373) fused to the C-terminus of GST	(Funakoshi *et al.*, 2002)
390	pCAL1	As pGEX-$DSK2_{UBA}$ but with two point mutations M342R and F344A in the UBA domain.	This study.
399	pGEX GGA3 VHS-GAT	*E. coli* expression vector encoding the VHS-GAT domain of hGGA3 (residues 1-146) fused to the C-terminus of GST	(Mattera *et al.*, 2004)
476	pCAL4	*S. cerevisiae* expression vector (*CEN, URA3*) encoding GLUT4 with an exofacial HA tag between residues 67 and 68, based on pNB701	This study
482	pRM35	Retroviral expression vector encoding HA-tagged GLUT4 6K/R (K109)	Constructed by Dr R. McCann
483	pRM36	Retroviral expression vector encoding HA-tagged GLUT4 6K/R (K495)	Constructed by Dr R. McCann
487	pGEX6P-1	*E. coli* expression vector with N-Terminal GST tag.	GE Healthcare
492	pCAL6	As pGEX GGA3 VHS-GAT with two point mutations in GAT domain (E250N D284G)	This study
498	pGEX USP25	*E. coli* expression vector encoding USP25 with an N terminal GST tag	(Meulmeester *et al.*, 2008)
515	pRM55	Retroviral expression vector encoding HA-tagged GLUT4. Constructed by excision of a *Psh*AI-*Bgl*II fragment	Constructed by Dr R. McCann

		from pHA-GLUT4 and ligating this fragment into *Psh*AI-*Bgl*II cut pRM36	
521	pCAL11	Retroviral expression vector encoding N terminally tagged myc-GGA3 short isoform.	This study
553	pCAL12	Retroviral expression vector encoding N terminally tagged myc-GGA3 short isoform with mutations in the GAT domain (E250N, D284G)	This study
597	pCAL13	Identical to pGEX-USP25 with a mutation in the putative tankyrase binding motif (R1049A)	This study

Table 2.3 Plasmids used in this study

Name	Target sequence	Description
Scrambled	GACGAACAAACCGCCACATAT	Scrambled control siRNA
30825	CCTGCTGGTTTAGTGCAGTTA	Targeted against USP25; sequence provided by Dr Nai-Wen Chi (UCSD)
30827	CCCAACGATCACTGCAAGAAA	As above

Table 2.4 siRNA target sequences used in this study

Number	Sequence (5′-3′)	Description
1	GATATTAAGAAAAACAAACTGTACAATCAAT CAATCAATCATCACATAAAATGCCGTCGGGC TTCCAACAGATA	*CUP1*hGLUT4
2	ATTATAACGTATTAAATAATATGTGAAAAAAG AGGGAGAGTTAGATAGGGATCAGTCGTTCTC ATCTGGCCCTAA	*3′UTR*hGLUT4
352	GACAACTAAACGACAGGGGCGCCTTCGATTT CGATAGAA	Mutation of residues 342 and 344 of Dsk2p UBA domain from methionine to arginine and phenylalanine to alanine respectively (mutagenic codons underlined)
353	GTTTCTATCGAAATCGAAGGCGCCCCTGTCG TTTATTGGTC	Reverse complement of 352
489	GTGGTCGACTCATAGGTTCCCCCACTGTTCC	*Sal*I GGA33′
511	TGAATTCATGGAACAAAAACTTATTTCTGAAG AAGATCTGGCGGAGGCGGAAGGGGAAACG	*Eco*RI myc GGA3 5′.
520	TCTTCCATCCGCGCCGTCTCTC	pBABE sequencing primer.
559	CATGTTGTCCCTCAGTGCAACTCCTGCTGAT GG	Mutation of residue 1049 of human USP25 from arginine to alanine (forward primer, mutagenic codons underlined)
560	CCATCAGCAGGAGTTGCACTGAGGGACAAC ATG	Reverse complement of 559
565	GACAGAGAGCTGATGAAGAACCTGTTTGATC AGTGTGAGAAC	Mutation of residue 250 of GGA3 GAT domain from glutamic acid to asparagine (forward primer, mutagenic codon underlined)
566	GTTCTCACACTGATCAAACAGGTTCTTCTTCA TCAGCTCTCTGTC	Reverse complement of 457
567	CTGCAAGCCAGTGGGAACCTCTCCCGGGTC	Mutation of residue 284 of GGA3 GAT domain from aspartic acid to glycine (forward primer, mutagenic codon underlined)
568	GACCCGGGAGAGGTTCCCACTGGCTTGCAG	Reverse complement of 459

Table 2.5 DNA oligonucleotides used in this study

Name	Genotype	Source
BL-21(DE3)	F^- *omp*T *hsd*S_B(r_B^-, m_B^-) *gal dcm* (DE3)	Invitrogen
TOP10	F^- *mcr*A (*mrr-hsd*RMS-*mcr*BC) 80*lac*ZM15 *lac*X74 *rec*A1 *ara*139 (*ara-leu*)7697 *gal*U *gal*K *rps*L (Str^R) *end*A1 *nup*G	Invitrogen
XL-1 Blue	*recA1 endA1 gyrA96 thi-1 hsdR17 supE44 relA1 lac* [F′ *proAB lacI*^{q}*ZΔM15* Tn*10* (Tet^r)]	Stratagene

Table 2.6 *E. coli* strains used in this study.

Name	Genotype	Source
SF838-9Dα	*MATα leu2-3, 112 ura3-52 his4-519 ade6 gal2 pep4-3*	(Rothman *et al.*, 1989)
YNL297C	*MATa his3Δ::pFA6aMON2-GFP leu2Δ0 met15Δ0 ura3Δ0*	Invitrogen, (Huh *et al.*, 2003)
BHNY1	*MATa his3Δ::pFA6aMON2-GFP leu2Δ0 met15Δ0 ura3Δ0 pep4-3*	This study

Table 2.7 *S. cerevisiae* strains used in this study.

Chapter 3 - Ubiquitination and insulin responsive trafficking of GLUT4

3.1 Introduction

GLUT4 is a 12-transmembrane domain-containing transporter protein, part of the larger family of GLUTs, which allows passive diffusion of glucose down a concentration gradient (Wood and Trayhurn, 2003). Insulin signalling results in an increase in the number of GLUT4 molecules at the cell surface, thus increasing the rate at which glucose enters the cell (Birnbaum, 1989;James *et al.*, 1989). This activity is responsible for the insulin-induced clearance of glucose from the bloodstream after a meal. In the absence of insulin, GLUT4 is retained intracellularly, continually cycling through compartments of the TGN/endosomal system including GLUT4 storage vesicles or GSVs (Bryant *et al.*, 2002). GSVs are defined as the compartment(s) from where GLUT4 is mobilised to the cell surface in response to insulin (discussed in more detail in sections 1.4.3 and 1.4.4). Although GSVs remain somewhat poorly defined, they are known to contain many proteins other than GLUT4. Notable amongst these are the insulin responsive aminopeptidase IRAP (Ross *et al.*, 1996;Ross *et al.*, 1997), the sorting receptor sortilin (Lin *et al.*, 1997;Morris *et al.*, 1998) and the SNARE protein VAMP2 (Cain *et al.*, 1992;Martin *et al.*, 1996).

The trafficking itinerary of GLUT4 bears some similarities to that of the yeast amino acid permease Gap1p (Roberg *et al.*, 1997;Bryant *et al.*, 2002) as discussed in section (1.5.2). When yeast cells are grown on optimal nitrogen sources such as glutamate, the transporter is delivered to the endosomal system. On less favourable nitrogen sources such as proline, the channel is directed to the plasma membrane to allow uptake of amino acids (Roberg *et al.*, 1997;Soetens *et al.*, 2001;Risinger and Kaiser, 2008).

The nitrogen-regulated trafficking of Gap1p is controlled by ubiquitination of the transporter by the ubiquitin ligase Rsp5p (Helliwell *et al.*, 2001), and subsequent Gap1p-Ub interaction with the coat proteins Gga1p/Gga2p (Scott *et al.*, 2004;Bilodeau *et al.*, 2004). Work in our laboratory has built upon the parallels between the regulated trafficking of Gap1p and GLUT4 to form the hypothesis that ubiquitination of GLUT4 plays a role in its trafficking in insulin-sensitive cells. A previous PhD student in the lab expressed human GLUT4 in yeast and found that it could only be detected by immunoblot analysis in cells lacking active vacuolar proteases, suggesting that it is trafficked to the proteolytically active endosomal system (McCann R.K., 2007). Indirect immunofluorescence

found that GLUT4 expressed in yeast displays a punctate staining pattern reminiscent of that reported for Gap1p (McCann R.K., 2007). This staining colocalises with the TGN marker Kex2p (McCann R.K., 2007). Proteins localise to the yeast TGN by continually cycling through a prevacuolar/endosomal compartment (Bryant and Stevens, 1997), an exaggerated form of which accumulates in the class E *vps* mutants (Raymond *et al.*, 1992). Consistent with its TGN localisation, GLUT4 localises to the class E compartment that accumulates in *vps27Δ* cells (McCann R.K., 2007) Again, this bears similarity to findings reported for Gap1p whose punctate distribution (on rich media) collapses into the class E compartment of *vps4* and *vps27* mutant cells (Rubio-Texeira and Kaiser, 2006).

The endosomal delivery of Gap1p on rich media is regulated by ubiquitination of the transporter (Soetens *et al.*, 2001). Ubiquitinated Gap1p is recognised by the Gga coat proteins, and trafficked from the TGN into the endosomal system (Scott *et al.*, 2004).

Immunoblot analysis of GLUT4 immunoprecipitated from yeast reveals that it is ubiquitinated in a lysine-dependent manner (McCann R.K., 2007). Ubiquitination of GLUT4 appears to be both necessary and sufficient for delivery into the proteolytically active endosomal system in yeast since a ubiquitin-resistant version (with all 7 cytosolically disposed lysine residues mutated to arginines) is not degraded by vacuolar proteases in yeast, whereas an in-frame version of ubiquitin to this mutant restores its trafficking (McCann R.K., 2007). In addition, as reported for Gap1p (Scott *et al.*, 2004), the ubiquitin-dependent delivery of GLUT4 to the yeast endsomal system requires the ubiquitin-binding Gga proteins (McCann R.K., 2007) (Figure 3.1).

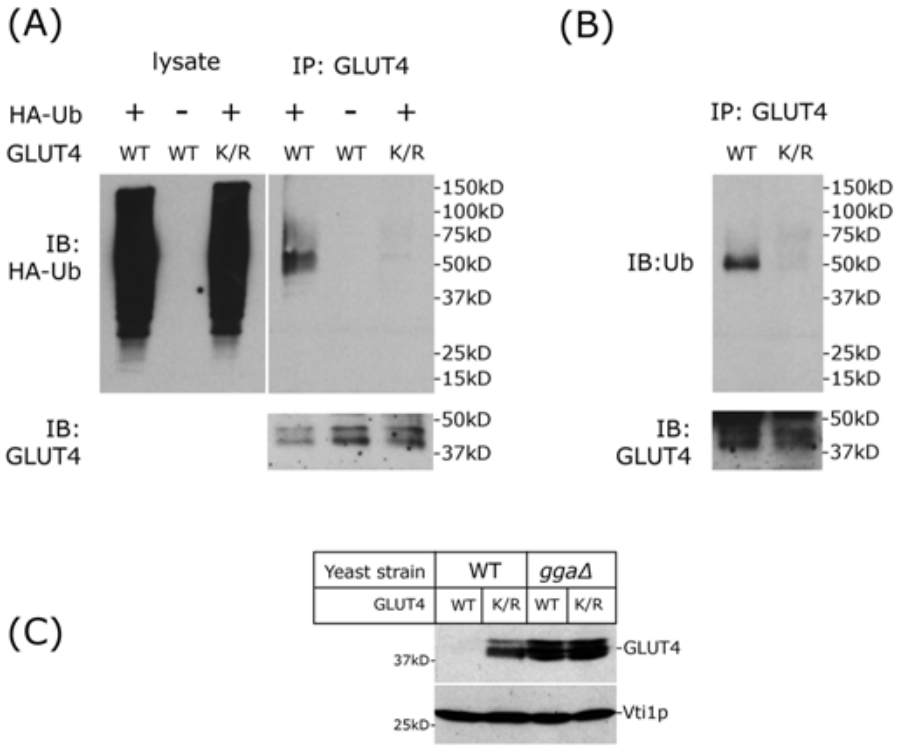

Figure 3.1 hGLUT4 expressed in yeast requires ubiquitin acceptor sites to enter the proteolytically active endosomal system.

Wild type (wt) GLUT4 expressed in yeast is conjugated to HA-Ub (A) and endogenous Ub (B) when expressed in vacuolar protease deficient SF838-9Dα yeast, whereas a ubiquitin resistant mutant (K/R) is not. (C) Yeast grown on rich media traffic wt GLUT4, but not GLUT4 7K/R, into the proteolytically active endosomal system, resulting in its degradation. GLUT4 is stabilized on rich media when expressed in a *ggaΔ* strain. Image used with permission from Dr. Rebecca McCann.

These studies were extended to the more physiologically relevant 3T3-L1 adipocyte cell line. Initial results suggested that GLUT4-7K/R does not enter GSVs and does not translocate to the cell surface in response to insulin. However the constructs used in these studies expressed wild type HA-GLUT4 at a significantly higher (approximately 20 fold greater) level than the ubiquitin resistant HA-7K/R, making it impossible to be sure that the differences seen in the trafficking of these molecules was due to differences in their ubiquitination status.

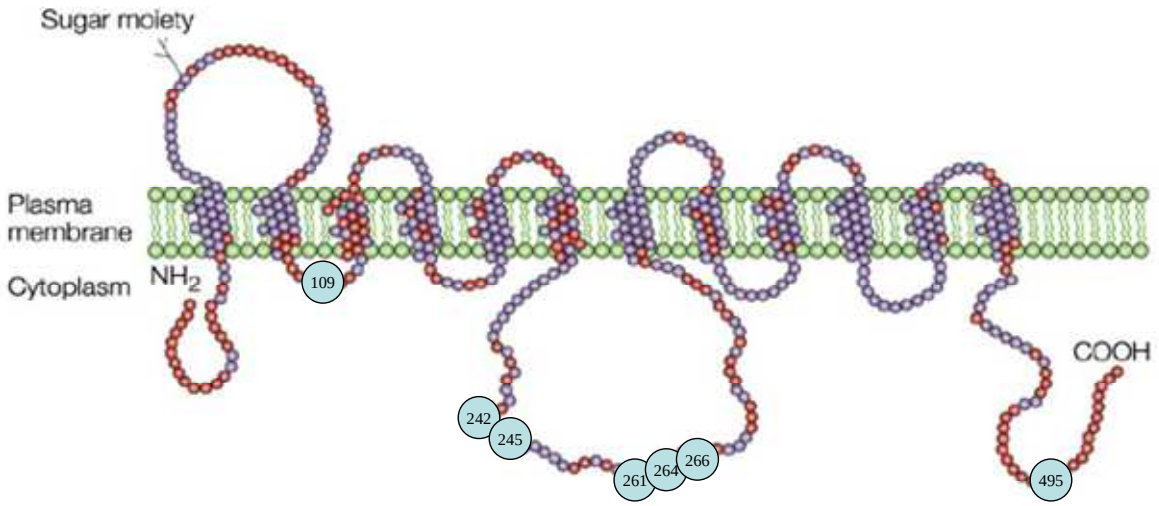

Figure 3.2 Schematic of GLUT4 in the plasma membrane with cytosolic lysines (putative ubiquitination sites) indicated.

Adapted with permission from Macmillan Publishers Ltd from Bryant et al., copyright (2002)

Another caveat with these experiments is that five of the seven potential ubiquitination sites (i.e. lysine residues that are predicted to be cytosolically disposed) (Birnbaum, 1989;James *et al.*, 1989) in GLUT4 are in the large intracellular loop (Figure 3.2). This portion of GLUT4 has been reported to interact with the ARF GAP protein ACAP1, and it has been proposed that this interaction is required to form functional clathrin coats on GSVs and permit recycling of GLUT4 (Li *et al.*, 2007). One of the important sites identified by Li *et al.* (2007) is a KR motif at residues 245-246, mutation of which to AA results in decreased interaction between GLUT4 and ACAP1. It is therefore possible that mutation of the five lysine residues within the loop results in impaired insulin-regulated trafficking of due to disruption of interaction with ACAP1. This chapter describes work performed by me to address the above concerns.

3.2 Aims of the chapter.

The aims of the work in this chapter were twofold; firstly, I set out to equalise expression of wild type HA-GLUT4 and the ubiquitin resistant HA-GLUT4 7K/R from their respective retroviral expression vectors; and secondly, I wanted to address concerns that impaired insulin-regulated trafficking of ubiquitin-resistant HA-GLUT4 7K/R may not be due to its lack of ubiquitination, but structural changes in the large intracellular loop, which may in turn disrupt

interactions with effector proteins required for the insulin regulated trafficking of GLUT4, such as ACAP1 (see above).

In order to investigate the latter point, I built on previous work that demonstrated that GLUT4 expressed in yeast can be ubiquitinated on any one of its seven cytosolically disposed lysine residues, and that ubiquitination of any one of these lysines is sufficient to direct GLUT4 delivery to the endosomal system (McCann R.K., 2007). I reasoned that if the same is true in adipocytes then I could test whether the mutations in the large intracellular loop were impairing the trafficking of HA-GLUT4 7K/R by creating versions in which single lysine residues outwith the large intracellular loop, at positions 109 or 495, had been reintroduced.

3.3 Expression of HA-GLUT4 and HA-GLUT4 7K/R

The HA-GLUT4 expression construct (pHA-GLUT4) used in our lab's initial studies on GLUT4 (described above) was generated in an earlier study (Shewan *et al.*, 2000). The cDNA from which the HA-GLUT4 fragment was generated contained 22 bases of untranslated sequence 5' to the GLUT4 coding region (Fukumoto *et al.*, 1989;Quon *et al.*, 1994) which may play a role in transcriptional and/or translational regulation of the *GLUT4* coding sequence. A comparison of pHA-GLUT4 and wild type GLUT4 coding sequence is shown in Figure 3.3.

The HA-GLUT4 7K/R expression vector (pRM4) was generated from the GLUT4-7K/R open reading frame present in a yeast expression vector for GLUT4-7K/R. This construct lacked the 22bp upstream sequence and its expression was solely controlled by the retroviral CMV promoter in the pBABE vector backbone (Morgenstern and Land, 1990). In order to create a retroviral expression vector that produces levels of wild-type HA-GLUT4 similar to those obtained for pHA-GLUT4 7K/R, I set out to remove the 22 bp, non-coding sequence found upstream of the coding sequence in pHA-GLUT4.

```
                    1                                                    50
GLUT4 human     (1) ----------------------------------------ATGCCGTC
  pHA-GLUT4     (1) GGATCCTCTAGACTCGACCGCGTCCAGCTCTTCTAAGACGAGATGCCGTC
                    51                                                   100
GLUT4 human     (9) GGGCTTCCAACAGATAGGCTCCGAAGATGGGGAACCCCCTCAGCAGCGAG
  pHA-GLUT4    (51) GGGCTTCCAACAGATAGGCTCCGAAGATGGGGAACCCCCTCAGCAGCGAG
                   101                                                   150
GLUT4 human    (59) TGACTGGGACCCTGGTCCTTGCTGTGTTCTCTGCGGTGCTTGGCTCCCTG
  pHA-GLUT4   (101) TGACTGGGACCCTGGTCCTTGCTGTGTTCTCTGCGGTGCTTGGCTCCCTG
                   151                                                   200
GLUT4 human   (109) CAGTTTGGGTACAACATTGGGGTCATCAATGCCCCTCAGAAGGTGATTGA
  pHA-GLUT4   (151) CAGTTTGGGTACAACATTGGGGTCATCAATGCCCCTCAGAAGGTGATTGA
                   201                          230
GLUT4 human   (159) ACAGAGCTACAATGAGACGTGGCTGGGGAG
  pHA-GLUT4   (201) ACAGAGCTACAATGAGACGTGGCTGGGGAG
```

Figure 3.3 DNA sequence alignment of HA-GLUT4 from pHA-GLUT4 and the hGLUT4 sequence.

The *Bam*HI site used to subclone HA-GLUT4 is indicated in blue, homologous sequences are in red. Sequences were aligned using Vector NTI (Invitrogen).

Also present in the lab at this time were HA-GLUT4 expression vectors (pRM35 and 36) encoding GLUT4 mutants with single cytosolic lysine residues (K109 and K495 respectively), constructed by Dr R. K. McCann. These constructs were based on pHA-GLUT4 7K/R and thus lacked the upstream sequence present in pHA-GLUT4 (Fukumoto *et al.*, 1989;Quon *et al.*, 1994). The presence of these reagents in the lab provided a straightforward way to generate wild type HA-GLUT4 in a background lacking the 5' upstream sequence (detailed in Figure 3.4), with the hope of obtaining vectors to produce comparable amounts of wild type HA-GLUT4, HA GLUT4 7K/R and the two "add back" mutants in 3T3-L1 adipocytes. A *Psh*AI-*Bgl*II fragment of HA-GLUT4 from base pairs 70-1469 of the GLUT4 coding sequence was excised from pHA-GLUT4 and inserted into *Psh*AI-*Bgl*II digested pRM36 which encoded HA-GLUT4 6K/R (495). The presence of the fragment was verified using a diagnostic restriction digest with *Tth*IIII. This work was carried out in collaboration with Dr. Rebecca McCann.

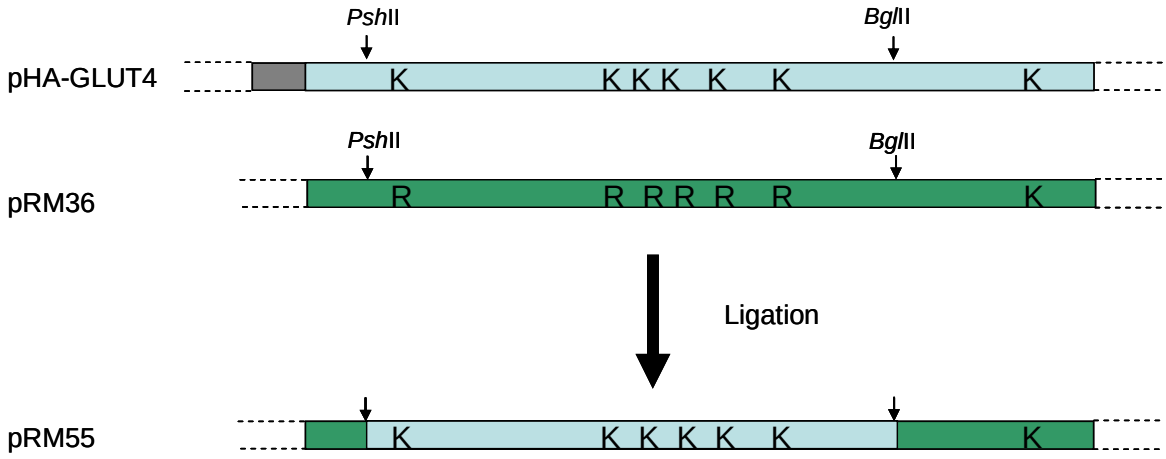

Figure 3.4 Construction of pRM55.

pHA-GLUT4 and pRM36 (encoding HA-GLUT4 6K/R K495) were simultaneously digested using *Psh*II and *Bgl*II restriction enzymes. The resulting fragment of HA-GLUT4 was ligated into gapped pRM36, generating pRM55. Relative positions of codons for cytosolically disposed lysine (K) and arginine (R) are indicated, the 22 bp 5' untranslated sequence is represented by the grey box in pHA-GLUT4.

All four HA-GLUT4 constructs (wild type, 7K/R and 6K/R 109 and 495), now in the same background (i.e. lacking the 22 bp sequence found in pHA-GLUT4) were transfected into Plat-E packaging cells to generate recombinant retrovirus as described in 2.3.4 and the resulting viruses were used to infect subconfluent 3T3-L1 fibroblasts. The fibroblasts were grown to confluency, differentiated into adipocytes and their HA-GLUT4 content analysed by immunoblotting. As shown in Figure 3.5 the expression of all four HA-GLUT4 variants was similar (using comparison to endogenously expressed GAPDH to control for loading). Having established conditions to express these 4 versions of HA-GLUT4 to similar levels in adipocytes, it was now possible to proceed with further characterisation of their trafficking without being concerned that any observed differences might be due to altered expression levels.

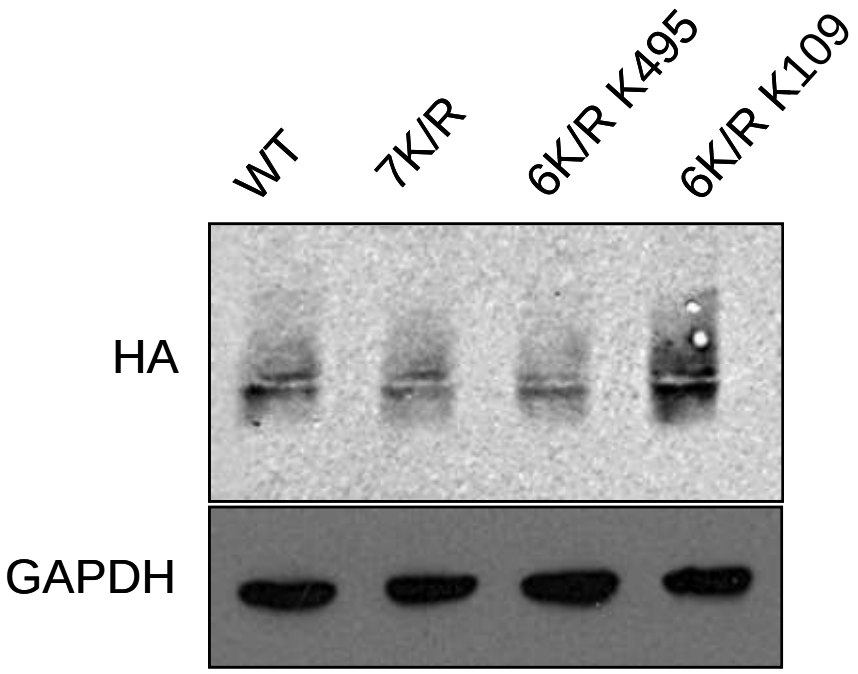

Figure 3.5 Expression of HA-GLUT4 and mutants in 3T3-L1 adipocytes.

Subconfluent 3T3-L1 fibroblasts were infected with recombinant retrovirus harbouring expression vectors encoding HA-GLUT4, HA-GLUT4 7K/R, HA-GLUT4 6K/R K495 and HA-GLUT4 6K/R 109, grown to confluency under selection with 2.5 µg/ml puromycin and differentiated as previously described. Between days 8 and 12 post-differentiation cells from one 10 cm plate were harvested in lysis buffer and the lysates equalized for protein content to approximately 5 mg/ml. The lysates were subjected to SDS-PAGE on 10 % (v/v) gels and immunoblotted for the HA epitope and GAPDH as a loading control.

3.4 A single ubiquitination site is sufficient to permit insulin-stimulated translocation of GLUT4.

3.4.1 HA-GLUT4 6K/R K109 and K495 are ubiquitinated in 3T3-L1 adipocytes.

As stated in 3.1, one of the major concerns with the use of the 7K/R mutant was that mutation of the five lysine residues within the large intracellular loop of GLUT4 may affect the structure of this region so that the altered trafficking of this mutant may be for reasons other than its altered ubiquitination status. To address this concern I made use of the observation that when present as the sole cytosolic lysine, any one of the seven lysines mutated in the 7K/R mutant serves as a ubiquitin acceptor site in yeast (McCann R.K., 2007). The two lysines located outside the large cytosolic loop are K109, located within the first intracellular domain, and K495, located within the C-terminal cytosolic region of

GLUT4 (Figure 3.2), a region known to contain several important GLUT4 trafficking motifs (Verhey *et al.*, 1995;Shewan *et al.*, 2000;2003). As discussed above, our lab has retroviral constructs (pRM35 and pRM36) to express versions of GLUT4 harbouring either one of these as the sole cytosolic lysine (HA-GLUT4 K109 and 495) that produce these proteins in 3T3-L1 adipocytes at levels comparable to HA-GLUT4 and HA-GLUT4 7K/R from their retroviral expression vectors (Figure 3.5) Recombinant retroviral particles were produced containing these two constructs and used to infect 3T3-L1 fibroblasts. These cells were grown to confluency in 10 cm dishes and differentiated into adipocytes.

To ask whether the presence of either K109 or K495 is sufficient for to restore the ubiquitination of HA-GLUT4 7K/R I used a GST-pull-down approach. The Dsk2p-UBA has been studied extensively and binds both mono- and poly-ubiquitin with high affinity (Funakoshi *et al.*, 2002;Ohno *et al.*, 2005;Raasi *et al.*, 2005). The molecular determinants of ubiquitin recognition by the UBA domain have been identified in an NMR solution structure of Dsk2p UBA in complex with ubiquitin (Funakoshi *et al.*, 2002), demonstrating the two residues within the UBA essential for interaction are methionine 342 and phenylalanine 344 (numbering relative to full length Dsk2p).

A fusion protein of Dsk2p UBA and glutathione-S-transferase (GST) had been generated in another study (GST-UBA) (Raasi *et al.*, 2005), and could be used to pull ubiquitinated proteins out of solution. Work in our lab by myself and others sought to use GST-UBA to detect ubiquitinated GLUT4 in 3T3-L1 adipocytes. As a negative control for these experiments I used site-directed mutagenesis to mutate M342 and F344 in the context of the GST-UBA fusion, generating GST-UBA M342R F344A (GST-UBA_{mut}). In collaboration with another member of our group (Dr. R.K. McCann) I used GST-UBA and GST-UBA_{mut} in pull-down assays to ascertain the ubiquitination status of endogenous GLUT4 in 3T3-L1 adipocytes. The results of these experiments are shown in Figure 3.6.

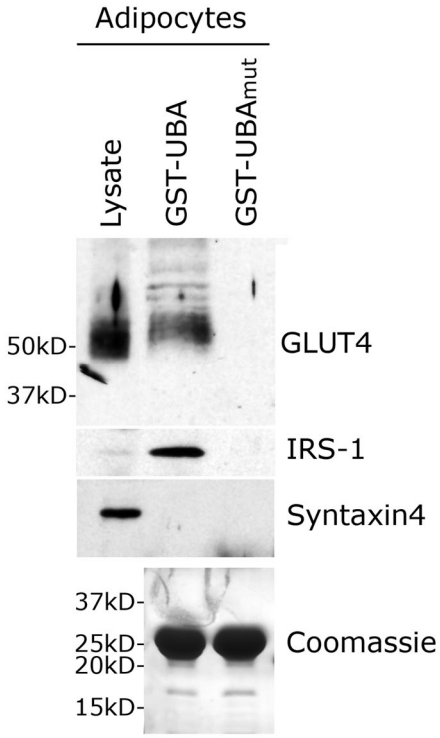

Figure 3.6 GLUT4 is ubiquitinated in 3T3-L1 adipocytes.

3T3-L1 adipocytes (two 10 cm plates per condition) were lysed in a buffer containing 1 % (v/v) Triton-X 100, 1 mM NEM and 1 mM EDTA, equalized for protein concentration to 5 mg/ml and 2 mg lysate protein incubated with 20 µl of a 50 % (v/v) slurry of GST-UBA immobilised on glutathione-Sepharose beads for two hours. After 3 washes in lysis buffer, bound protein was eluted from the beads with 15 µl 2xLSB at 65 ℃ for 10 minutes. The eluate was su bjected to SDS-PAGE on a 10 % (v/v) gel alongside 1.25 % (v/v) of the input lysate and immunoblotted for the HA epitope, IRS-1 as a control for ubiquitination and syntaxin 4 as a negative control. Equal loading of GST-UBA and GST-UBA$_{mut}$ is shown in the Coomassie stained gel.

These results not only show that GST-UBA can bind endogenous ubiquitinated proteins such as IRS-1 (Zhande *et al.*, 2002), and this binding can be ablated by the M342R F344A mutation, but also that a proportion of GLUT4 is ubiquitinated in 3T3-L1 adipocytes, represented by the protein recognised by an anti-GLUT4 antibody at just above 50 kD in the GST-UBA pulldown lane in Figure 3.6. The small increase in molecular weight would suggest that GLUT4 is modified with a single ubiquitin moiety, as endogenous GLUT4 has an apparent molecular weight of 45 kD by SDS-PAGE (James *et al.*, 1989) and ubiquitin has a molecular weight of approximately 8 kD (Ciechanover, 2005). Armed with this assay for detection of GLUT4 ubiquitination, I proceeded to analyse the ubiquitination status of HA-GLUT4, HA-GLUT4 7K/R and the two “add-back” mutants.

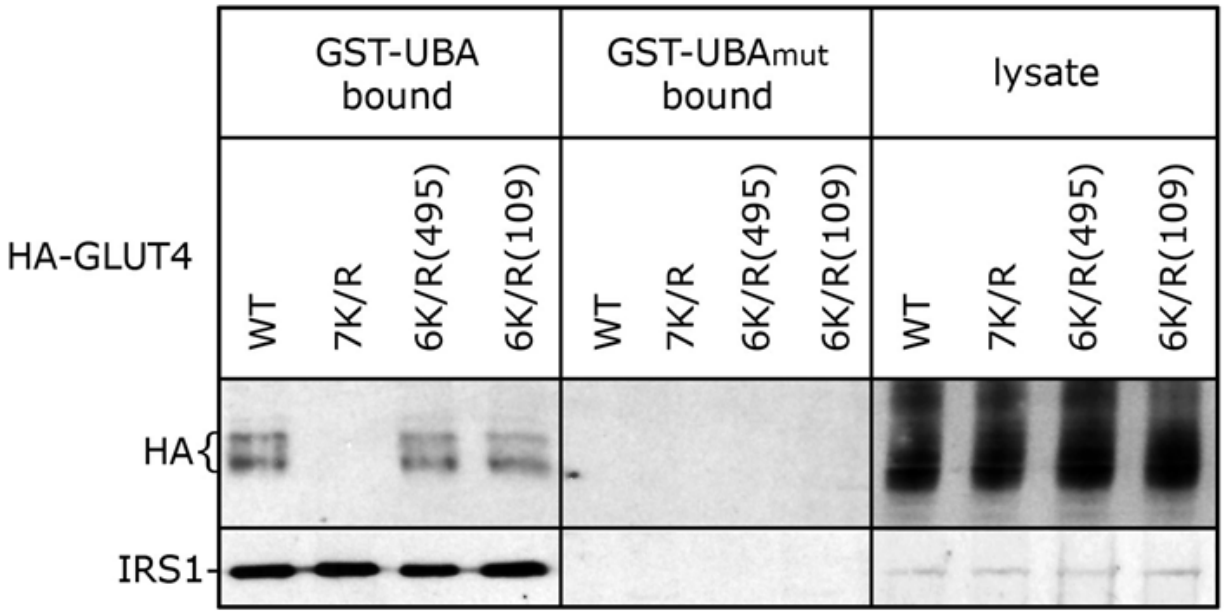

Figure 3.7 Ubiquitination of HA-GLUT4 variants in 3T3-L1 adipocytes.

3T3-L1 adipocytes expressing the indicated retroviral constructs (two 10 cm plates per construct) were lysed in a buffer containing 1 % (v/v) Triton-X 100, 1 mM NEM and 1 mM EDTA, equalized for protein concentration to 5 mg/ml and 2 mg lysate protein incubated with 20 µl of a 50 % (v/v) slurry of GST-UBA immobilised on glutathione-Sepharose beads for two hours. After 3 washes in lysis buffer, bound protein was eluted from the beads with 15 µl 2xLSB at 65 ℃ for 10 minutes. The eluate was subjected to SDS-PAGE on a 10 % (v/v) gel alongside 1.25 % (v/v) of the input lysate and immunoblotted for the HA epitope and IRS-1 as a control for ubiquitination. Blots are representative of 2 independent experiments.

As demonstrated in Figure 3.7, similar amounts of HA-GLUT4 and the two 6K/R variants are pulled down by GST-UBA, which suggests that they are ubiquitinated to a similar extent. As anticipated from the yeast studies, HA-GLUT4 7K/R is not detected in the pull-down, indicating that it is not ubiquitinated. As a control the blots were also probed for insulin receptor substrate-1 (IRS1) which is an abundant, endogenous adipocyte protein known to be ubiquitinated (Zhande *et al.*, 2002). These data are in agreement with the findings from yeast (McCann R.K., 2007) that all seven cytosolic lysines represent potential sites of ubiquitination and also validates using K109 and 495 to test the sufficiency of a single ubiquitination site outside the large intracellular loop for GLUT4 translocation.

3.4.2 HA-GLUT4 7K/R cannot translocate in response to insulin.

As described in 3.1, the relatively low expression of HA-GLUT4 7K/R compared to its wild-type counterpart made interpretation of previously generated data showing that HA-GLUT4 7K/R does not translocate in response to insulin problematic, as its altered trafficking may simply be due to its lower expression levels. Having normalised expression levels between HA-GLUT4, HA 7K/R and the two 6K/R "add back" mutants (K109 and K495), I could now compare the translocation of the wild type ubiquitinated and ubiquitin resistant transporters. pRM4 (HA-7K/R), pRM55 (HA-GLUT4), pRM35 (HA-GLUT4 K109) and pRM36 (HA-GLUT4 K495) were transfected into Plat-E cells to generate recombinant retrovirus and the virus used to infect 3T3-L1 fibroblasts. The fibroblasts were grown to confluency and differentiated into adipocytes on sterile coverslips. The adipocytes were stimulated with 200 nM insulin or left in the basal condition, fixed and processed for confocal microscopy. The fixed cells were first stained for the HA epitope with out permeablisation to detect HA-GLUT4 localised at the adipocyte plasma membrane (as the HA tag is located in the first extracellular loop of GLUT4 (Quon *et al.*, 1994)), followed by permeablisation and a second round of anti-HA staining to detect total HA-GLUT4. This technique shows the extent to which HA-GLUT4 and the three mutants can translocate in response to insulin.

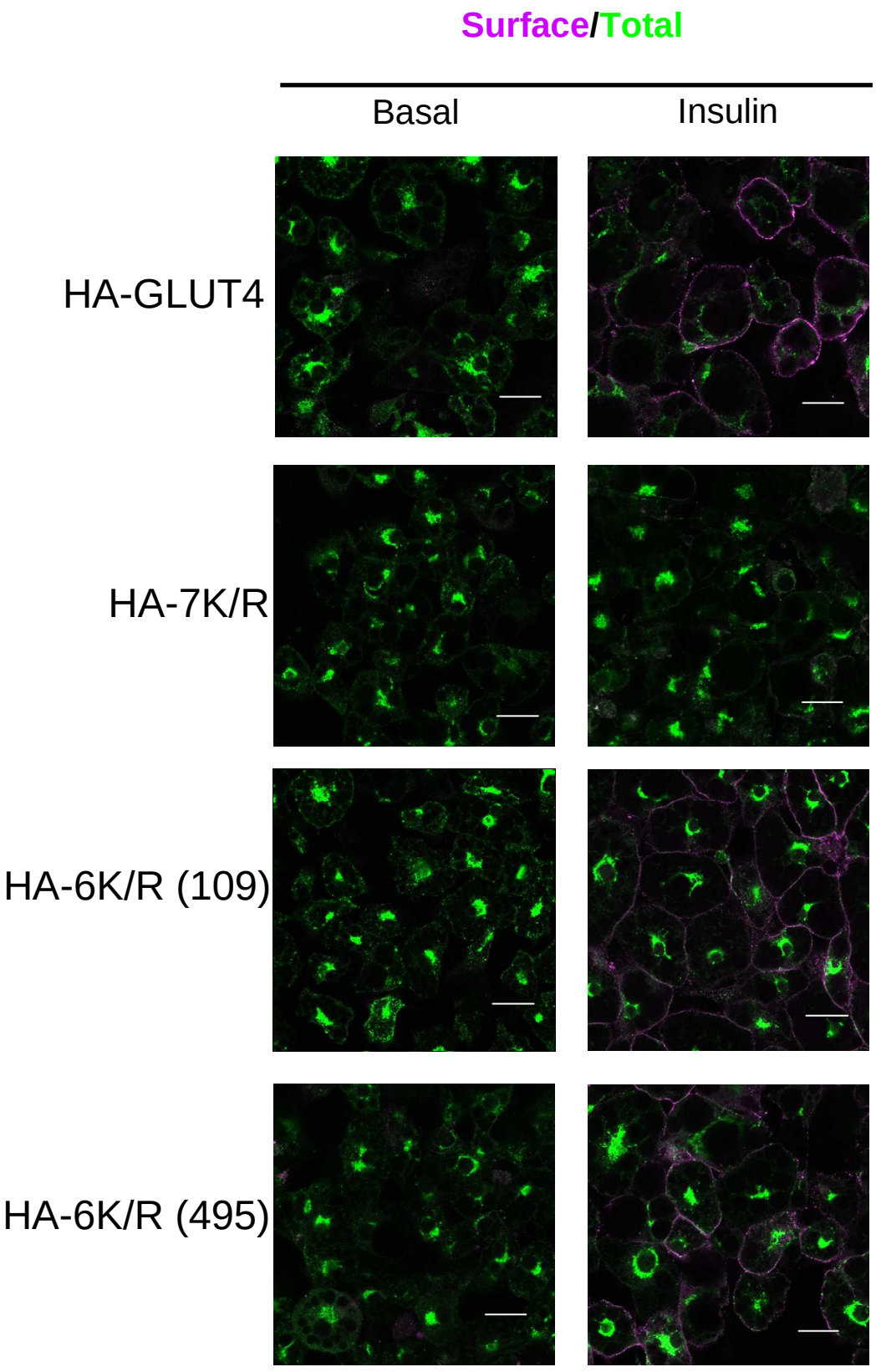

Figure 3.8 HA-GLUT4 7K/R cannot translocate in response to insulin.

Subconfluent 3T3-L1 fibroblasts were infected with the retroviral constructs encoding the indicated HA-GLUT4 variants, grown to confluency on sterile coverslips under selection with 2.5 µg/ml puromycin and differentiated into adipocytes. Between days 8 and 12 post differentiation, the cells were either treated with 200 nM insulin for 15 minutes (Insulin) or not (Basal), fixed using 3 % (v/v) paraformaldehyde and stained for surface (magenta) and total HA epitope (green). Images are representative of three independent experiments. Scale bar = 20 µm.

	Basal	Insulin
HA-GLUT4	0	90.97 (±1.69) %
HA-GLUT4 7K/R	0.55 (±0.55) %	22.12 (±4.36) % (*)
HA-GLUT4 6K/R (495)	0.62 (±0.62) %	91.32 (±6.06) %
HA-GLUT4 6K/R (109)	1.23 (±1.23) %	86.17 (±2.96) %

Table 3.1 Percentage translocation of HA-GLUT4 and mutants thereof in response to 200 nM insulin.

At least 50 cells from three fields of view (prepared as in Figure 3.8) were scored for the presence or absence of cell surface HA immunoreactivity (rim fluorescence) as a measure of HA-GLUT4 translocation. Results shown in the table are the mean of three experiments, expressed as percentage of counted cells exhibiting rim fluorescence. * $p < 0.001$ compared to the HA-GLUT4 insulin stimulated condition, student's unpaired T-test.

The upper four panels of Figure 3.8 compare the insulin regulated translocation of wild type and 7K/R HA-GLUT4. HA-GLUT4 7K/R exhibits severely impaired translocation in response to 200 nM insulin stimulation, whereas HA-GLUT4 translocates readily. The immunofluorescence data is quantified in Table 3.1, and show that while approximately 90 % of cells expressing HA-GLUT4 exhibit translocation in response to 200 nM insulin, only 20 % of those expressing HA-GLUT4 7K/R do. These data indicate that ubiquitination of GLUT4 is essential for its insulin responsive translocation. However, they still left open the possibility that the 5K/R mutations in the large central loop of HA-GLUT4 7K/R were affecting its translocation, rather than the lack of target lysines *per se*, due to the inability of ACAP1 to bind the loop and induce clathrin coat formation (Li *et al.*, 2007).

3.4.3 HA-GLUT4 6K/R K109 and K495 translocate readily in response to insulin stimulation.

Having determined that the two HA-GLUT4 6K/R "add back" mutants are ubiquitinated (Figure 3.7), I was able to use the translocation assay described in 3.4.2 to observe whether they can still respond to insulin with a single intact ubiquitination site outwith the large intracellular loop. The results of these experiments are shown in the lower four panels of Figure 3.8. Both HA-GLUT4 6K/R variants translocate readily in response to 200 nM insulin, in a manner indistinguishable from HA-GLUT4 (upper two panels). These data demonstrate that a single site of ubiquitination of GLUT4 permits its insulin responsive translocation, and that despite mutation of residues within the large cytosolic

loop in both 6K/R variants there is no effect on translocation. This argues that if ACAP1 binding is required for sorting into and thus clathrin coat formation on GSVs (Li *et al.*, 2007) is not affected by the 5K/R mutations introduced into the large intracellular loop.

The mutations introduced into the large cytosolic loop of GLUT4 by Li *et al.* (2007) were alanine scanning mutations, so the basic lysine residue with a bulky R-group was being replaced with neutral alanine which has a much smaller R group. However in the present study the lysines were being replaced with another bulky basic residue, arginine, which would be expected to alter the charge and structure of the large intracellular loop much less significantly.

3.5 Does the 7K/R mutation affect loading of GLUT4 into the insulin responsive compartment?

In insulin responsive tissues GLUT4 occupies two overlapping trafficking cycles. Cycle 1 is a prototypical recycling pathway between the endosomes and the cell surface; cycle 2 is a much slower pathway between the *trans*-Golgi network (TGN) and endosomes (discussed extensively in 1.4.3). As part of this cycle, GLUT4 occupies GLUT4 storage vesicles (GSVs); the compartment from where GLUT4 is mobilised to the cell surface in response to insulin (Bryant *et al.*, 2002). GSVs are a component of the low density microsome (LDM) fraction of adipocytes and contain various proteins aside from GLUT4; these include sortilin (Lin *et al.*, 1997), the insulin responsive aminopeptidase IRAP (Ross *et al.*, 1996;Ross *et al.*, 1997) and LRP1 (low density lipoprotein receptor related protein 1) (Jedrychowski *et al.*, 2010). Translocation of GSVs is largely responsible for the approximately 11-fold increase in plasma membrane GLUT4 on insulin stimulation (Yang *et al.*, 1992;Ross *et al.*, 1998;Kupriyanova *et al.*, 2002).

The hypothesis that HA-GLUT4 7K/R is not trafficked into GSVs was formed following colocalisation studies between HA-GLUT4, HA-GLUT4 7K/R and the TGN resident SNARE syntaxin 16 (McCann R.K., 2007). HA-GLUT4 is present in the TGN and punctate cytoplasmic structures which represent GSVs (Martin *et al.*, 2000). However, while HA-GLUT4 7K/R, like its wild type counterpart, colocalises with syntaxin 16 to the TGN, it is conspicuously absent from these

puncta. Although the data presented in Figure 3.8 support the hypothesis that HA-GLUT4 7K/R is not trafficked into GSVs, it is also a possibility that the mutant's defective translocation arises due to impaired trafficking from GSVs to the cell surface.

To distinguish between these possibilities I undertook subcellular fractionation to separate GSVs from other GLUT4 containing membranes of adipocytes expressing HA-GLUT4 and mutants thereof. One approach that was initially considered was that of iodixanol gradient centrifugation. This process as described by Hashiramoto and James (2000), involves isolating a LDM fraction from 3T3-L1 adipocytes in a high sucrose buffer (HES) and subjecting this to high velocity centrifugation in a self forming iodixanol gradient. Thirteen fractions are collected from the gradient and fractions 2-13 immunoblotted. GLUT4 fractionates into a "heavy" and "light" peak in fractions 2-6 and 7-12 respectively – the GLUT4 content of the heavy peak is depleted on insulin stimulation which indicates that these fractions contain the insulin responsive compartment (Hashiramoto and James, 2000).

I initially set out to use this approach on basal adipocytes expressing HA-GLUT4. However it proved difficult to obtain consistent fractionation profiles for even the wild-type protein. Three example gradients for HA-GLUT4 are shown in Figure 3.9 and indicate the lack of consistency between experiments –the protein was generally located primarily in one or another peak, rather than being evenly distributed between the two. This variation meant it would be difficult to ascertain whether the fractionation profile of any of the HA-GLUT4 mutants was altered when compared to the wild type.

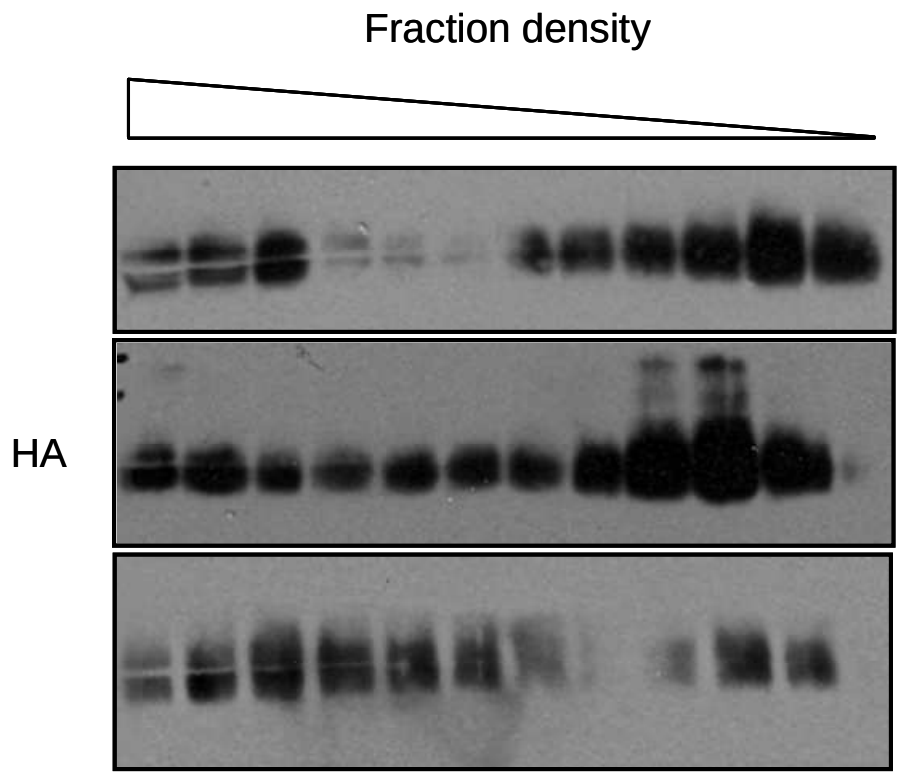

Figure 3.9 Three example iodixanol gradient fractionation profiles of HA-GLUT4 in 3T3-L1 adipocytes.

Low density microsomes from serum-starved 3T3-L1 adipocytes were resuspended in HES buffer and centrifuged at 295 000 xg for 1 hour on a self-forming iodixanol gradient. Thirteen fractions were collected from the bottom of the gradient, combined with sample buffer and fractions 2-12 subjected to SDS-PAGE on a 10 % gel. The fractions were then immunoblotted with an anti-HA antibody to detect HA-GLUT4.

Another method for isolating the insulin responsive compartment has been developed in the laboratory of Konstantin Kandror (Boston University School of Medicine). As outlined in several publications (Xu and Kandror, 2002;Kupriyanova *et al.*, 2002;Li and Kandror, 2005;Li *et al.*, 2007), a subcellular fraction enriched in GSVs can be obtained from adipocytes homogenised in PBS and subjected to a 20 minute centrifugation at 16 000 xg. The resultant pellet contains heavy membranes including the lysosomes, Golgi membranes, endoplasmic reticulum and plasma membrane, whereas the supernatant contains the GSV compartment and transport vesicles (Xu and Kandror, 2002;Kupriyanova *et al.*, 2002).

I employed this method to analyse the partitioning of HA-GLUT4, HA-GLUT4 7K/R and the two 6K/R (K109 and K495) mutants between the pellet and GSV containing supernatant fractions. Basal adipocytes were fractionated using the

protocol outlined in 2.12 and subsequently immunoblotted for the HA epitope and IRAP as a marker for GSVs. The results of these experiments are shown in Figure 3.10. From three independent experiments there was a consistent reduction in the amount of HA-GLUT4 7K/R in the supernatant fraction compared to HA-GLUT4 (31 % ± 1.02 % compared to 53.8 ± 0.57 %), indicating that HA-GLUT47K/R is impaired in its ability to reach GSVs. This correlates with the unpublished data concerning the absence of HA-GLUT4 7K/R from the cytosolic puncta thought to represent GSVs (McCann R.K., 2007). It also provides an explanation as to why HA-GLUT4 7K/R cannot translocate in response to insulin (as demonstrated in Figure 3.8) as the mutant is impaired in its ability to reach GSVs.

Importantly, both the 6K/R mutants are partitioned between the pellet and supernatant fractions in a manner similar to HA-GLUT4 (HA-GLUT4 6K/R (495) 53.5 % ± 3.9 %, HA-GLUT4 6K/R (109) 54.2 % ± 2.4% in supernatant fraction). These data support the hypothesis that a single ubiquitination site on GLUT4 is sufficient to allow the entry of the transporter into the insulin responsive compartment, and provides further evidence that mutation of the 5 lysine residues within the large intracellular loop does not affect the loading of GLUT4 into GSVs.

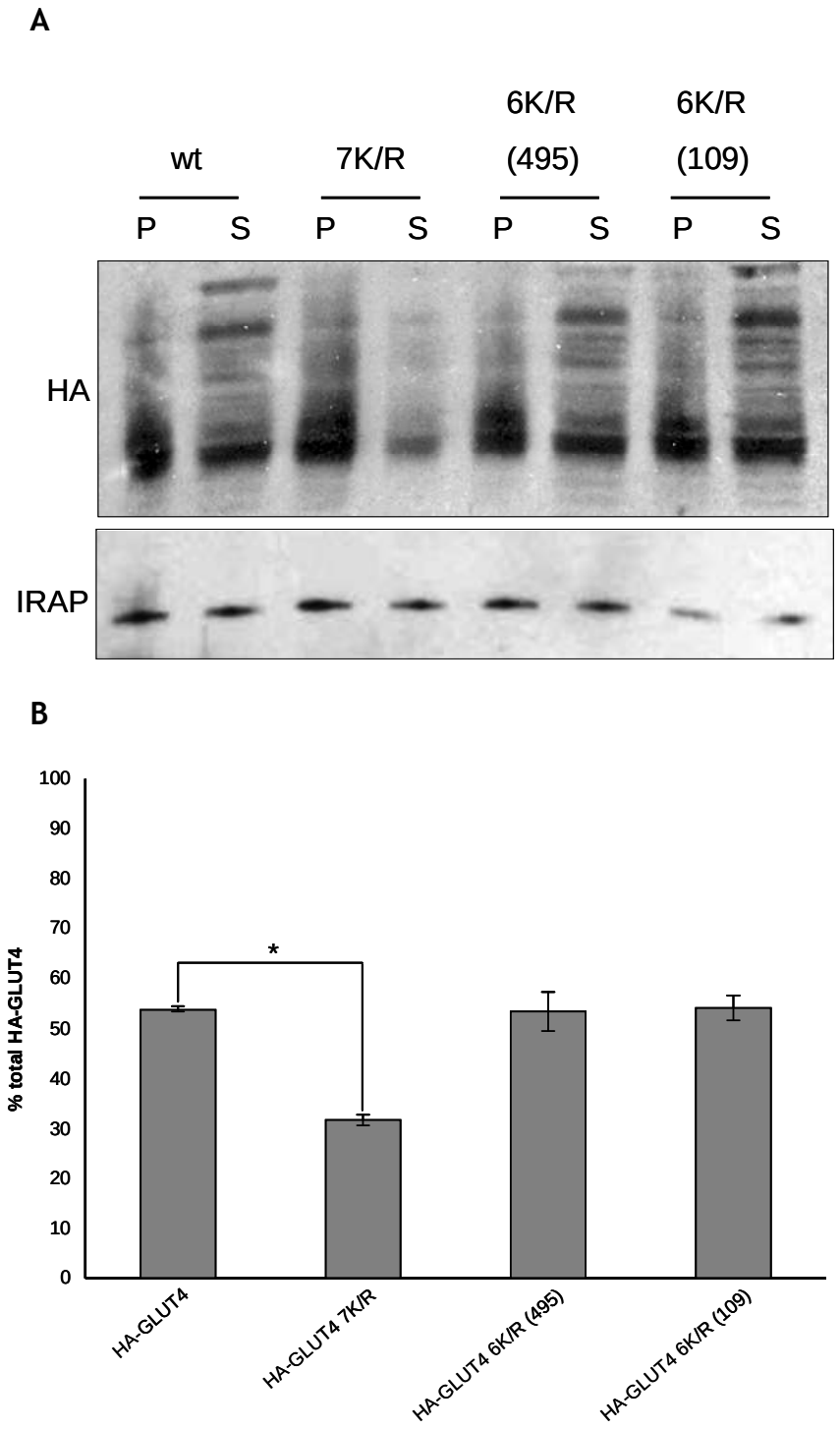

Figure 3.10 HA-GLUT4 7K-R cannot enter the insulin responsive compartment.

Adipocytes were homogenised with 12 strokes with a syringe and needle then centrifuged at 2000 xg for 10 minutes. The soluble phase of this step was subject to further centrifugation at 16 000 xg for 20 minutes. The pellet and supernatant from this centrifugation step were analysed by immunoblotting (A), loading 5 µg pellet protein and 20 µg supernatant protein. B. The partitioning of HA-GLUT4 between pellet and supernatant was compared using image analysis software (ImageJ, NIH) to quantify the optical density of the bands on the blot. The percentage of total HA-GLUT4 in the supernatant fraction is plotted. n = 3, * statistically significant difference ($p < 0.001$, unpaired Student's T-test). Error bars ± standard error of the mean.

3.6 Chapter discussion

The aim of the experiments in this chapter was to test the hypothesis that ubiquitination of GLUT4 is required for its insulin responsiveness. To test this hypothesis, I initially set out to equalise the levels of HA-GLUT4 and HA-GLUT4 7K/R expression from their retroviral expression vectors as previous studies in our lab had used vectors which expressed HA-GLUT4 at much higher levels than HA-7K/R. The second aim was to use these new constructs to study the trafficking of HA-GLUT4, HA-GLUT4 7K/R and two "add back" mutants with single cytosolic lysines (i.e. potential ubiquitination sites) outwith the large intracellular loop (K109 and K495). This would indicate whether a single ubiquitination site is sufficient for entry into GSVs and thus insulin responsive GLUT4 translocation, and whether mutation of the five lysine residues within the large intracellular loop alters GLUT4 trafficking.

Removal of sequences 5' of the HA-GLUT4 coding sequence in pHA-GLUT4 using subcloning techniques resulted in HA-GLUT4 and HA-GLUT4 7K/R being expressed at similar levels (Figure 3.5), addressing concerns that any difference in their trafficking properties might be due to differences in their expression levels. Going forward with these new reagents, I demonstrated that HA-GLUT4 7K/R is not be ubiquitinated in 3T3-L1 adipocytes (Figure 3.7) and that translocation of this mutant in response to insulin is blunted compared to the wild type protein (Figure 3.8). The ability of HA-GLUT4 7K/R to enter the GSV compartment is also significantly impaired, as shown by a subcellular fractionation approach (Li and Kandror, 2005) (Figure 3.10), which indicates that the lack of HA-GLUT4 7K/R translocation is due to its inability to enter the insulin responsive compartment rather than a defect in exit from GSVs.

A recent study indicated that the large intracellular loop, specifically the 245-246 KR motif, is involved in recruitment of the Arf6 GAP ACAP1 which plays a role in GLUT4 recycling (Li *et al.*, 2007). Potentially, the 5K/R mutations located within the large cytosolic loop could disrupt the binding interface between the ACAP1 and GLUT4, raising concerns that the defective insulin regulated trafficking of the 7K/R mutant was not due to its loss of ubiquitination. This led to the use of two "add back" mutants which have single ubiquitin-acceptor sites outwith the large intracellular loop (HA-GLUT4 6K/R 109 and 495). Both these mutants behaved in a manner similar to HA-GLUT4 – they

were ubiquitinated in adipocytes (Figure 3.7), enter GSVs (Figure 3.10) and translocate to the cell surface in response to insulin (Figure 3.8) and. It is therefore possible to say that mutation of the lysine residues within the large intracellular loop does not affect GLUT4 traffic in itself. From these data it can also be stated that the exact residue on which GLUT4 is ubiquitinated is not important; any of the single cytosolic lysine residues can provide a suitable substrate for ubiquitination and subsequent development of insulin responsiveness. This corroborates unpublished data from yeast where immunoprecipitation experiments demonstrated that GLUT4 can be ubiquitinated to the same extent on any one of its seven cytosolically disposed lysine residues (McCann R.K., 2007).

The finding that a single GLUT4 ubiquitination site is sufficient for its ubiquitination and translocation may seem surprising. However, previous studies attempting to map the ubiquitination sites of other protein substrates using lysine to arginine mutations has shown that these mutants retain almost wild type levels of ubiquitination. Examples include the T cell receptor ζ subunit (Hou *et al.*, 1994) and c-Jun (Treier *et al.*, 1994).

How does my data correlate with previous findings? Work on other receptors and channel proteins in mammalian cells has shown ubiquitination is a signal for internalisation and degradation, rather than sorting from the TGN to a secretory compartment (Geetha *et al.*, 2005;Kamsteeg *et al.*, 2006;Shin *et al.*, 2006;Shenoy, 2007). Examples of proteins being sorted into secretory compartments in a ubiquitin dependent manner are rare. One example is Fas ligand (FasL) which is secreted by cytotoxic leukocytes and natural killer cells to induce apoptosis (Zuccato *et al.*, 2007). FasL is secreted from compartments known as secretory lysosomes, which are highly vesiculated structures with the intralumenal vesicle membranes containing FasL. A combination of phosphorylation and ubiquitination is required to sort FasL into the intralumenal vesicles of secretory lysosomes (Zuccato *et al.*, 2007). However this sorting process may have more in common with ESCRT dependent multivesicular body sorting than formation of classical secretory compartments such as GSVs (Blott and Griffiths, 2002). The finding that ubiquitination of GLUT4 is required for its sorting into the insulin responsive compartment is, therefore, novel in the context of mammalian cells.

Previously, parallels have been drawn between the nitrogen-regulated trafficking of *S. cerevisiae* Gap1p and GLUT4 traffic (Roberg *et al.*, 1997;Bryant *et al.*, 2002). Gap1p is sorted to the cell surface when yeast are grown on poor nitrogen sources such as proline, but diverted to the endosomal system when yeast are provided with a rich nitrogen source such as glutamate (Roberg *et al.*, 1997). GLUT4 is directed to the cell surface in response to insulin, whereas in the absence of insulin it is retained intracellularly in a cycle containing GSVs (Bryant *et al.*, 2002;Muretta *et al.*, 2008) – in both cases an extracellular stimulus is determining whether the transporter remains intracellular or reaches the plasma membrane.

The data presented in this chapter highlight the differences between the two systems. Gap1p is only ubiquitinated in response to optimum nitrogen sources (e.g. glutamate), whereupon it traffics directly from the *trans*-Golgi network to the endosomal system (Soetens *et al.*, 2001;Magasanik and Kaiser, 2002) whereas it appears that GLUT4 is constitutively ubiquitinated to reach GSVs. Unpublished data from our laboratory has also shown that the ubiquitination status of GLUT4 is unchanged on stimulation with 100 nM insulin (Lamb *et al.*, 2010).

Collectively, the data presented in this chapter support the hypothesis that GLUT4 requires ubiquitination to enter the insulin responsive compartment. The molecular mechanisms underlying how ubiquitination has this effect will be investigated in subsequent chapters.

Chapter 4 - The ubiquitin binding GAT domain of GGA3 in ubiquitin mediated GLUT4 traffic.

4.1 Introduction

The GGA proteins are a family of clathrin adaptor proteins which sort proteins based on their ubiquitination status at the *trans*-Golgi network (Mattera *et al.*, 2004;Pelham, 2004;Scott *et al.*, 2004;Kawasaki *et al.*, 2005). They have a conserved modular structure, with (from N to C terminus) a VHS domain (Vps27, Hrs and STAM) which interacts with acidic dileucine motifs, a GAT domain(GGA and Tom1) which has binding sites for Arf-GTP and ubiquitin, a clathrin binding hinge region and a C-terminal γ adaptin ear (GAE) which binds accessory factors such as epsin related proteins (Bonifacino, 2004;Pelham, 2004) (Figure 1.5). The structural basis of the GAT-ubiquitin interaction was resolved independently by two groups for the GGA3 GAT domain (Bilodeau *et al.*, 2004;Kawasaki *et al.*, 2005). The latter study carried out mutagenic analyses which suggested that residues 250 and 284 (glutamic acid and aspartic acid respectively) were vital for the Ub-GAT interaction, as substitution of both residues resulted in loss of ubiquitin binding.

The prototypical Gga cargo in yeast is the general amino acid permease Gap1p. When yeast are grown on rich nitrogen sources, Gap1p is trafficked to the endosomal system in a ubiquitin and Gga dependent manner where it is degraded by vacuolar proteases (Roberg *et al.*, 1997;Soetens *et al.*, 2001;Magasanik and Kaiser, 2002). In contrast to wild type cells, in the absence of Ggas the endosomal sorting of Gap1p is delayed on a shift from a poor nitrogen source (proline) to a rich one (glutamate) and when the only Gga protein present lacks the GAT domain, Gap1p is trafficked to the vacuole via the plasma membrane (Scott *et al.*, 2004). Collectively these data show that Ggas sort ubiquitinated Gap1p into the endosomes via their GAT domain when yeast are grown on a rich nitrogen source. Intriguingly a version of Gga2p which has the GAT domain of human GGA3 can rescue the sorting defects observed in *ggaΔ* cells (Bilodeau *et al.*, 2004), suggesting that the ubiquitin binding function of GGAs is conserved from yeast to mammals.

The sorting of ubiquitinated substrates by mammalian GGAs is less well characterized. It has been known for some time that GGAs, notably GGA3, can interact with components of the ESCRT machinery such as TSG101 (Puertollano and Bonifacino, 2004;Mattera *et al.*, 2004), which sorts ubiquitinated substrates to the lysosome (Raiborg and Stenmark, 2009), and that sorting of ubiquitinated

substrates such as the EGF receptor from the TGN to early endosomes is perturbed by depletion of GGA3 (Puertollano and Bonifacino, 2004).

Another example of GGA dependent protein sorting is beta-site amyloid precursor protein-cleaving enzyme 1 (BACE1), involved in the production of the toxic beta-amyloid protein thought to be responsible for Alzheimer's disease (Tesco *et al.*, 2007). Depletion of GGA3 through caspase activation or RNAi stabilizes BACE1 (Tesco *et al.*, 2007), due to defective lysosomal sorting of the enzyme (Tesco *et al.*, 2007). More recent data has demonstrated that ubiquitination of BACE1 is required for its GGA3 dependent sorting to the lysosome (Kang *et al.*, 2010). Mutation of the putative BACE1 ubiquitination site at K501 or expression of a ubiquitin binding deficient mutant of GGA3 both result in impaired sorting of BACE1 to the lysosome (Kang *et al.*, 2010). These data demonstrate that GGA and ubiquitin dependent sorting of proteins is conserved from yeast to mammals.

The GGAs have been implicated in the sorting of GLUT4 into GSVs. Expression of a fragment of GGA2 which has dominant interfering effects for all three GGAs (VHS-GAT) in 3T3-L1 adipocytes alters the fractionation profile of GLUT4 , with significantly less being found in a fraction enriched in GSVs (Li and Kandror, 2005). VHS-GAT also causes a block in budding of GSVs *in vitro* (Li and Kandror, 2005). Consistent with these findings, adipocytes expressing VHS-GAT display a blunted translocation of GLUT4 to the cell surface in response to insulin (Li and Kandror, 2005). The acquisition of insulin responsiveness of newly synthesised GLUT4 is severely impaired in 3T3-L1 adipocytes (Watson *et al.*, 2004), however translocation of endogenous GLUT4 already present in GSVs is unaffected (Watson *et al.*, 2004). These data indicate that the GGAs are involved in sorting newly synthesised GLUT4 from the TGN into GSVs.

On expression in yeast, ubiquitin dependent GLUT4 sorting into the proteolytically active endosomal system is impaired in a *ggaΔ* strain (Lamb *et al.*, 2010). Taking the above data supporting a role for the GGA proteins in the sorting of GLUT4 from the TGN into GSVs, together with the data presented in the previous chapter supporting a role for GLUT4 ubiquitination in GLUT4 sorting into GSVs, it seems plausible that the GGAs recognize the ubiquitin modification on GLUT4 at the TGN and sort it into GSVs.

4.2 Aims of the chapter.

The aim of the work presented in this chapter was to investigate the role of the ubiquitin-binding GAT domain of GGA3 in the sorting of GLUT4 into GSVs. GGA3 was selected for study as it has the highest affinity for ubiquitin of all three mammalian GGAs (Shiba *et al.*, 2004), and published structural data for the GGA3 GAT domain in complex with ubiquitin was available to facilitate analysis of the interaction (Bilodeau *et al.*, 2004;Kawasaki *et al.*, 2005). I utilised two approaches in this investigation: firstly, an *in vitro* pull-down approach to determine whether GLUT4 can interact with GGAs and whether this interaction is dependent on the ubiquitin binding function of the GAT domain; and secondly an *in vivo* approach, expressing an epitope-tagged versions of wild-type and a ubiquitin binding deficient mutant of GGA3 in 3T3-L1 adipocytes, to investigate their effect on GLUT4 sorting into GSVs.

4.3 Ubiquitin and GLUT4 interaction with the GGA3 GAT domain.

4.3.1 Mutagenesis of the GAT domain ablates ubiquitin binding in vitro.

As has been previously discussed, studies have indicated that the GAT domain of GGAs is the region of the proteins which binds ubiquitin (Scott *et al.*, 2004;Bilodeau *et al.*, 2004;Kawasaki *et al.*, 2005). The lab was previously gifted a construct encoding recombinant GST-GGA3 VHS-GAT (pGEX *GGA3 VHS-GAT* (Dell'Angelica *et al.*, 2000)), and I planned to use this construct to study the interactions between GGAs and GLUT4. I first carried out site directed mutagenesis of this construct to mutate the two key residues implicated by Kawasaki *et al.*(2005) in ubiquitin binding, generating pCAL6 (Table 2.3) which encodes recombinant GST-GGA3 VHS-GAT E250N D284G (referred to as GST-VHS-GAT$_{mut}$; please see section 2.4.5 for a detailed description of how this construct was made and the oligonucleotide pairs used).

A

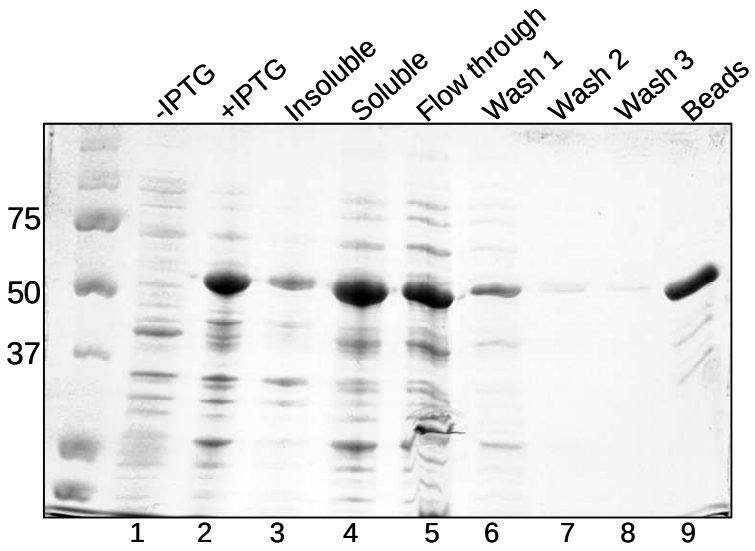

B

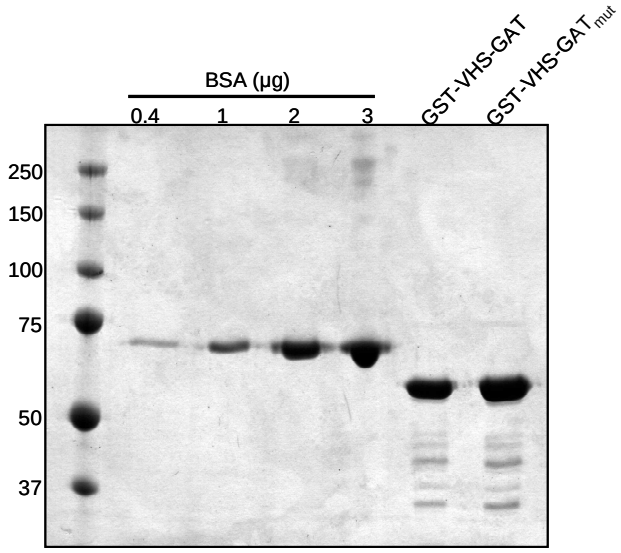

Figure 4.1 Purification of GGA3 VHS-GAT$_{mut}$.

A. BL-21 (DE3) *E. coli* were transformed with pCAL6 and grown to an OD_{600} of 0.6 in 400 ml Terrific Broth (1). The cells were induced for 4 hours with 1 mM IPTG (2), then lysed by treatment with 1 mg/ml lysozyme (4 ℃ for 30 minutes) and sub sequent sonication. The lysates were centrifuged at 17000 xg to separate insoluble (3) and soluble (4) components. The soluble proteins were incubated with glutathione-Sepharose beads for 1 hour with continual mixing. The flow through was collected from this incubation (5) and several washes with PBS were also performed (6-8). Bound protein was eluted from the beads at a 1 in 400 dilution (9) and 5 µl of all samples run on a 10% SDS-PAGE gel. B. GST-VHS-GAT and GST-VHS-GAT$_{mut}$ were expressed and purified as in A, and run on a 10% SDS-PAGE gel with samples containing known amounts of BSA to allow an estimation of fusion protein concentration.

Although the expression of GST-VHS-GAT has already been reported, I analysed the expression of the newly generated GST-VHS-GAT$_{mut}$ as demonstrated in

Figure 4.1. Panel A shows aliquots taken at various stages of the expression and purification process of GST-VHS-GAT$_{mut}$ from BL-21 *E. coli*. A band of approximately 60 kD is induced after 4 hours of induction with IPTG, corresponding to the predicted molecular weight of the GGA3 VHS-GAT domains fused to GST (Dell'Angelica *et al.*, 2000). The majority of this protein remains in the soluble fraction of the lysate. Although some of GST-VHS-GAT$_{mut}$ remains in the flow through (lane 5), a large amount binds to the beads (lane 9). In panel B equivalent dilutions of GST-VHS-GAT and GST-VHS-GAT$_{mut}$ are run on the same gel as a set of BSA standards. This demonstrates that GST-VHS-GAT and GST-VHS-GAT$_{mut}$ can be expressed, purified and immobilised on glutathione-Sepharose beads at similar levels, allowing for comparisons in their ability to bind proteins to be made.

pGEX *GGA3 VHS-GAT* and pCAL6 were transformed into BL-21 *E. coli* and the recombinant proteins purified as described in 2.5.6, immobilised on glutathione Sepharose beads. The proteins were used in pull-down assays from lysates of 3T3-L1 adipocytes. Immobilised material was subsequently immunoblotted using antibodies raised against ubiquitin (Figure 4.2).

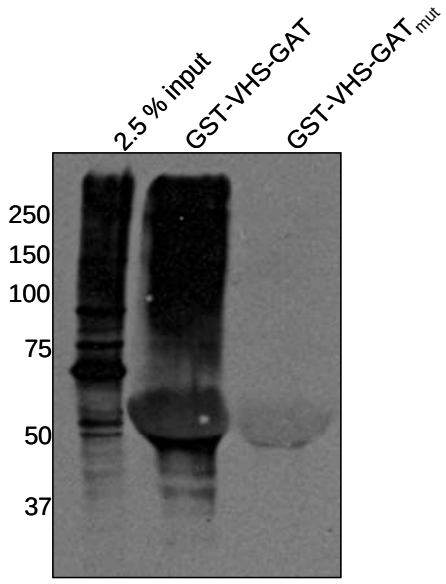

Figure 4.2 Mutation of the GAT domain ablates ubiquitin binding *in vitro*.

Recombinant GST-GGA3 VHS-GAT and GST-GGA3 VHS-GAT$_{mut}$ were immobilised on glutathione Sepharose beads and 20 μl of the bead suspension exposed to detergent lysates of 3T3-L1 adipocytes for 2 hours. After three washes with 1 ml lysis buffer the pull-downs and 2.5% of the input lysates were subjected to SDS-PAGE on a 10% gel and immunoblotted for ubiquitin. Blot is representative of two independent experiments.

The immuoblot in Figure 4.2 demonstrates GST-VHS-GAT$_{mut}$ does not pull down the smear of ubiquitinated proteins seen for GST-VHS-GAT from an adipocyte lysate. This result indicates that mutation of E250 and D284 in the context of GST-VHS-GAT severely impairs the ability of the protein to bind ubiquitinated proteins, as expected from the published structures of the GGA3 GAT domain (Bilodeau *et al.*, 2004;Kawasaki *et al.*, 2005).

4.3.2 Expression of HA-GLUT4 and HA-GLUT4 7K/R in yeast.

Given that our lab has demonstrated that GLUT4 expressed in yeast is ubiquitinated (Lamb *et al.*, 2010) I decided to use this system to investigate the binding between GLUT4 and the GGA3 constructs generated above. Our lab has also found that the heterologously expressed transporter traffics in a nitrogen responsive manner (R. McCann and N. Bryant, unpublished). This bears considerable similarity to the trafficking of the nitrogen-regulated amino acid transporter Gap1p (Roberg *et al.*, 1997;Bryant *et al.*, 2002). Gap1p has been shown to require at least one of the two yeast GGAs for its ubiquitin-dependent post-Golgi trafficking to the endosomal system when yeast are grown on rich nitrogen sources (Scott *et al.*, 2004). The sorting of Gap1p and Gga1/2p depends on the presence of a ubiquitin binding GAT domain (Bilodeau *et al.*, 2004).

Importantly, replacement of the two yeast GGAs with a single chimaeric protein consisting of yeast Gga2p with its GAT domain replaced with that of hGGA3 can fully complement the loss of the yeast Ggas in a *gga1/gga2Δ* strain (Bilodeau *et al.*, 2004) which suggests that the ubiquitinated cargo binding function of this domain is conserved from yeast to mammals. With this in mind I set out to express an epitope tagged form of GLUT4 in yeast cells.

I used PCR with primers 1 and 2 (Table 2.5) on plasmids harbouring cDNAs encoding human GLUT4 with haemagglutinin epitope tags (HA) in the first extracellular loop (pRM55; Table 2.3) to amplify the cDNAs with the 3'UTR of *PHO8* and a 5' region homologous to the 3' end of the *CUP1* promoter. The PCR product was transformed into SF838-9Dα yeast, along with the gapped pNB701 plasmid. pNB701 contains the ORF for RS-ALP (Struthers *et al.*, 2009). By gapping the plasmid within the RS-ALP ORF using a *Xho*I/*Sal*I restriction digest

this allowed the GLUT4-HA and GLUT4 7K/R-HA fragments to repair the plasmid by homologous recombination. The whole scheme is illustrated in Figure 4.3.

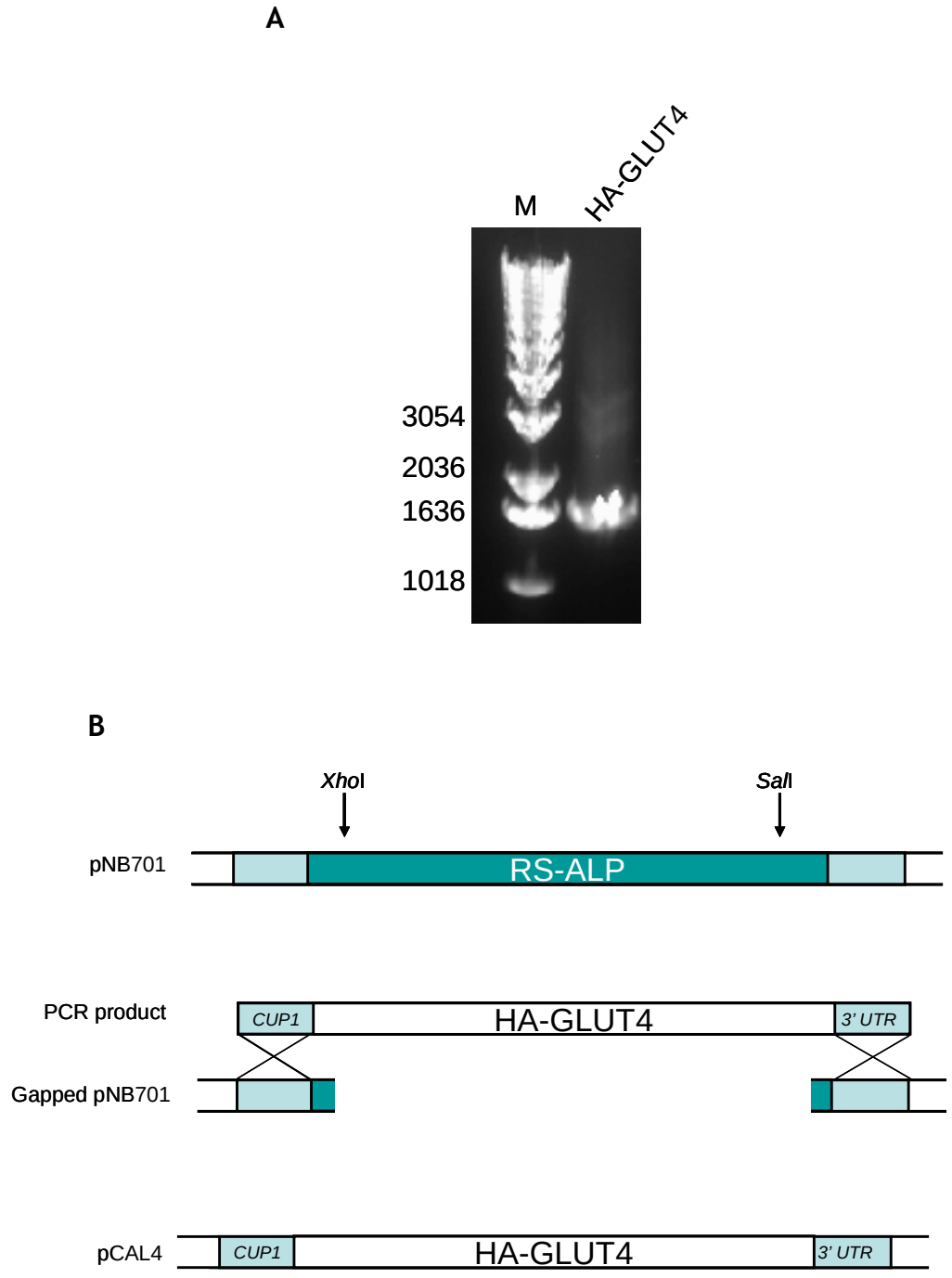

Figure 4.3 Generation of pCAL4.

A. The ORF of HA-GLUT4 was amplified from pRM55 using oligonucleotide primers 1 and 2 (detailed inTable 2.5). B. Schematic of homologous recombination in yeast. pNB701 was gapped by a restriction digest using *Xho*I and *Sal*I restriction enzymes, co-transformed into SF838-9Dα yeast with the PCR products from A allowing homologous recombination and plasmid repair to take place, generating pCAL4.

pCAL4 harbours the ORF of HA-GLUT4 under the control of the *CUP1* promoter. The *CUP1* gene encodes a metallothionein protein which mediates yeast cell resistance to high concentrations of Cu^{2+} (Winge *et al.*, 1985;Mascorro-Gallardo *et al.*, 1996), and its promoter region is more effective with higher concentrations of copper – thus resulting in titrateable expression of genes from this promoter. SF838-9Dα cells, deficient in vacuolar protease activity (Table 2.7) transformed with pCAL4 grown in selective media supplemented with 100 μM $CuSO_4$ produce a HA-immunoreactive protein of approximately 42 kD (Figure 4.4), which corresponds to the molecular weight of GLUT4 expressed in yeast (Kasahara and Kasahara, 1997;Lamb *et al.*, 2010).

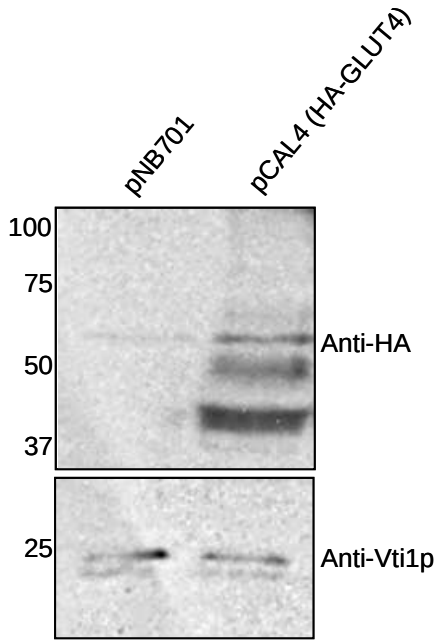

Figure 4.4 Expression of HA-GLUT4 in yeast.

SF838-9Dα cells harbouring pNB701 (empty vector), pCAL4 or pCAL5 were grown overnight in selective media in the presence of 100 μM $CuSO_4$, resuspended in TWIRL buffer as in 2.2.3. Equivalent amounts of cells were subjected to SDS-PAGE on a 10 % acrylamide gel and immunoblotted for the HA epitope and Vti1p.

4.3.3 Construction of the yeast strain BHNY1.

The reagents generated in 4.3.1 and 4.3.2 provide a basis on which to test the requirement for ubiquitination to mediate the interaction between the GAT domain of GGA3 and heterologously expressed GLUT4. As an initial test for whether mutation of the ubiquitin binding GAT domain would affect the ability

of GST-VHS-GAT to interact with GLUT4 I carried out a pull-down assay from lysates prepared from SF8389Dα yeast expressing HA-GLUT4. The results of this are shown in Figure 4.5. HA-GLUT4 is detected at the expected molecular weight of approximately 42 kD in both GST-VHS-GAT and GST-VHS-GAT$_{mut}$ pull-downs. However a higher band is present that may be caused by the excess of recombinant GST tagged protein in the lanes. Most interestingly there is a decrease in the amount of HA-GLUT4 pulled out of the yeast lysate when the GAT domain is mutated.

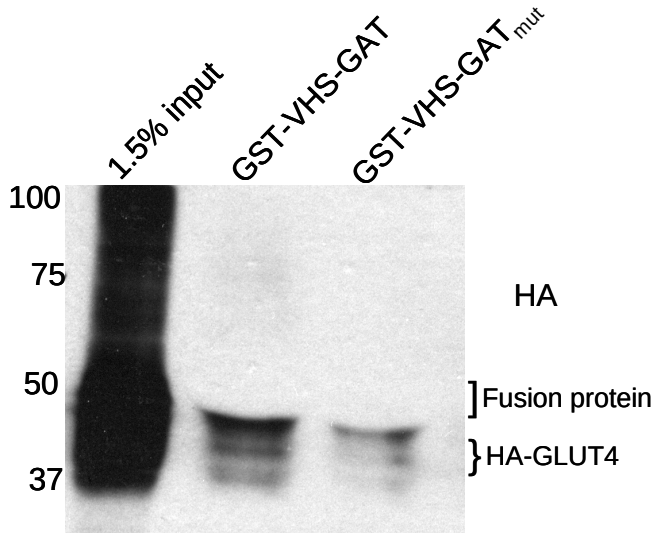

Figure 4.5 HA-GLUT4 expressed in yeast interacts with GST-VHS-GAT.

A 400ml culture of SF8389Dα yeast harbouring pCAL4 (HA-GLUT4) were grown to mid log phase in selective media supplemented with 100 µM $CuSO_4$. The cells were harvested by centrifugation, converted to spheroplasts and lysed in 500 µl of a buffer containing 1 % Triton-X100 and 1 mM NEM. 250 µl of the resulting lysates were incubated with 20 µl of a 50 % GST-VHS-GAT or GST-VHS-GAT$_{mut}$ bead slurry for 2 hours with continual mixing. After three washes with lysis buffer bound protein was eluted from the beads by heating for 10 minutes in 20 µl 2xLSB. Eluted proteins were subjected to SDS-PAGE alongside 2.5 % input lysate and immunoblotted for the HA epitope,

These initial data from SF8389Dα yeast suggest that GLUT4 interacts with GGA3 in a manner that is at least partially ubiquitin dependent; however this preliminary experiment would benefit from further controls. An ideal control for this experiment would be a yeast protein that can interact with GGAs via the VHS domain alone with no ubiquitin dependence. Although several mammalian proteins are known to bind the GGA VHS domain through their acidic dileucine sorting motifs, including sortilin and the mannose-6-phosphate receptors (Nielsen *et al.*, 2001;Tortorella *et al.*, 2007) only a single yeast protein has been shown to exhibit VHS domain binding. This protein is Mon2p (Monensin sensitivity), also known as Ysl2p, a *trans*-Golgi resident protein related to Arf

GTP-exchange factors, which is involved in maintenance of Golgi architecture and has been shown to bind isolated VHS and VHS-GAT domains (Efe *et al.*, 2005;Gillingham *et al.*, 2006;Singer-Kruger *et al.*, 2008).

I utilized the commercially available yeast strain YNL297C expressing green fluorescent protein (GFP) tagged Mon2p (Invitrogen; (Huh *et al.*, 2003)). In order to detect GLUT4 in yeast grown on rich media, it is necessary to inactivate vacuolar proteases as the transporter is delivered to the proteolytically active endosomal system (Lamb *et al.*, 2010).

The *PEP4* gene product, which activates many of the proteases present in the yeast vacuole (van den Hazel *et al.*, 1992), was disrupted in GFP-Mon2p expressing YNL297C using the loop in/loop out method by transforming the cells with *Eco*RI digested (linearised) pPLO2010, which contains the *URA3* gene flanked with sequences homologous to *PEP4* and further sequences which permit looping out of the *URA3* cassette (Nothwehr *et al.*, 1995). Integration of this fragment was selected for by plating transformants onto solid SD-URA media. To select for transformants which had looped out the *URA3* cassette, they were plated onto media containing 5-fluoroorotic acid (5-FOA). The *URA3* gene product is orotine-5'monophosphate dicarboxylase, which converts 5-FOA to toxic fluorodeoxyuridine (Boeke *et al.*, 1984). Therefore only those cells lacking *URA3* survive on 5-FOA containing media.

A selection of 5-FOA resistant colonies were collected and tested for the *pep4-3* mutation in the APNE overlay assay (Wolf and Fink, 1975). This assay detects the activity of carboxypeptidase Y (CPY) which is activated by the *PEP4* gene product proteinase A (van den Hazel *et al.*, 1992). CPY activity releases β-napthol from APNE. β-napthol reacts with the Fast Garnet GBC salt present in the overlay mixture producing an insoluble red dye; thus strains which secrete CPY are red, whereas strains that missort (and thus do not activate) CPY remain white due to a lack of active CPY.

A single 5-FOA resistant *pep4-3* colony was selected in this manner and named BHNY1.

4.3.4 An in vitro *interaction between GLUT4 and GST-GGA3-VHS-GAT is partly ubiquitin dependent.*

Armed with the reagents generated in 4.3.1, 4.3.2 and 4.3.3 I set out to test whether there is a ubiquitin dependent *in vitro* interaction between hGLUT4 expressed in yeast and GST-GGA3-VHS-GAT. 400 ml cultures of BHNY1 yeast transformed with pCAL4 or 5 (encoding HA-GLUT4 and HA-GLUT4 7K/R respectively) were grown to an OD_{600} of 0.5, harvested and lysates prepared. The lysates were incubated with GST-VHS-GAT and GST-VHS-GAT_{mut} immobilized on beads. Bound proteins were eluted from the beads and subject to SDS-PAGE alongside a sample of the input lysate.

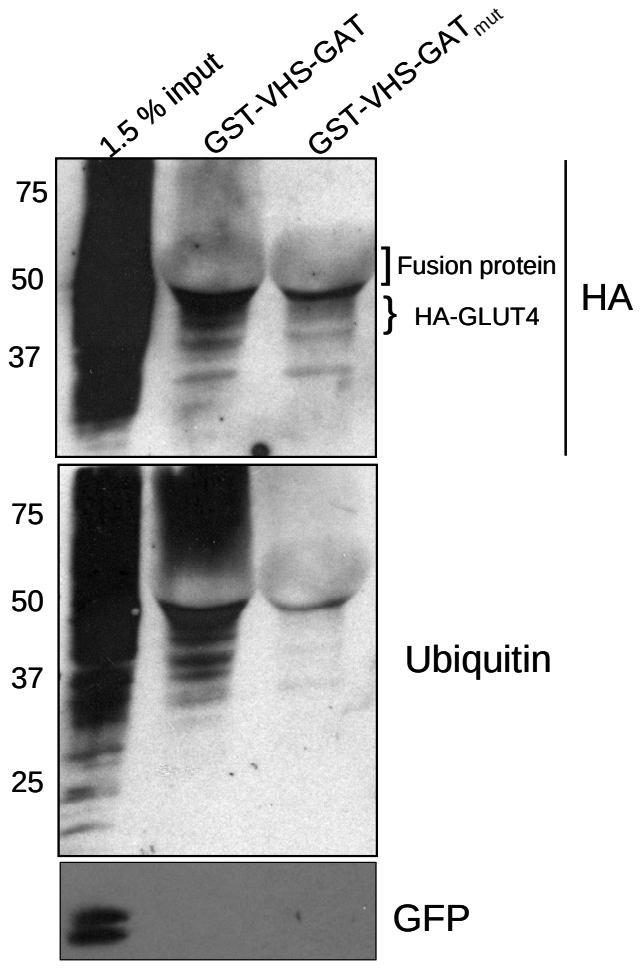

Figure 4.6 GLUT4 expressed in yeast interacts with GST-VHS-GAT in a ubiquitin dependent manner.

400ml cultures of BHNY1 yeast harbouring pCAL4 (HA-GLUT4) were grown to mid log phase in selective media supplemented with 100 µM $CuSO_4$. The cells were harvested, lysed and used in pull-down assays as described for Figure 4.5. Eluted proteins were subjected to SDS-PAGE alongside 2.5 % input lysate and immunoblotted for the HA epitope, GFP and ubiquitin. Results are representative of three independent experiments.

A typical result for this experiment is shown in Figure 4.6. As observed for SF8389Dα yeast, HA-GLUT4 expressed in BHNY1 shows a detectable interaction between HA-GLUT4 and GST-VHS-GAT, and there is a less pronounced interaction between HA-GLUT4 and GST-VHS-GAT$_{mut}$. However as previously discussed the GST fusion proteins distort the HA-GLUT4 band due to the high levels of fusion protein present in the pull-down reactions making these experiments somewhat difficult to interpret.

These data suggest that there is an interaction between heterologously expressed HA-GLUT4 and the VHS-GAT domain of GGA3 and this interaction is at least partially dependent on the presence of a functional ubiquitin-binding site in the GAT domain of GST-VHS-GAT. As expected, and demonstrated in Figure 4.2, there is reduced binding of ubiquitin to GST-VHS-GAT$_{mut}$ (compared to GST-VHS-GAT) in these experiments. One caveat with this result is that although BHNY1 expresses detectable amounts of Mon2p-GFP (input lane) there is no detectable interaction observed with either GST-VHS-GAT or GST-VHS-GAT$_{mut}$. Previous studies have suggested that isolated VHS domain alone interacts more readily with Mon2p than VHS-GAT (Singer-Kruger *et al.*, 2008), so perhaps the level of interaction between Mon2p and GST-VHS-GAT is undetectable because of this effect.

I decided to extend this study to insulin responsive 3T3-L1 adipocytes to investigate whether an interaction between endogenous GLUT4-Ub and GST-VHS-GAT can be detected. The results of this experiment are shown in Figure 4.7. Although, as was previously demonstrated in Figure 4.2, GST-VHS-GAT readily pulls down a smear of ubiquitinated substrates, there is no discernible interaction between endogenous GLUT4 and GST-VHS-GAT.

Although there was no interaction detected between endogenous GLUT4 and recombinant GGA3-VHS-GAT in adipocytes, the data from yeast suggested that the ubiquitin binding GAT domain of GGA3 could interact with a small pool of GLUT4. Ubiquitinated species are enriched in the BHNY1 strain due to an absence of vacuolar proteases (4.3.3) and previous data from our lab has indicated that in 3T3-L1 adipocytes approximately 0.1 % of the total GLUT4 pool is ubiquitinated (Lamb *et al.*, 2010). Coupled with the relatively low affinity of the GGA3 GAT domain for ubiquitin (K_d = 231 μM)(Kawasaki *et al.*, 2005) this is

likely to make detection of ubiquitinated GLUT4 binding to GST-VHS-GAT by a pull-down method rather challenging.

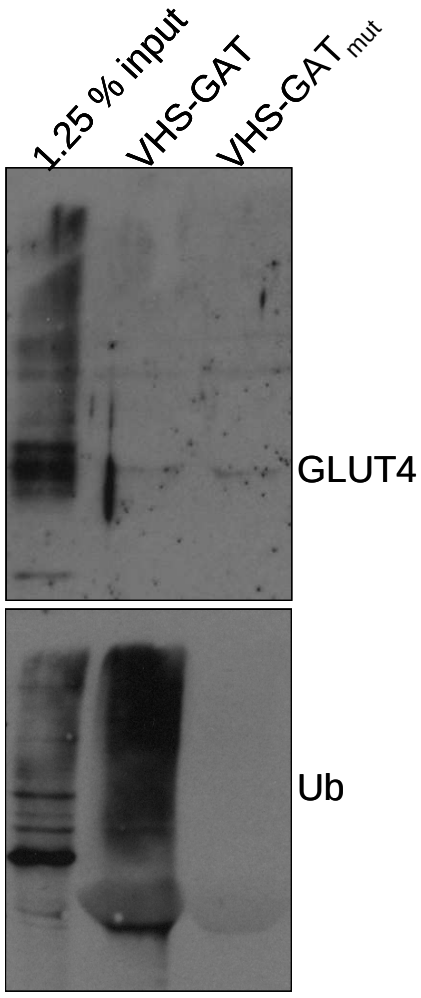

Figure 4.7 GST-VHS-GAT pull-down assay on 3T3-L1 adipocyte lysates.

4 plates of 3T3-L1 adipocytes were serum starved for 2 hours and lysed in a buffer containing 1 % Triton-X100 and 1 mM NEM. 500 µl of the clarified lysates was incubated with with 20 µl of a 50 % GST-VHS-GAT or GST-VHS-GAT$_{mut}$ bead slurry for 2 hours with continual mixing. After three washes with lysis buffer bound protein was eluted from the beads by heating for 10 minutes in 20 µl 2xLSB. Eluted proteins were subjected to SDS-PAGE alongside 1.25 % input lysate and immunoblotted for GLUT4 and ubiquitin. Results are representative of three independent experiments.

4.4 Expression of a ubiquitin-binding mutant of myc-GGA3 in 3T3-L1 adipocytes.

As the biochemical approaches I had initially set out to use were not suitable for detecting an effect on interaction of endogenous GLUT4-Ub with GGA3, I decided to express epitope tagged versions of wild type, full length GGA3 and a mutant version predicted to abolish ubiquitin binding (harbouring the same E250N D284G substitutions as the the recombinant GST-VHS-GAT$_{mut}$ used in

4.3.4) in 3T3-L1 adipocytes and observe any effect of overexpression of these proteins on GLUT4 loading into GSVs and/or the ability of insulin to stimulate glucose transport into the cells. Expression of a dominant negative GGA construct (EGFP-VHS-GAT) resulted in reduced budding of GLUT4 vesicles in an *in vitro* assay, impaired loading of GLUT4 into GSVs, and reduced insulin responsiveness of the transporter (Watson *et al.*, 2004;Li and Kandror, 2005). Therefore if the ubiquitin binding function of the GGA proteins is required to sort GLUT4 into GSVs, I would predict that expression of the non-ubiquitin-binding myc-GGA3$_{mut}$ would reduce GLUT4 loading into GSVs and thus impair insulin stimulated glucose uptake.

To test this, I generated a chimeric gene incorporating a 5' sequence encoding the myc epitope tag fused to the *GGA3* short isofom cDNA in the pBABE puro retroviral expression vector (Morgenstern and Land, 1990) (pCAL11), and used site directed mutagenesis of pCAL11 to produce a construct encoding myc-GGA3 E250N D284G (myc GGA3$_{mut}$) (pCAL12) which is predicted to be impaired in ubiquitin binding function according to data from this and previous studies (section 4.3.1, (Bilodeau *et al.*, 2004;Kawasaki *et al.*, 2005)).

pCAL11, pCAL12 (encoding myc-GGA3 and myc-GGA3$_{mut}$ respectively) and pBABE puro (as an empty vector control) were transfected into Plat-E packaging cells (Morita *et al.*, 2000), resulting in production of retroviral particles. 3T3-L1 fibroblasts were stably infected with each of the viruses, grown to confluency and differentiated into adipocytes. Lysates were subsequently prepared for western blot analysis. Blotting for the myc epitope and GAPDH (as a loading control) showed that cells infected with pCAL11 and 12 retroviruses exhibited an immunoreactive band at approximately 85 kD as has been previously reported for the GGA3 short isoform (Wakasugi *et al.*, 2003). However, myc-GGA3$_{mut}$ was consistently detected at much higher levels than the wild type protein (Figure 4.8).

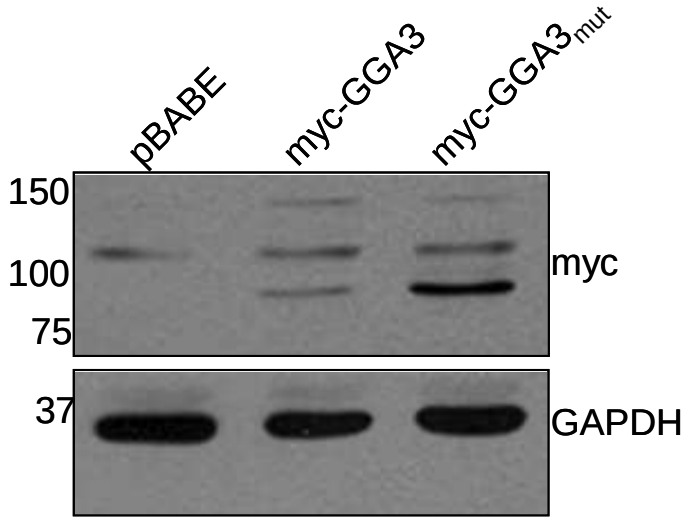

Figure 4.8 Expression of myc-GGA3 and myc-GGA3$_{mut}$ in 3T3-L1 adipocytes.

3T3-L1 fibroblasts were infected with the retroviral constructs pBABE puro (pBABE), pCAL11 (myc GGA3) and pCAL12 (myc-GGA3$_{mut}$), plated onto 2 10 cm plates per construct, grown to confluency and differentiated into adipocytes. Cells were harvested in 250 µl PBS supplemented with protease inhibitors per plate, homogenised with 12 strokes through a syringe and needle (10 x 25G, 2 x 26G) and the homogenate clarified by centrifugation. The homogenates were equalized for protein content and 20 µg protein subjected to SDS-PAGE on 10 %(v/v) gels, followed by immunoblotting for the myc epitope and GAPDH as a loading control. Blots are representative of three independent experiments.

This difference in levels of the wild type and mutant versions of myc-GGA3 has several possible explanations. It may be that the myc-GGA3$_{mut}$ viral stock infects 3T3-L1 fibroblasts more readily, or that myc-GGA3$_{mut}$ is more stable than myc-GGA3. To address whether the observed difference was due to differing levels of retroviral infection I performed a titration of the retroviral stock used to stably infect the 3T3-L1 cells. The pCAL11 (myc-GGA3) and pCAL12 (myc-GGA3$_{mut}$) virus stocks were used in a series of six tenfold dilutions (10^{-1} to 10^{-6}) to infect 3T3-L1 fibroblasts on 6 well plates. After a week of selection using DMEM supplemented with 10 % FBS and 2.5 µg/ml puromycin, the number of colonies present on the highest dilution plate was recorded. The pCAL11 viral stock gave 1 x 10^6 colony forming units per ml (cfu/ml) whereas the pCAL12 stock gave 9 x 10^5 cfu/ml. This result suggests that the observed differences in expression between myc-GGA3 and myc-GGA3$_{mut}$ are not due to differences in the ability of the two viruses to infect 3T3-L1 cells, but may be due to post-infection events such as the relative stability of the myc-GGA3 and myc-GGA3$_{mut}$ proteins. This possibility will be discussed in more detail at the end of the chapter.

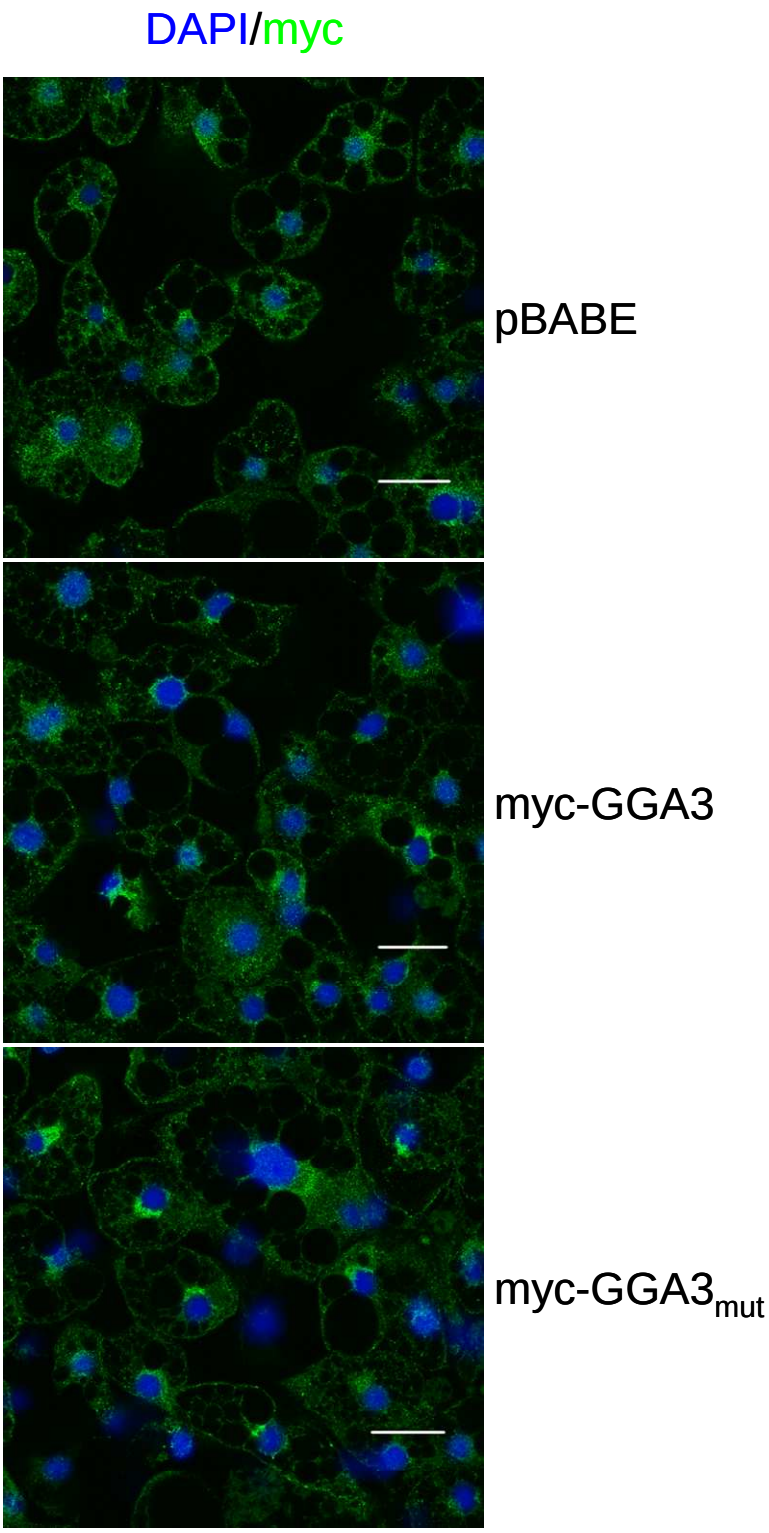

Figure 4.9 Localisation of myc-GGA3 and myc-GGA3$_{mut}$ expressed in 3T3-L1 adipocytes.

3T3-L1 fibroblasts infected with either empty pBABE puro (pBABE), pCAL11 (myc-GGA3) or pCAL12 (myc-GGA3$_{mut}$) virus were grown to confluency on sterile coverslips, differentiated into adipocytes and processed for confocal microscopy, staining for the myc epitope and nuclear DNA with DAPI. Images are representative from three experiments. Scale bar = 20 µm

To address whether the two constructs have differences in subcellular localisation, the infected cells were plated onto coverslips and stained for the myc epitope and DAPI to mark the nucleus. When visualized by confocal microscopy (Figure 4.9) both myc-GGA3 and myc-GGA3$_{mut}$ exhibited the perinuclear localization characteristic of the GGAs (Dell'Angelica *et al.*, 2000;Hirst *et al.*, 2000). Qualitatively there appears to be an increase in the amount of perinuclear staining in cells expressing myc-GGA3$_{mut}$. This suggests that despite the relatively high expression level of myc-GGA3$_{mut}$ there is no change in the subcellular localisation of the mutant compared to the wild type protein.

4.4.1 *Does expression of myc-GGA3 and myc-GGA3$_{mut}$ alter GLUT4 loading into the insulin responsive compartment?*

To assess the functional consequences of expressing myc-GGA3 and myc-GGA3$_{mut}$ in 3T3-L1 adipocytes I first used a subcellular fractionation approach, as detailed in 3.5, to assess the proportion of GLUT4 loaded into the GSV enriched 16,000 xg supernatant of 3T3-L1 cells (Xu and Kandror, 2002;Kupriyanova *et al.*, 2002;Li and Kandror, 2005). Previously, expression of dominant negative EGFP-VHS-GAT has been shown to impair loading of GLUT4 into GSVs using this system (Li and Kandror, 2005). If either myc-GGA3 or myc-GGA3$_{mut}$ had a dominant negative effect on GLUT4 loading into GSVs, I would anticipate a lower proportion of GLUT4 would be found in the supernatant fraction. The results of this experiment are detailed in Figure 4.10. 40.3 % (± 3.5 %) of the total GLUT4 was found in the supernatant fraction in cells harbouring pBABE puro. The situation was similar in cells expressing myc-GGA3 - although 44.7 % (± 2 %) of total GLUT4 was found in the supernatant, this increase did not reach statistical significance ($p = 0.18$, Student's T-test). However on expression of myc-GGA3$_{mut}$ in adipocytes only 30.6 % (± 2.4 %) of total GLUT4 was found in the supernatant, which was significantly different from both cells expressing empty pBABE puro ($p < 0.05$) and those expressing myc GGA3 ($p < 0.01$).

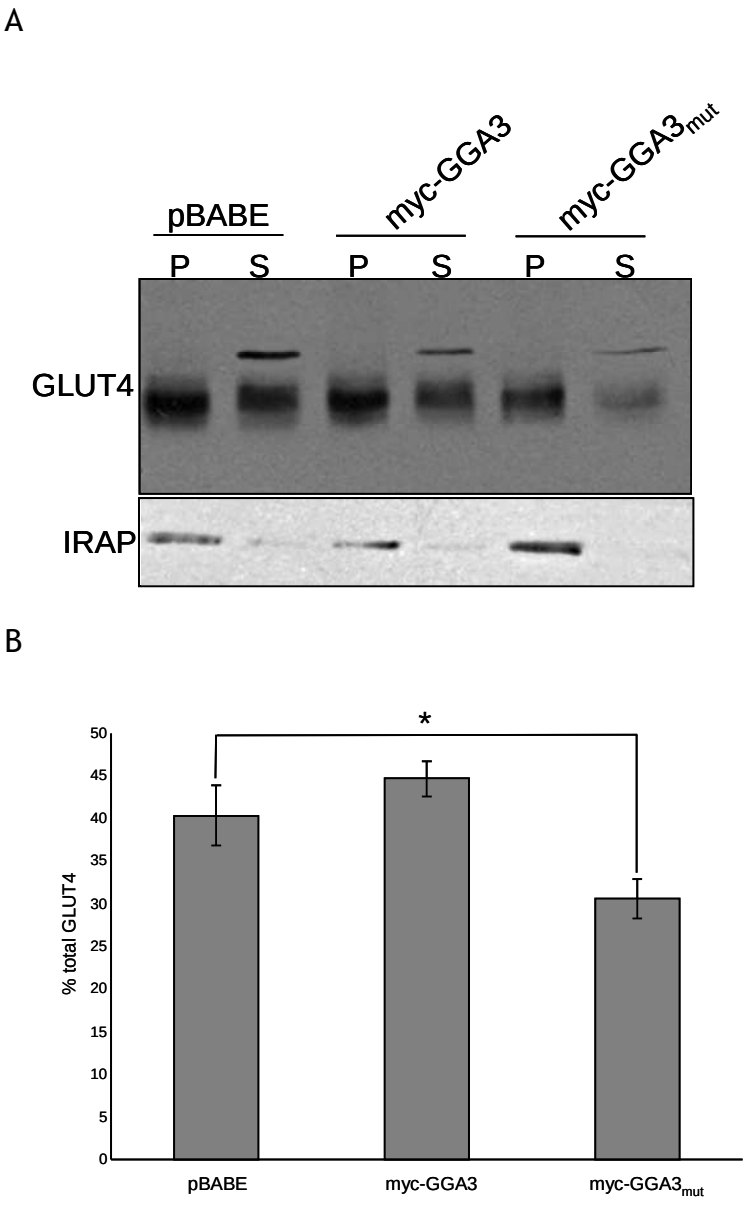

Figure 4.10 GLUT4 loading into the 16,000 xg supernatant is reduced by expression of myc-GGA3$_{mut}$.

(A) 3T3-L1 adipocytes (2 10 cm plates per construct) harbouring empty pBABE puro (pBABE), pCAL11 (myc-GGA3) or pCAL12 (myc-GGA3$_{mut}$) retrovirus were homogenised in 250 µl PBS supplemented with protease inhibitors (PBS + I) per plate by passage through a syringe and needle (10 x 25G, 2 X 26G) and insoluble components removed by centrifugation at 2000 xg for 10 minutes at 4 ℃. The resulting supernatants were c entrifuged at 16,000 xg for 20 minutes at 4 ℃, separating pellet (P) and supernatant (S) fractions. The pellet was resuspended in 500 µl PBS + I and both fractions equalized for protein content. 30 µg of both pellet and supernatant was subject to SDS-PAGE on 10 % (v/v) gels and blotted for IRAP and GLUT4. Blots are representative of three independent experiments. (B) The percentage of total GLUT4 present in the supernatant fraction was measured from three independent experiments using image analysis software (ImageJ, NIH) and plotted. * significantly different from cells harbouring pBABE ($p < 0.05$, Student's T-test)

As a control, the pellet and supernatant fractions were also blotted for the insulin responsive aminopeptidase IRAP. IRAP is another GSV cargo which occupies the same trafficking itinerary as GLUT4 (Ross *et al.*, 1997). The

distribution of IRAP between supernatant and pellet fractions was not altered significantly by expression of myc-GGA3 or myc-GGA3$_{mut}$, with the greater proportion of IRAP found in the pellet fraction for all three groups of cells.

This result is interesting in that expression of the ubiquitin-binding deficient myc-GGA3$_{mut}$ appears to have a mild dominant negative effect on GLUT4 loading into GSVs, reducing the amount of total GLUT4 found in the 16,000 xg supernatant by 10 % relative to controls. myc-GGA3 could still potentially have an effect on GLUT4 traffic; however its low expression level in this system may mask any possible phenotypes.

4.4.2 *Does expression of myc-GGA3 and myc-GGA3$_{mut}$ alter insulin responsive [^{3}H]2-deoxyglucose uptake?*

As GLUT4 loading into the insulin responsive 16,000 xg supernatant is impaired by mutation of the GAT domain in the context of myc-GGA3, I wanted to test whether this altered loading translated to impaired insulin responsive GLUT4 translocation. It would be technically challenging to use the HA-GLUT4 translocation assay as it would involve co-infection of 3T3-L1 cells with two different retroviruses. I therefore decided to use an indirect measure of GLUT4 translocation, namely the [^{3}H]2-deoxyglucose uptake assay (Millar *et al.*, 1999). This assay measures the uptake of the radiolabelled glucose analogue [^{3}H]2-deoxyglucose into cells with and without insulin stimulation. As previously discussed in 1.4.2 the increase in glucose uptake on insulin stimulation is almost entirely due to GLUT4 translocation (Saltiel and Kahn, 2001) so a perturbation in [^{3}H]2-deoxyglucose uptake would indicate altered GLUT4 translocation.

A reduction in insulin stimulated glucose uptake on expression of EGFP-VHS-GAT in 3T3-L1 adipocytes compared to cells harbouring an empty vector control has previously been reported (Li and Kandror, 2005). To test whether this would also be the case for overexpression of myc-GGA3$_{mut}$, I carried out [^{3}H]2-deoxyglucose uptake assays on cells stably infected with pBABE puro, pCAL11 and pCAL12 (encoding myc-GGA3 and myc-GGA3$_{mut}$ respectively).

As shown in Figure 4.11, expression of myc-GGA3 does not alter insulin stimulated glucose uptake compared to cells harbouring empty vector. There is a slight decrease in insulin stimulated glucose uptake on expression of myc-

GGA3$_{mut}$; however this does not reach statistical significance when compared to cells harbouring empty vector (p = 0.18, Student's T-test). It is difficult to draw any firm conclusions from this assay due to the variability of results between experiments. The mean values for glucose uptake (in pmoles/min/cell) for each of the 4 replicate experiments are detailed in Appendix I and illustrate the variability between experiments, ranging from 0.0118 to 0.0713 nmoles/min/well in the case of myc-GGA3. This suggests great variation in the glucose uptake between batches of cells which was unexpected as the cell lines used in these experiments were all products of a single infection, with each experiment being from a different passage number of the same cell line.

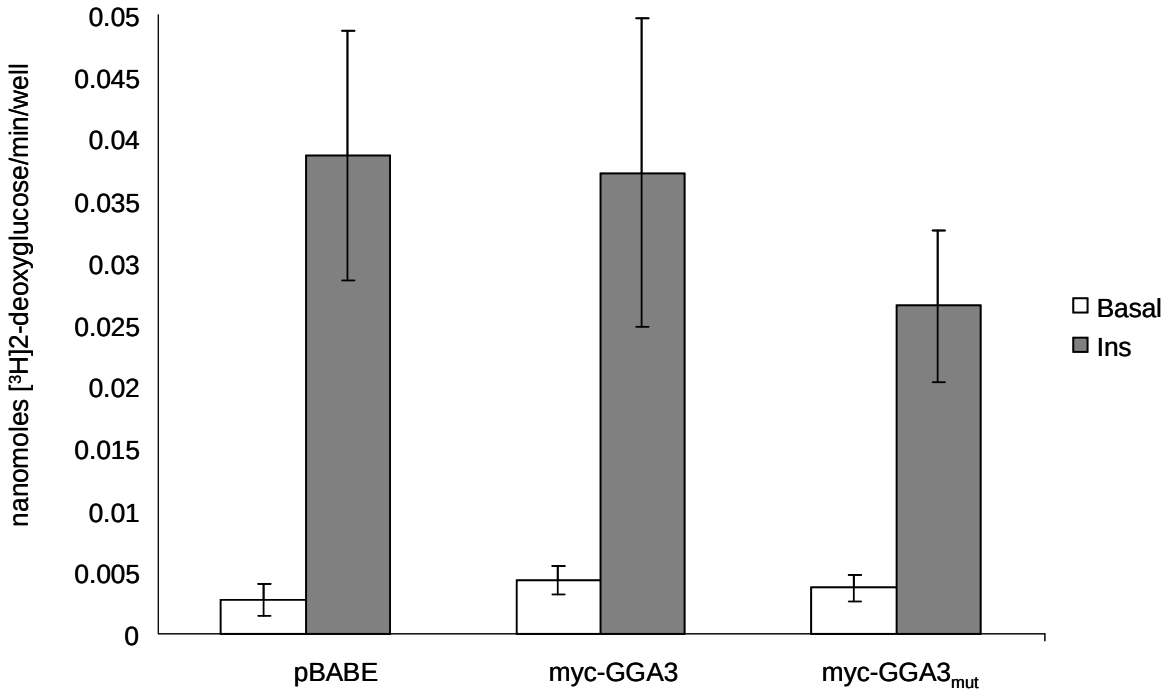

Figure 4.11 Insulin stimulated glucose uptake rate is not affected by expression of myc-GGA3 or myc-GGA3$_{mut}$.

12 well plates of 3T3-L1 adipocytes harbouring either pBABE puro (pBABE), pCAL11 (myc-GGA3) or pCAL12 (myc-GGA3$_{mut}$) were either stimulated with 100 nM insulin (Insulin) or not (Basal) for 30 minutes, followed by incubation with 50 µM [^{3}H]2-deoxyglucose per well for 5 minutes. After the incubation excess [^{3}H]2-deoxyglucose was washed from the cells using cold PBS. The plates were dried, cells lysed in 1 ml 1 % (v/v) Triton X-100 and cell associated radioactivity measured using liquid scintillation spectrophotometry. n = 4, results are presented ± standard error of the mean.

4.5 Chapter Discussion

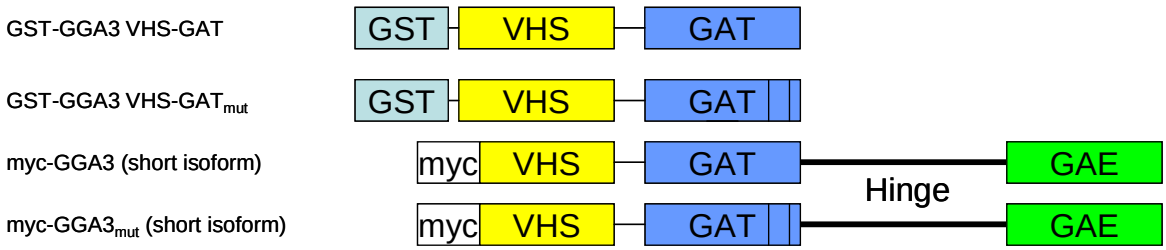

Figure 4.12 Recombinant GGA3 proteins used in this chapter.

Glutathione S-transferase (GST) purification and myc epitope tags are indicated. Black vertical bars in GAT domain indicate sites of E250N and D284G mutations.

In this chapter I set out to investigate whether GGA ubiquitin binding is required for their role in sorting GLUT4 into the insulin responsive compartment. To do this I took advantage of the published crystal and solution structures of the GGA3 GAT domain in complex with ubiquitin (Bilodeau *et al.*, 2004;Kawasaki *et al.*, 2005), to generate mutant versions of GGA3 which are severely impaired in their ability to bind ubiquitin.

I first used site directed mutagenesis to mutate E250 and D284 of the GGA3 GAT domain in the context of a fusion protein consisting of GST fused to the VHS-GAT domains of GGA3 (GST-VHS-GATmut). As shown in Figure 4.2, GST-VHS-GATmut could not pull ubiquitinated proteins out of a 3T3-L1 adipocyte cell lysate. I then set out to test whether HA-GLUT4 expressed in yeast could interact with immobilised GST-VHS-GAT.

As shown in Figure 4.6, HA-GLUT4 can bind GST-VHS-GAT. This interaction appears to be partially dependent on the ubiquitin binding function of the GAT domain as it is decreased when the GAT domain of the fusion protein is mutated. Despite the VHS domain of both GST-VHS-GAT and GST-VHS-GAT$_{mut}$ being intact, as the original GST-VHS-GAT expression construct (pGEX GGA3 VHS-GAT) was generated from the long isoform of GGA3 (Dell'Angelica *et al.*, 2000), no interaction was observed between either fusion protein and GFP tagged Mon2p, which is the only *S. cerevisiae* protein known to interact with GGA VHS domains (Singer-Kruger *et al.*, 2008). However the interaction between the VHS domain and Mon2p is less effective when the GAT domain is also present (Singer-Kruger

et al., 2008) which could explain the lack of binding observed in this experiment.

Unfortunately I was not able to extend this *in vitro* study of GLUT4 and GGA3 GAT interaction to 3T3-L1 adipocytes. The low affinity of the GAT domain for ubiquitin (Kawasaki *et al.*, 2005) in combination with the low abundance of ubiquitinated GLUT4 in 3T3-L1 cells (Lamb *et al.*, 2010), will likely prove technically challenging in using this pull-down approach to studying the interaction further.

I next went on to clone myc-GGA3 and generate a ubiquitin-binding deficient mutant thereof (myc-GGA3$_{mut}$) and express these constructs in 3T3-L1 cells, using the pBABE puro retroviral expression system (Morgenstern and Land, 1990). Despite infection of 3T3-L1 fibroblasts with similar numbers of viral particles harbouring pCAL11 and pCAL12 (section 4.4), the expression of myc-GGA3 was much lower than myc-GGA3$_{mut}$ when compared by Western blotting. Although myc-GGA3$_{mut}$ was relatively overexpressed both proteins had a similar perinuclear localisation (Figure 4.9).

What possible explanations are there for the observed difference in expression? The answer may lie with ubiquitination of GGA3 itself. Previous studies have shown that GGA3 is ubiquitinated (Shiba *et al.*, 2004;Pak *et al.*, 2006) and that this ubiquitination depends on the ubiquitin binding ability of the GAT domain, as single amino acid substitutions introduced within the ubiquitin binding portion of the GAT domain severely impair GGA3 ubiquitination (Shiba *et al.*, 2004). This study did not report an increase in the levels of GGA3 expression as a consequence of GAT mutation; however the GGA3 expression constructs used by Shiba *et al*. were for transient expression of GGA3. As I was using the pBABE retroviral system (Morgenstern and Land, 1990) to stably express myc-GGA3 and myc-GGA3$_{mut}$ in polyclonal pools of cells, it is hard to compare the two sets of data and further investigation of the role of the GAT domain in GGA3 stability would certainly be valuable. It may be that myc-GGA3 is more readily ubiquitinated than myc-GGA3$_{mut}$ and is thus degraded more rapidly by the proteasome, although without further analysis this remains purely speculation.

I went on to analyse the phenotypic effects of myc-GGA3 and myc-GGA3$_{mut}$ expression in 3T3-L1 adipocytes. Firstly I used a subcellular fractionation approach to isolate a GSV enriched vesicular fraction from 3T3-L1 adipocytes (Xu

and Kandror, 2002;Li and Kandror, 2005) harbouring either an empty vector control, pCAL11 or pCAL12 retrovirus. On expression of myc-GGA3 the loading of GLUT4 into the 16,000 xg supernatant is unaffected, however expression of myc-$GGA3_{mut}$ lowers the proportion of total GLUT4 present in the supernatant fraction, from 40.3 % (± 3.5 %) to 30.6 % (± 2.4 %) (Figure 4.10). These data substantiate the previous study outlining a role for GGAs in the sorting of GLUT4 into the insulin responsive compartment (Li and Kandror, 2005), as this study found that expressing a dominant negative version of GGA (EGFP fused to the VHS-GAT domains of GGA2) reduced the proportion of GLUT4 present in the GSV fraction compared to cells harbouring an empty vector.

The dominant negative effect of myc-$GGA3_{mut}$ expression is less than that observed for EGFP-VHS-GAT (Li and Kandror, 2005). The most obvious explanation is the structure of the two mutants. EGFP-VHS-GAT was derived from human GGA2, and thus would be expected to bind VHS domains more readily than ubiquitin modifications (Nielsen *et al.*, 2001;Puertollano and Bonifacino, 2004;Shiba *et al.*, 2004), whereas myc-$GGA3_{mut}$ was derived from the short isoform of GGA3 (see Figure 4.12). It has been predicted that the short isoform of GGA3 cannot bind dileucine motifs; the crystal structure of GGA1 VHS in complex with the C-terminal acidic dileucine motif of the cation independent mannose-6-phosphate receptor has been published, and GGA1 VHS residues involved in this interaction identified (Shiba *et al.*, 2002). These residues are conserved in full length GGA3, however they are absent from GGA3 short (Wakasugi *et al.*, 2003).

Therefore in terms of dominant negative activity, EGFP-VHS-GAT can interfere with the recruitment of endogenous GGAs to membranes (via Arf-GTP recruitment) and interaction with dileucine motifs. myc-$GGA3_{mut}$ (derived from GGA3 short) would be predicted to block membrane association of endogenous GGAs and to sequester factors which bind to the hinge region and GAE domain; these include clathrin and the BAR domain containing protein enthprotin, which are involved in formation of clathrin coated vesicles (Hirst *et al.*, 2001;Mills *et al.*, 2003).

IRAP and sortilin are two acidic dileucine-containing proteins which can bind GGA VHS domains and are present in GSVs (Nielsen *et al.*, 2001;Hou *et al.*,

2006). More recently, the sortilin, IRAP and GLUT4 lumenal domains have been shown to interact physically (Shi and Kandror, 2007;Shi *et al.*, 2008).

From these data I propose a model for GGA binding to GSV cargoes at the TGN (Figure 4.13). Sortilin (or IRAP) and GLUT4-Ub cluster together at the TGN, brought into close proximity by their lumenal interactions. The GGAs, with their modular structure, can bind to GLUT4-Ub via the GAT domain, and to the acidic dileucine motifs present in the other cargo molecules, recruiting clathrin and accessory proteins resulting in vesicle budding. This model would account for the larger effect EGFP-VHS-GAT expression on GLUT4 loading into GSVs, as EGFP-VHS-GAT would prevent endogenous GGAs from interacting with GLUT4-Ub, ARF:GTP and the cytosolic domains of IRAP or sortilin.

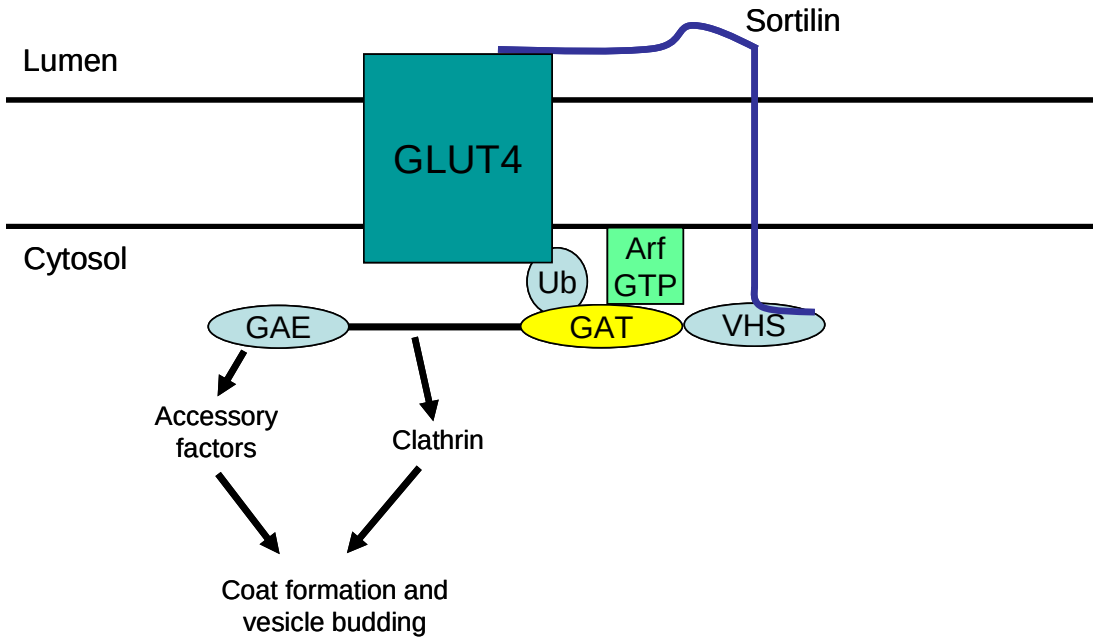

Figure 4.13 A model for GGA function in GSV cargo recruitment.

Sortilin and GLUT4 are brought into proximity by their lumenal interactions. GGAs bind to the ubiquitinated GLUT4 cytosolic domain and the acidic dileucine motif in the sortilin cytoplasmic tail, resulting in clathrin coat formation and vesicle budding.

The proposed model is supported by work with truncation mutants of sortilin. A full length version of sortilin co expressed with GLUT4 in 3T3-L1 fibroblasts induces formation of an insulin responsive compartment in these normally non insulin responsive cells (Shi and Kandror, 2005). However a version of sortilin lacking the lumenal domain, and therefore not capable of interacting with the

lumenal region of GLUT4, can only partially recapitulate this effect (Shi and Kandror, 2005).

In cells expressing myc-GGA3$_{mut}$ there is a slight reduction in insulin stimulated glucose uptake, however this reduction does not reach statistical significance (Figure 4.11). As discussed in section 4.4.2, there is large variability in the results for insulin stimulated glucose uptake for all three constructs. As the effect of myc-GGA3$_{mut}$ on GLUT4 loading into the GSV enriched 16,000 xg supernatant is apparently quite small with only a 10 % loss of total GLUT4 from this fraction, the large variability in the glucose transport assay data may be masking any effect of myc-GGA3$_{mut}$ expression on glucose uptake.

In summary, the data presented in this chapter implicate the ubiquitin binding region of the GAT domain of GGA3 in the sorting of GLUT4 into the insulin responsive compartment. When taken together with data from the preceding chapter that GLUT4 sorting into GSVs requires its ubiquitination, and data from a study by our group implicating the yeast Ggas in ubiquitin dependent sorting of GLUT4 from the TGN to the proteolytically active endosomal system (Lamb *et al.*, 2010), this lends weight to the hypothesis that GLUT4 ubiquitination is one of the signals required for GGA dependent sorting of GLUT4 into the GSV compartment.

Chapter 5 - Deubiquitination and GLUT4 traffic.

5.1 Introduction

Although work in our group (this study, Chapter 3, (McCann R.K., 2007;Lamb *et al.*, 2010)) has implicated ubiquitin in the loading of GLUT4 into GSVs, one potential flaw in the hypothesis that ubiquitination is required to sort GLUT4 into GSVs is that ubiquitination of membrane proteins is canonically thought of as a modification resulting in protein degradation at the lysosome (Hicke and Dunn, 2003;Urbe, 2005). Ubiquitin dependent delivery of proteins to the lysosome is facilitated through MVBs, with ubiquitin acting as a signal for ESCRT-dependent sorting of membrane proteins into the intralumenal vesicles of MVBs (Wollert *et al.*, 2009;Raiborg and Stenmark, 2009). Work from our group has shown that a constitutively ubiquitinated version of GLUT4 (GLUT4 7K/R-Ub) is effectively trafficked into the yeast endosomal system (McCann R.K., 2007) indicating that the modification is sufficient for GGA dependent sorting into the endosomal system.

While it is clear that ubiquitination of GLUT4 is required for the transporter to become insulin sensitive, our lab estimates that only about 0.1 % of cellular GLUT4 is ubiquitinated in 3T3-L1 adipocytes (Lamb *et al.*, 2010). This suggests that the ubiquitin modification on GLUT4 is a transient one, and introduces the possibility that deubiquitinating enzymes may play a role in GLUT4 traffic.

Deubiquitinating enzymes (DUBs) function at various levels of cellular regulation, including maintenance of free ubiquitin levels and promotion of protein stability (Komander *et al.*, 2009;Reyes-Turcu *et al.*, 2009). In the endosomal system, DUBs have been shown to play a role in receptor recycling and resensitisation; examples include the β2 adrenergic receptor which is deubiquitinated by USP20 and USP33 (Berthouze *et al.*, 2009), and the *Drosophila* Wnt receptor Frizzled which is deubiquitinated by USP8 (Mukai *et al.*, 2010). In both these cases, a proportion of the internalised receptor is deubiquitinated, thus being rescued from lysosomal degradation and returned to the cell surface for further stimulation. I therefore reasoned that DUB activity may be required to remove the ubiquitin modification from GLUT4 after interaction with GGA proteins had sorted it into the endosomal system, allowing it to avoid lysosomal trafficking.

The GSV resident insulin responsive aminopeptidase (IRAP) traffics in an identical manner to GLUT4 under both basal and insulin stimulated conditions in fat and muscle cells (Ross *et al.*, 1997). siRNA mediated depletion of IRAP in

3T3-L1 cells has been shown to blunt insulin stimulated GLUT4 translocation, however GLUT4 depletion does not seem to have the same effect on IRAP (Yeh *et al.*, 2007;Jordens *et al.*, 2010). Intriguingly, IRAP knockout mice show a significant decrease in relative amounts of total GLUT4 (Keller *et al.*, 2002). These data implicate IRAP in GLUT4 sorting into the insulin responsive compartment, and also suggest that IRAP may form part of a cellular machinery to maintain the stability of GLUT4. Could this include a deubiquitinating enzyme?

A potential link between IRAP and a DUB has been identified through the work of Nai-Wen Chi (UCSD) and colleagues over a number of years. IRAP has been shown to bind the poly-ADP ribose polymerase (PARP) tankyrase, via a minimal tankyrase binding motif (RXX(P,A)DG) (Chi and Lodish, 2000;Sbodio and Chi, 2002). Tankyrase 1 was initially localized to the nucleus where it plays a role in telomere maintenance and spindle assembly (Smith *et al.*, 1998;Hsiao and Smith, 2008). In 3T3-L1 adipocytes a proportion of tankyrase 1 is also Golgi resident (Chi and Lodish, 2000) and siRNA mediated depletion of tankyrase 1 blunted insulin stimulated GLUT4 translocation in a manner similar to IRAP depletion (Yeh *et al.*, 2007).

Tankyrase has been shown, via yeast two hybrid analysis, to interact with the deubiquitinating enzyme USP25 (which contains a putative tankyrase binding motif) (Sbodio *et al.*, 2002). USP25 has three isoforms in humans; the ubiquitously expressed USP25a and b, and the muscle specific USP25m; USP25b is absent in murine tissues (Valero *et al.*, 2001) and has also been shown to modulate the levels of a specific substrate, MyBPC1, on the basis of USP25 catalytic activity (Bosch-Comas *et al.*, 2006). From these data a model can be inferred whereby tankyrase acts as a scaffold, linking USP25 to GSVs via IRAP.

My hypothesis for this part of the project is that USP25 serves to deubiquitinate GLUT4 once it has been sorted into the endosomal system and thus regulates GLUT4 entry into GSVs as part of a complex with IRAP and tankyrase. This deubiquitination of GLUT4 prevents its traffic to the lysosome and thus the transporter becomes localised to GSVs marked by IRAP (which localises USP25 to this compartment).

5.2 Aims of the chapter

I sought to substantiate the published data of a yeast two hybrid interaction of USP25 and the tankyrases by carrying out *in vitro* pull-down assays using immobilized USP25, and to determine whether the interaction was dependent on the putative tankyrase binding motif of USP25 (Sbodio and Chi, 2002). I also employed transient siRNA mediated depletion of USP25 to test the hypothesis that USP25 is required to deubiquitinate GLUT4 thus stabilizing the transporter, allowing it to reach GSVs and preventing its traffic to the lysosome. I will also discuss my efforts to generate a USP25 antiserum for use in Western blotting.

5.3 *In vitro* interaction of USP25 with tankyrase 1.

Studies over the last decade have identified a number of tankyrase binding partners, including IRAP, TAB182 (tankyrase 1 binding protein of 182 kilodaltons), NuMA (nuclear/mitotic antigen 1) and TRF1 (telomere repeat binding factor 1) (Chi and Lodish, 2000;Sbodio and Chi, 2002). All these proteins include a tankyrase binding motif RXX(P,A)DG (Sbodio and Chi, 2002). Human USP25 has also been found to contain this motif (RTPADG) one amino acid removed from the C terminus of the protein, and an interaction between tankyrase and USP25 has been demonstrated using yeast 2-hybrid analysis (Sbodio and Chi, 2002). The RTPADG motif, and its positioning, appears to be conserved in vertebrates. Figure 5.1 shows an alignment between known USP25 protein sequences from human and mouse databases, and predicted sequences for rat, *Xenopus laevis* and *Danio rerio*.

Unpublished data from our collaborator's laboratory (Nai-Wen Chi, UCSD) has shown, using a co-immunoprecipitation approach, that USP25 and tankyrase 1 and 2 interact *in vivo* – however this interaction may not be direct and could require a "bridging" molecule. In order to corroborate this data I sought to determine whether USP25 and tankyrase could interact directly in an *in vitro* pull-down assay, and whether any interaction observed is dependent on the putative tankyrase binding motif.

```
          USP25 human  (1034) HELCERFARIMLSLSR--TPADGR
    Usp25 Danio rerio  (1049) LELFERFGRVMTSLTMGRTPADGR
 Usp25 Xenopus laevis  (1025) HELCERFARIMLSLSR--MPADGR
          Usp25 mouse  (1034) HELCERFARIMLSLSR--TPADGR
            Usp25 rat  (1034) HELCERFARIMLSLSR--TPADGR
```

Figure 5.1 Protein sequence alignment of vertebrate USP25.

The C-termini of known sequences for human and mouse USP25, and predicted sequences for rat, frog (*Xenopus laevis*) and zebrafish (*Danio rerio*) from the UniProt database were aligned using Vector NTI (Invitrogen). The tankyrase binding motif is in green text.

5.3.1 Expression and purification of recombinant GST-USP25.

The GST-USP25 expression vector used in this study was a gift from the laboratory of Frauke Melchior (University of Gottingen). The vector was transformed into BL-21 DE3 *E. coli* and GST-USP25 purified as described in 2.5.6. A sample gel of the purification is shown in Figure 5.2. A major band of the correct molecular weight for GST-USP25 (approximately 165 kD) is observed in lane 1. Some of this protein seems to be lost in the insoluble fraction (lane 3), however after binding to glutathione-Sepharose beads and several wash steps (lanes 6-8) a large amount of this protein is bound to the beads (lane 9). There is also a second major band at approximately 25 kD (lane 9); this may represent an incomplete translation product of GST-USP25, or a degradation product, as the pGEX USP25 vector used in these studies contains a protease cleavage site C terminal to the GST tag.

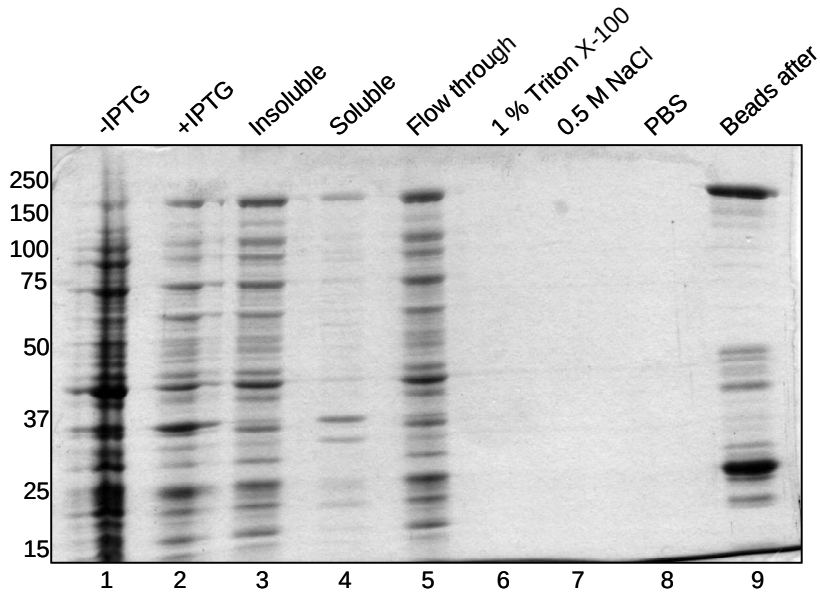

Figure 5.2 Coomassie stained SDS-PAGE gel of GST-USP25 purification.

A. BL-21 DE-3 *E. coli* were transformed with pGEX USP25 and grown to an OD_{600} of 0.6 in 2 l Terrific Broth (1). The cells were induced for 4 hours with 1 mM IPTG (2), then lysed using a Microfluidizer M-110P cell disruptor set at 10,000 psi. The lysates were centrifuged at 17000 xg to separate insoluble (3) and soluble (4) components. The soluble proteins were incubated with glutathione-Sepharose beads for 1 hour with rotation. The flow through was collected from this incubation (5) and nine wash steps were performed – 3 x PBS + 1 % Triton-X (6), 3 x PBS + 0.5 M NaCl (7) and 3 x PBS (8). Bound protein was eluted from a 20 µl sample of the beads after the wash steps by heating at 65 ℃ in 20 µl 2xLSB for 1 0 minutes (9).

5.3.2 Pull-down assay on adipocyte lysates using GST and GST-USP25

To control for nonspecific interactions with the GST tag I included GST in the experiments. As a much smaller, soluble protein (Sassenfeld, 1990) GST is much more highly expressed than GST-USP25, so this protein was purified from 200 ml of culture in an effort to equalize amounts of the two immobilized proteins. Nevertheless, GST alone had an approximately fivefold higher expression than GST-USP25, as shown in Figure 5.3.

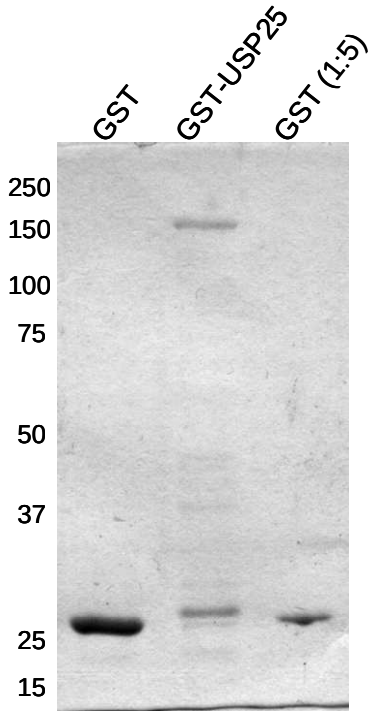

Figure 5.3 Comparison of GST-USP25 and GST protein expression levels.

GST and GST USP25 were purified as in 5.3.1 from 200 ml and 2 l of BL-21 (DE3) *E. coli* culture respectively. 20 µl of bead suspension was heated at 37 ℃ in 200 µl 2xLSB for 30 minutes to elute bound proteins. 20 µl of each elution was subjected to SDS-PAGE on a 10 % gel. Additionally, 4 µl of the GST elution was run alongside (GST (1:5)).

The immobilized fusion proteins were used in pull-down assays from 3T3-L1 adipocyte lysates as described in section 2.7. To overcome the problem of GST being highly expressed compared to GST-USP25, proteins from the GST pull-down were eluted in a fivefold greater volume of 2 x LSB than the GST-USP25 one, and equal volumes of each eluate immunoblotted for tankyrase 1 and 2 using an antibody that recognised both proteins (Table 2.1). This experiment was carried out in collaboration with Iain Adamson, a placement student in the lab.

Figure 5.4 shows a representative result for one of these experiments. It appears that in this system only tankyrase 1 binds to USP25; a lower molecular weight band is observed but it does not coincide with the molecular weight of tankyrase 2 (compare band marked by lower arrowhead in GST-USP25 lane with the lower band, representing tankyrase 2, in the input lane). A similar result was observed if the pull-downs were eluted in the same volume of 2 x LSB. The data presented here corroborate the yeast 2-hybrid studies (Sbodio and Chi, 2002) and the *in vivo* immunoprecipitation data (N-W Chi, personal communication) that USP25 and tankyrase interact.

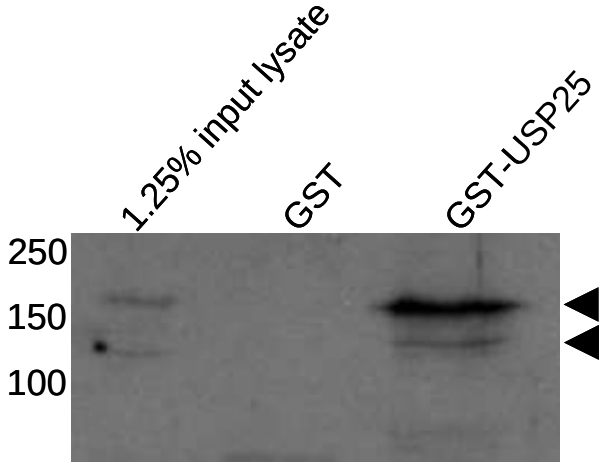

Figure 5.4 Pull-down assay on adipocyte lysates using immobilised recombinant GST and GST-USP25.

20 µl of each recombinant protein immobilized on glutathione-Sepharose beads was incubated with 400 µl 3T3-L1 adipocyte lysate (approximately 10 mg/ml protein content) for 2 hours with rotation. The beads were washed with lysis buffer and bound proteins eluted. 15 µl of each eluate was subjected to SDS-PAGE on a 10 % (v/v) gel and immunoblotted for tankyrase 1 and 2, alongside a sample of the input lysate. Representative of three independent experiments

5.3.3 Does mutation of the putative tankyrase binding motif of USP25 disrupt the in vitro *interaction with tankyrase?*

As discussed in 5.3, USP25 is one of a number of proteins which contain a tankyrase binding motif (Chi and Lodish, 2000;Sbodio and Chi, 2002). Previously mutational analyses have shown that disruption of this motif ablates tankyrase binding to human IRAP, TRF1 and TAB182 in *in vitro* pull-down assays and immunoprecipitation of epitope tagged proteins (Sbodio and Chi, 2002). I therefore reasoned that mutation of the RTPADG motif in USP25 would prevent its *in vitro* interaction with tankyrase 1 as described in 5.3.2, and thus set out to mutate its conserved arginine residue using site directed mutagenesis.

Site directed mutagenesis of pGEX-USP25 using primer pair 555 and 556 (detailed in Table 2.5) generated pCAL13, encoding a GST-USP25 variant with the conserved arginine residue at position 1049 mutated to alanine (GST-USP25 R1049A). Both pGEX-USP25 and pCAL13 were transformed into BL-21 *E. coli* and recombinant GST-USP25 and GST-USP25 R1049A purified as detailed in Figure 5.2. Figure 5.5 shows the results of this purification, indicating that GST-USP25 and GST-USP25 R1049A can be purified at similar levels.

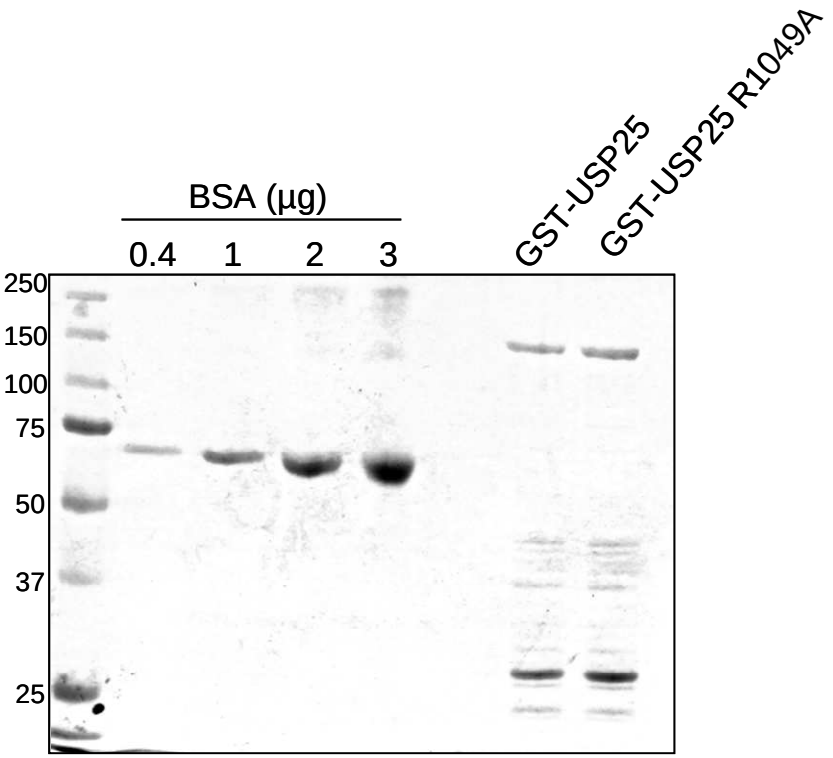

Figure 5.5 Quantification of purified GST-USP25 and GST-USP25 R1049A.

BL-21 (DE3) *E. coli* were transformed with pGEX-USP25 and pCAL13, and recombinant fusion proteins purified as in 5.3.1. 10 µl of 1 in 10 dilutions of the immobilised fusion proteins were subject to SDS-PAGE on 10 % (v/v) gels, alongside samples of BSA at standard concentrations.

Both immobilized GST fusions were introduced into the pull-down assay described in 5.3.2, and bound proteins subjected to SDS-PAGE and immunoblotted with tankyrase specific antibodies. A typical result for this experiment is shown in Figure 5.6. It appears that binding of tankyrase 1 to GST-USP25 is ablated on mutation of the conserved R1049 within the tankyrase binding motif. This result is consistent with previous data for other tankyrase binding motif-containing proteins, such as IRAP, TAB182 and TRF1 (Chi and Lodish, 2000;Sbodio and Chi, 2002;Sbodio *et al.*, 2002), as shortening or point mutation of the conserved RXX(A,P)DG motif in these proteins results in loss of tankyrase 1 interaction.

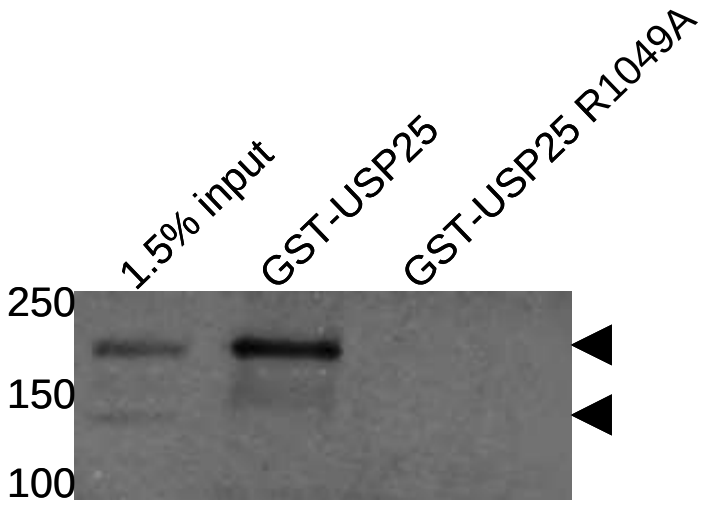

Figure 5.6 Mutation of the conserved arginine residue in the USP25 tankyrase binding motif prevents interaction with tankyrase 1.

Pull-down assays were performed as in Figure 5.4, using immobilised GST-USP25 and GST-USP25 R1049A. Eluted proteins were subject to SDS-PAGE on 10 % (v/v) gel alongside 1.25 % of the input lysate, and immunoblotted for tankyrase 1 and 2. Arrows indicate molecular weights of tankyrase 1 (upper) and 2 (lower). Result is representative of three independent experiments.

5.4 siRNA mediated depletion of USP25 in 3T3-L1 adipocytes reduces GLUT4 stability

RNA interference (RNAi) using short interfering RNAs (siRNA) is a well established method for depleting proteins of interest in cells without having to knock out or inactivate the corresponding gene (Elbashir *et al.*, 2001). I attempted to deplete USP25 using the Mirus TransIT-TKO ® transfection system (see 2.3.3) and two oligonucleotide duplexes (siRNA25 and siRNA27, detailed in Table 2.4), the sequences for which were identified by our collaborator (Nai-wen Chi, UCSD, personal communication). 3T3-L1 adipocytes were transfected with 50 nM siRNA on days 6 and 7 post differentiation and subsequently harvested on day 8 in PBS supplemented with protease inhibitors. Equal amounts of proteins were run on 10 % SDS-PAGE gels prior to immunoblot analyses with antibodies against USP25, GLUT4, Fatty acid synthase (FAS) and GAPDH. The immunoblots were quantified using ImageJ software by normalizing the intensities of USP25, GLUT4 and FAS against GAPDH (which served as a loading control). The results are shown in Figure 5.7.

These data indicate that USP25 is substantially depleted by both siRNA 25 and 27 when compared to a scrambled siRNA control to 35 % ± 3.3 % and 19 % ± 3 % respectively. A concomitant reduction is observed for GLUT4 which is reduced

to 69 % ± 5.8 % (siRNA25) and 75% ± 8.8 % (siRNA27) of control levels. These reductions are statistically significant when compared to the alteration of amounts of the untargeted protein FAS (USP25: $p < 0.01$, GLUT4: $p < 0.05$ for both duplexes, unpaired Student's T-test). These data indicate that USP25 has a role in maintaining GLUT4 stability.

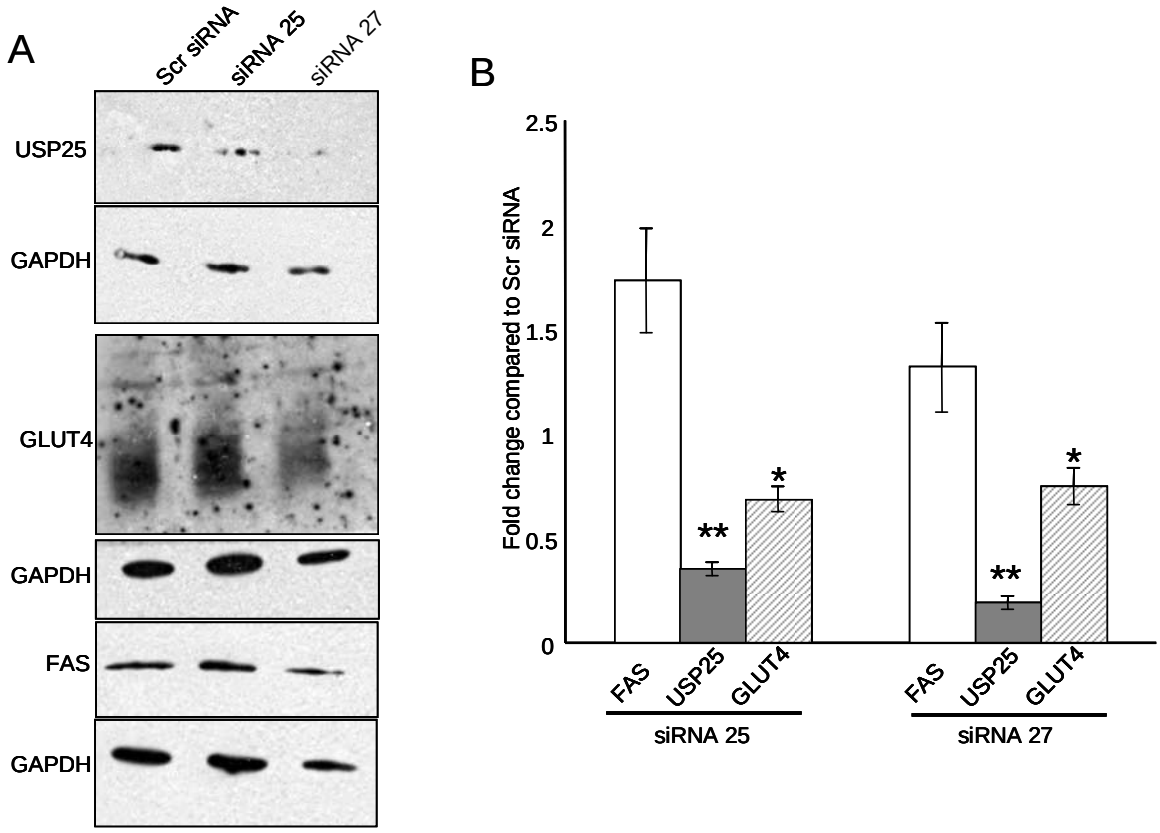

Figure 5.7 siRNA mediated depletion of USP25 results in a reduction in GLUT4 protein levels.

(A) 3T3-L1 adipocytes were treated with 50 nM of the indicated siRNA using Mirus TransIT TKO Transfection reagent on days 6 and 7 post-differentiation, harvested on day 8 and blotted for the indicated proteins. (B) Levels of USP25, GLUT4 and FAS were quantified using ImageJ software and normalized against GAPDH. Levels of USP25 and GLUT4 were compared to the non-targeted FAS using an unpaired student's T-test (* - $p < 0.05$, ** - $p < 0.01$). Error bars represent ± standard error of the mean, n = 4.

5.4.1 Is GLUT4 redirected to the lysosome as a consequence of USP25 depletion?

The depletion of GLUT4 observed in Figure 5.7 are consistent with the hypothesis stated at the beginning of this chapter, in that they are consistent with a model in which GLUT4 is trafficked to the lysosome in response to USP25 depletion. However, the mechanism by which GLUT4 is degraded in the

knockdown cells is not identified. Canonically, ubiquitinated membrane protein are degraded at the lysosome (Urbe, 2005). This led me to attempt to investigate whether lysosomal degradation is the fate of GLUT4 in USP25 depleted cells by inhibiting the lysosomal peptidases of the knockdown cells. Treatment of cultured cells with weak bases such as ammonium chloride (NH_4Cl) raises the pH of acidic compartments (including the lysosome) due to accumulation of protonated forms of the base. This pH rise inactivates lysosomal hydrolases (Amenta and Brocher, 1980).

To test whether GLUT4 in USP25 depleted cells was being redirected to the lysosome, I set out to inhibit the activity of lysosomal proteases using 15 mM ammonium chloride. Previous studies have shown this concentration of NH_4Cl to be effective in blocking peptidase activity in 3T3-L1 cells (Chandler and Ballard, 1983). The results of this experiment are shown in Figure 5.8. There appears to be knockdown of USP25 for cells transfected with siRNA27, however this is not observed for cells transfected with siRNA25. For both siRNAs there appears to be a relative increase in GLUT4 levels compared to cells transfected with scrambled control siRNA.

Although this initial experiment seemed to suggest that GLUT4 could be rescued from degradation by addition of NH_4Cl (at least in the case of siRNA27), repetition of the experiment proved problematic as USP25 knockdown appeared compromised in the cells treated with NH_4Cl. This may have been due to the method used to transfect siRNA duplexes into mature 3T3-L1 adipocytes. The transfection reagent (Mirus TransIT-TKO®) uses a polycation based method to allow siRNA to enter cells. This type of method relies on endocytosis of nanoparticles formed of siRNA duplexes and polycations from the reagent, and subsequent dissociation of the complex as the endosomal lumen acidifies, leading to release of the siRNA into the cytosol (Gary *et al.*, 2007). Inhibition of the acidification of the endosomal system by using NH_4Cl would prevent uptake of siRNA and therefore severely compromise the efficiency of knockdown.

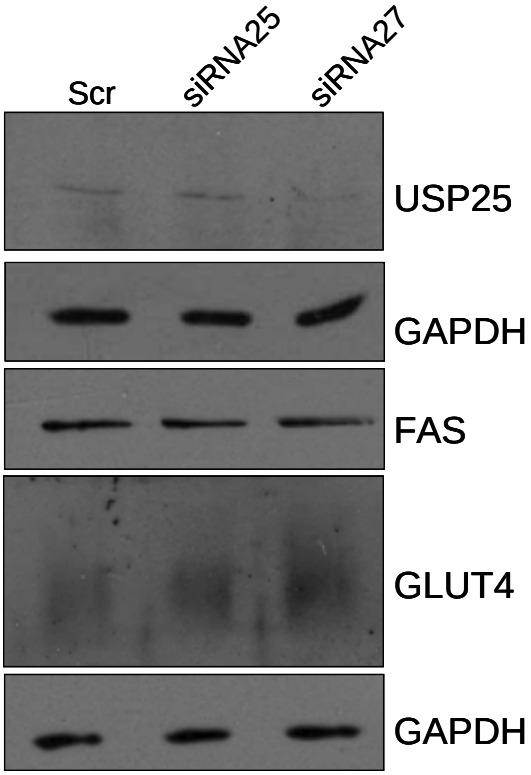

Figure 5.8 Treatment of siRNA transfected 3T3-L1 adipocytes with 15 mM NH_4Cl.

On days 6 and 7 post differentiation, 3T3-L1 adipocytes were transfected with siRNA duplexes as described in Figure 5.7, and simultaneously treated with 15 mM NH_4Cl. On day 8 cells were harvested and immunoblotted for USP25, GLUT4, FAS and GAPDH as a loading control (lower GAPDH blot is the loading control for FAS and GLUT4 blots)

5.4.2 Is glucose uptake affected by depletion of USP25?

As my hypothesis states that USP25 is required to sort GLUT4 into GSVs, it is important to identify whether depletion of USP25 affects the insulin stimulated uptake of glucose into adipocytes. If the insulin stimulated increase in glucose transport is impaired it would suggest there is reduced loading of GLUT4 into GSVs. To address this, [^{3}H] 2-deoxyglucose transport assays (Millar *et al.*, 1999) were carried out on 12 well plates of 3T3-L1 adipocytes treated with the two siRNA duplexes against USP25 and the scrambled control.

As shown in Figure 5.9, there is a reduction in fold change in [^{3}H] 2-deoxyglucose uptake on insulin stimulation in USP25 depleted cells. Results are expressed as fold change rather than absolute values due to the transient transfection method used (detailed in section 2.3.3). Unlike a cell line stably expressing an siRNA or shRNA construct there may be varying knockdown efficiencies and levels of cytotoxicity between batches of cells used for each experiment; this means it is more meaningful to compare the transport activities of cell populations within

experiments rather than use absolute values, however these are recorded in Appendix II.

The reduction in [^{3}H] 2-deoxyglucose uptake in USP25 depleted cells, coupled with the data from Figure 5.7, indicates that the reduced stability of GLUT4 in USP25 depleted cells is responsible for their reduced glucose uptake capacity.

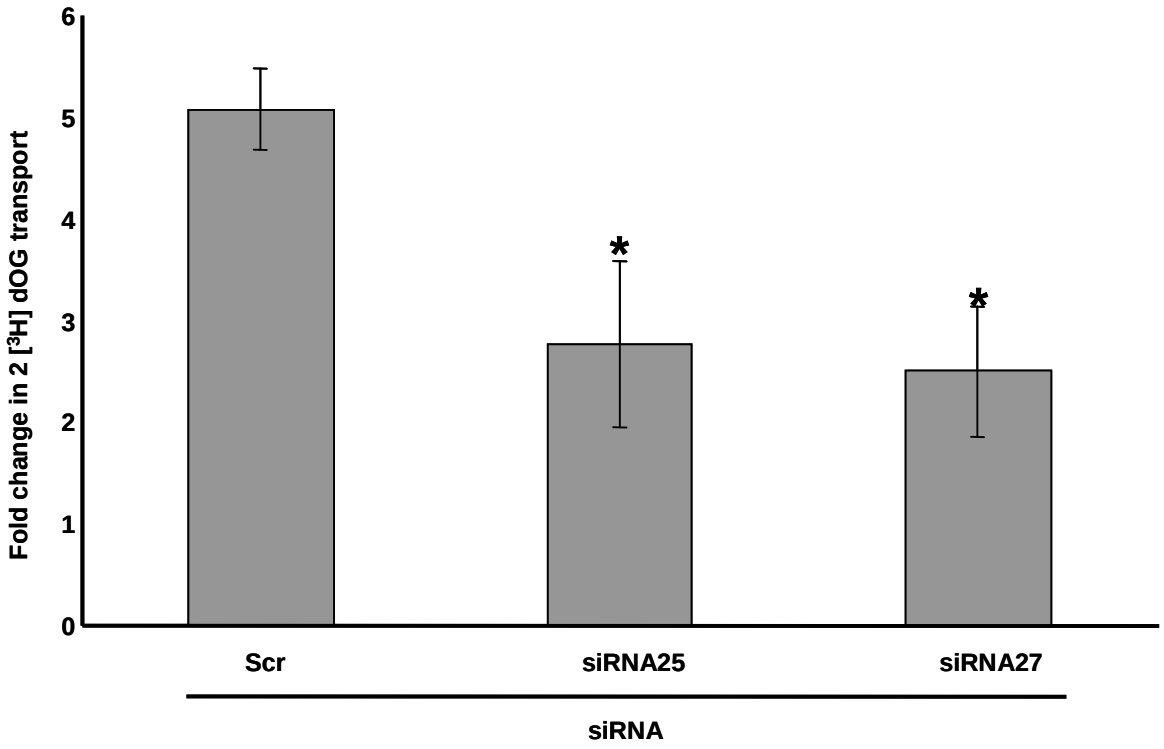

Figure 5.9 Fold change in [3^H] 2-deoxyglucose uptake is reduced on insulin stimulation of USP25 depleted 3T3-L1 adipocytes.

12-well plates of 3T3-L1 adipocytes were treated with the indicated siRNA as described, and assayed for uptake of [3^H] 2-deoxyglucose on day 8 post differentiation. Results were analysed using an unpaired student's T-test. * - $p < 0.05$. Error bars represent ± standard error of the mean, n = 3. The raw data for this figure are presented in Appendix II.

5.5 Generation and characterisation of USP25 antisera.

The anti-USP25 antibody used in this study was a gift from the laboratory of Gemma Marfany (Universitat di Barcelona). To allow larger scale experiments to be carried out I set out to generate antisera against USP25 which could be used in future experiments.

I initially produced recombinant GST-USP25 on glutathione-Sepharose beads as described in 5.3.1, and cleaved untagged USP25 from the beads using thrombin. The pGEX 4T-1 vector used in these experiments contains a thrombin cleavage site at the C-terminus of the GST tag.

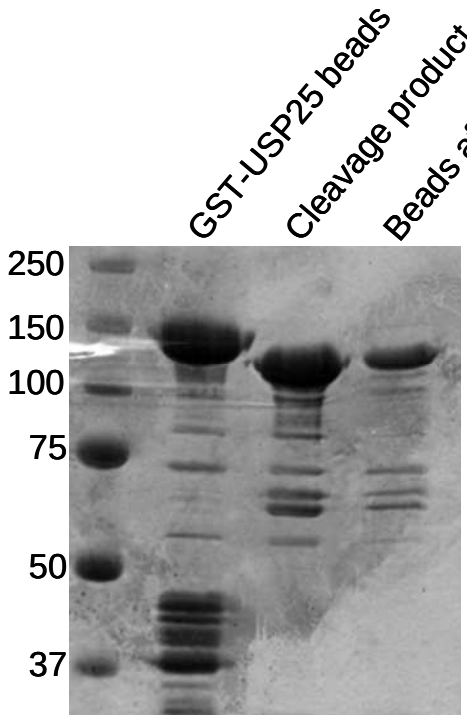

Figure 5.10 Thrombin cleavage of GST-USP25.

Recombinant GST-USP25 was purified as described in 5.3.1 on glutathione-Sepharose beads. The beads were treated with 0.04 units/µl thrombin in thrombin cleavage buffer (50 mM Tris-HCl pH 8.0, 150 mM NaCl, 2.5 mM $CaCl_2$) for 2 hours at room temperature, and untagged USP25 collected in the supernatant after brief centrifugation at 500 xg and 4 ℃. 20 µl samples of beads before cleavage (GST-USP25 beads), supernatant (Cleavage product) and beads after cleavage were heated at 37 ℃ for 30 minutes with 20 µl 2xLS B and 20 µl of the eluate subjected to SDS-PAGE on a 10 %(v/v) gel. Bands were visualized by Coomassie staining and subsequent destaining.

The untagged USP25 was used to immunize two New Zealand white rabbits, with serum collected at the time points described in Materials and Methods section 2.5.4. I tested the sera for immunoreactivity against purified GST and GST-USP25. The results of this experiment are shown in Figure 5.11 As expected, the pre immune serum from both rabbits does not detect GST-USP25. The small bleed from 2198 detects GST-USP25 at a low level. However the large and final bleeds of both 2198 and 2199 show increased immunoreactivity against GST-USP25. Importantly the large and final bleeds from 2199 show the least cross-reaction with the GST purification tag (visible at approximately 25 kD) which suggests that the sera from 2199 may be more suited for use in future experiments.

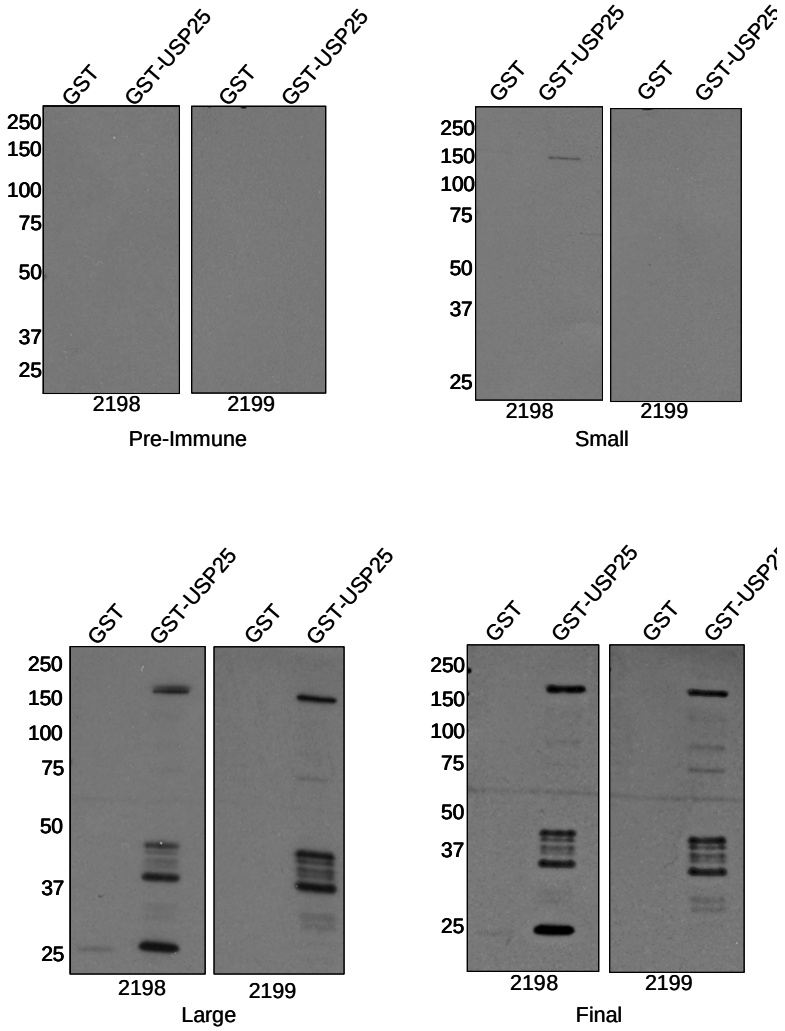

Figure 5.11 Sera from rabbits 2198 and 2199 tested against recombinant GST and GST-USP25.

Pre-immune, small, large and final bleeds of rabbits 2198 and 2199 were tested for immunoreactivity against 1 µg of either GST or GST USP25, subjected to SDS-PAGE on 10 % (v/v) gels, immunoblotted and incubated with each of the sera at 1:1000 dilution overnight at 4 ℃

I went on to analyse whether the 2198 and 2199 sera could be used to detect USP25 from a mammalian cell lysate. I ran two sets of 3T3-L1 adipocyte lysate samples, with decreasing amounts of protein, and probed them with a 1:1000 dilution of both 2198 and 2199 sera from the final bleed. After ECL visualization, the same membranes were stripped and reprobed with the two antisera, this time incubated with 8 µg GST-USP25. As this fusion protein contains the antigen against which 2198 and 2199 was raised its presence would be expected to reduce the immunoreactivity of endogenous USP25 on the blots by competing for USP25 specific antibodies.

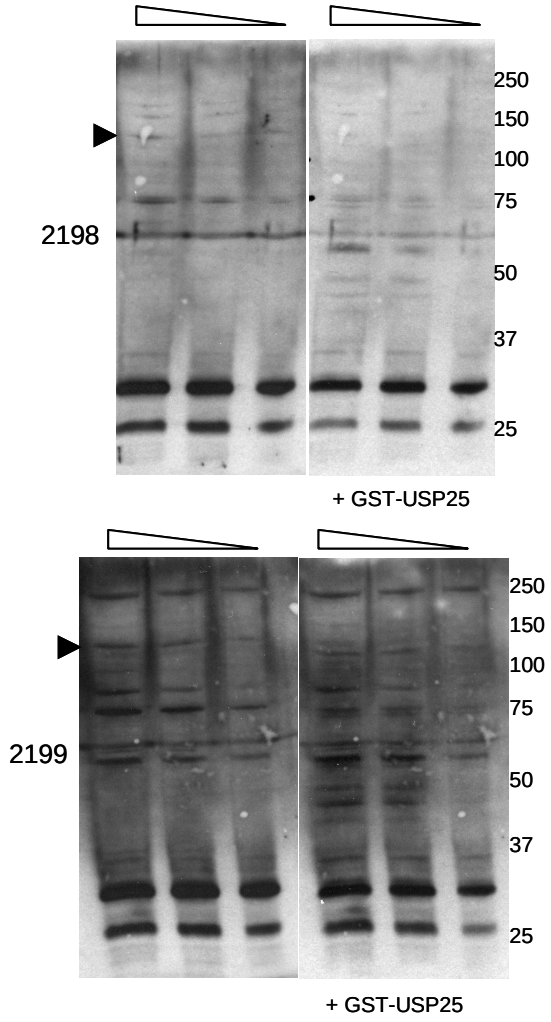

Figure 5.12 Testing sera 2198 and 2199 against 3T3-L1 adipocyte lysates.

Decreasing amounts of 3T3-L1 adipocyte lysates (30, 20 and 10 µg protein added) were subject to SDS-PAGE and blotted with 2198 and 2199 antisera at 1:1000 dilution (left panels). After visualization, the membranes were stripped using stripping buffer (100 mM glycine, 150 mM NaCl, pH 2) for 20 minutes, blocked and re probed with the two antisera in the presence of 8 µg GST-USP25 (right panels). Arrow indicates putative USP25 band.

The results of this experiment are shown in Figure 5.12. Unfortunately it appears that both sera recognise a number of antigens in the adipocytes lysates. However there are noticeable bands at approximately 140 kD in all three lanes for both sera, which corresponds to the molecular weight of USP25 from previous studies (Meulmeester *et al.*, 2008). These bands appear to be depleted on incubation with GST-USP25, which indicates that these bands may represent endogenous USP25. However this result is very preliminary as the experiment was only carried out once and has been included here primarily for documentation purposes.

5.6 Chapter Discussion.

In this chapter I set out to test the hypothesis that USP25 is recruited by tankyrase (through its interaction with IRAP) to GSVs, where it deubiquitinates GLUT4 and prevents the transporter from being delivered to the lysosome. I followed two lines of investigation to test this hypothesis. Firstly, I used an *in vitro* pull-down approach to indentify whether USP25 can interact directly with tankyrase, as predicted by yeast-2-hybrid analysis (Sbodio and Chi, 2002). Secondly I transiently depleted USP25 from adipocytes using siRNA, and analysed the effect on GLUT4 stability and insulin responsiveness in these cells.

I purified recombinant GST-USP25 and GST, immobilized on glutathione-Sepharose beads. The GST-USP25 fusion protein pulled tankyrase 1 down from a 3T3-L1 adipocyte lysates, whereas GST alone did not. This shows that USP25 and tankyrase can interact, as previously demonstrated by yeast-2-hybrid analysis (Sbodio and Chi, 2002;Seimiya and Smith, 2002).

To investigate whether this interaction is dependent on the putative tankyrase binding motif, as found for other tankyrase binding substrates (Chi and Lodish, 2000;Sbodio and Chi, 2002;Seimiya and Smith, 2002) I mutated the conserved arginine residue at position 1049 within the motif, and introduced GST-USP25 R1049A in to the pull-down assay. This approach resulted in ablation of binding of tankyrase 1 to USP25.

Of note, in these assays there is no obvious interaction with tankyrase 2, despite the fact that tankyrase 2 contains the same ankyrin repeat domains required for interaction as tankyrase 1 (Sbodio *et al.*, 2002;Hsiao and Smith, 2008). This result is not particularly surprising as tankyrase 2 is not present at high enough levels in 3T3-L1 adipocytes to interact with GST-IRAP at detectable levels in a pull-down assay (Sbodio *et al.*, 2002), indicating that there may be no detectable interaction with USP25 for similar reasons.

The findings from the pull-down studies indicate that USP25 is a *bona fide* tankyrase binding partner, with a functional tankyrase binding motif. These data have been substantiated by immunoprecipitation experiments, showing an interaction between tankyrase and USP25 *in vivo* (N-W Chi, personal communication). Given that tankyrase contains multiple sites that can interact with partner proteins in its ankyrin repeat domains (Seimiya and Smith, 2002), it

seems plausible that tankyrase can act as a scaffold protein at GSVs, binding the GSV cargo protein IRAP and recruiting USP25.

To investigate the role of USP25 in GLUT4 trafficking I depleted USP25 using siRNA. After two consecutive days of transfection with siRNA duplexes targeted against USP25, there was ~35 % less GLUT4 compared to cells transfected with an untargeted siRNA duplex. This suggests that GLUT4 is stabilised by the presence of USP25, which is consistent with my hypothesis of the role of USP25 in deubiquitinating GLUT4, preventing its lysosomal degradation and "trapping" it in GSVs.

These data are interesting in the context of recent data concerning the role of DUBs in plasma membrane receptor recycling. Plasma membrane receptors including the *Drosophila* Wnt receptor Frizzled and the β2-adrenegic receptor (Shenoy *et al.*, 2009;Berthouze *et al.*, 2009;Mukai *et al.*, 2010) can, after ubiquitin-dependent internalization, be stabilized by deubiquitination, allowing them to recycle to the cell surface and preventing their lysosomal degradation. However my finding is novel in the context of intracellular traffic from the TGN to a secretory compartment – ubiquitinated proteins sorted from the TGN into the endosomal system are thought to only be deubiquitinated by ESCRT-associated DUBs such as AMSH and Doa4p before entry into multivesicular bodies (Swaminathan *et al.*, 1999;Agromayor and Martin-Serrano, 2006;Nikko and Andre, 2007).

Further characterization of the USP25 depleted cells by lysosome inhibition proved problematic as the method used for inhibition of lysosomal hydrolases, treatment with 15 mM NH_4Cl (Amenta and Brocher, 1980;Chandler and Ballard, 1983), generally reduced the effectiveness of USP25 knockdown (Figure 5.8 and data not shown). The reduced effectiveness of the knockdown was probably due to the inhibition of endosome acidification by NH_4Cl (Gary *et al.*, 2007); this would prevent release of the siRNA from nanoparticles and its uptake into the cytosol.

Another possible method for investigating whether the lysosome is involved in GLUT4 degradation would be to use a pulse chase experiment. For example the USP25 knockdown adipocytes could be treated with siRNA duplexes for two days (as described in 5.4). These cells could be subsequently treated with a lysosome inhibitor such as 15 mM NH_4Cl and the half life of newly synthesised GLUT4

followed using pulse-chase labelling followed by immunoprecipitating GLUT4 at various timepoints. The difference between the half life of GLUT4 in cells with and without lysosome inhibition could then be compared – if GLUT4 is degraded at the lysosome the half life of GLUT4 would be expected to be longer in cells treated with 15 mM NH_4Cl. Measuring the rate of degradation of newly synthesised GLUT4 in this manner would circumvent the problem of reduced siRNA uptake in the presence of an inhibited endosomal system. Another possibility would be to use a lysosomal inhibitor that did not alter the acidification of the endosomal system and instead inhibits the lysosomal peptidases directly, an example being leupeptin (Maeda *et al.*, 1971). This method may not interfere with the pH dependent release of siRNA from the endosomal system (Gary *et al.*, 2007).

On assaying the glucose transport activity of the USP25 knockdown cells, they were found to have a reduced fold change in insulin stimulated glucose transport compared to cells transfected with an untargeted siRNA (Figure 5.9). This suggests that GLUT4 is being trafficked away from the insulin responsive pool, or that the GLUT4 present in the insulin responsive pool of the knockdown cells is less able to respond to insulin. When taken together with the data from Figure 5.7 it seems possible that the observed GLUT4 depletion is responsible for the reduced glucose transport – perhaps the population of GLUT4 normally routed to GSVs (and therefore ubiquitinated) is being diverted to the lysosome in USP25 depleted cells, resulting in the observed reduction in fold change on insulin stimulation.

The attempt to generate a USP25 antiserum was partially successful. Recombinant GST-USP25 could be detected by both sera. However endogenous USP25 from 3T3-L1 adipocytes was harder to detect, with a number of other bands being recognised by the sera. Use of antigen competition seemed to show that USP25 was amongst the bands detected by the two sera – although this result remains preliminary as the competition experiment was only carried out once. If this result stands up to repetition, the population of USP25 specific IgG would need to be immunopurified from the sera – the sera could be passed over a column of immobilised USP25 (antigen), allowing binding of USP25 specific IgG to the antigen. Nonspecific antibodies could then be washed off and USP25 specific IgG eluted.

Overall, the data presented in this chapter support the model that USP25 associates with GLUT4 containing compartments via a complex of IRAP and tankyrase, acting as a scaffolding protein, in a manner dependent on its C-terminal RTPADG motif, and that USP25 is required for maintenance of GLUT4 stability. However, more work clearly needs to be done to elucidate the underlying molecular mechanisms. As discussed in 5.1, in yeast a constitutively ubiquitinated version of GLUT4 (GLUT4 7K/R-Ub) is sorted into the yeast endosomal system and degraded (McCann R.K., 2007). However, when this fusion protein is expressed in adipocytes, it remains in the TGN, neither being degraded at the lysosome nor translocating in response to insulin (McCann R.K., 2007). These data do not necessarily implicate a DUB step in GLUT4 traffic. It may be that in the case of GLUT4 in 3T3-L1 adipocytes the architecture of the C-terminal ubiquitin fusion is not adequate to induce GGA dependent sorting out of the TGN to the endosomal system, unlike ubiquitination on a cytosolic lysine residue (this study, chapter 3, (Lamb *et al.*, 2010)).

My findings that USP25 depletion results in depletion of GLUT4 and alterations to its insulin responsive traffic are also interesting in the context of studies where IRAP and tankyrase are depleted. IRAP knockout mice have normal glucose tolerance, but exhibit depletion in total GLUT4 levels and reduced insulin responsive glucose uptake in certain tissues (Keller *et al.*, 2002). In studies of 3T3-L1 adipocytes depleted of IRAP (Yeh *et al.*, 2007;Jordens *et al.*, 2010) and tankyrase (Yeh *et al.*, 2007) the insulin responsive translocation of GLUT4 is blunted – both these lines of evidence support a role for a putative IRAP-tankyrase-USP25 complex at GSVs. However, studies of tankyrase deficient mice have yielded conflicting data. Tankyrase-1 knockout mice apparently have an expanded cellular pool of GLUT4 and a corresponding increase in insulin stimulated fold change in glucose transport (Yeh *et al.*, 2009). In contrast, tankyrase-2 knockout mice do not exhibit any significant perturbation in insulin stimulated glucose transport (Chiang *et al.*, 2008). Further study of tankyrase depletion and its effects on GLUT4 would clearly be valuable.

Overexpression of dominant interfering or dominant negative versions of DUBs is a technique often used to interpret their function (Mukai *et al.*, 2010). Given the data I have presented a catalytically inactive mutant such as that described in previous studies (Denuc *et al.*, 2009), where the conserved catalytic cysteine (C178) residue is mutated could be used. This could theoretically prevent

active, endogenous USP25 binding to the tankyrase scaffold and potentially replicate the phenotype seen for USP25 knockdown cells. In the aforementioned study this mutant was used to study the stability of a specific USP25 substrate, MyBPC1 (Denuc *et al.*, 2009).

Another useful tool would be a 3T3-L1 fibroblast cell line with a stable USP25 knockdown, or a knockdown which is under the control of an inducible system. This would make it possible to "add back" an siRNA resistant USP25 and observe whether the knockdown phenotype is rescued. As 3T3-L1 adipocytes are relatively difficult to work with in terms of generating a stable cell line due to the limited number of times the cells can be passaged, one possibility for generation of a stable cell line is to use a more tractable cell line where insulin signalling has been reconstituted. Chinese hamster ovary (CHO) cells expressing GLUT4 have been shown to recapitulate aspects of the insulin responsive GLUT4 trafficking pathway seen in 3T3-L1 adipocytes (Dobson *et al.*, 1996;Lampson *et al.*, 2000) and may prove a useful model system for testing effects of USP25 knockdown and overexpression before moving to work on adipocytes.

The USP25 R1049A mutant, which I showed to be deficient in tankyrase binding, could also be expressed in this background. If interaction with tankyrase is required for USP25 to exert its stabilising effect on GLUT4, the tankyrase binding deficient R1049A mutant would be expected not to have this effect. A stable knockdown of USP25 would also be helpful in addressing the issue of how GLUT4 is depleted in the absence of USP25. It would be possible to use lysosome inhibitors such as NH_4Cl or leupeptin on this cell line as there would be no issues with transfection reagents altering siRNA uptake. Another possibility for interfering with lysosomal function in USP25 depleted cells would be to knock down expression of components of the ESCRT machinery as this would interfere with multivesicular body formation and thus lysosomal protein degradation. Depletion of ESCRTI, II and III subunits has previously been shown to stabilise EGFR and prevent internalisation into MVBs (Bache *et al.*, 2006;Malerod *et al.*, 2007).

In summary, the data in this chapter substantiate the yeast two hybrid (Sbodio and Chi, 2002) and *in vivo* immunoprecipitation (N-W Chi, unpublished) data that tankyrase and USP25 can interact, and moreover demonstrate that the interaction is dependant on the RTPADG motif between residues 1049 and 1054

of USP25. Additionally, the data indicate that USP25 is involved in maintaining GLUT4 stability. These findings support my hypothesis that a deubiquitination step is required for the insulin responsive traffic of GLUT4.

Chapter 6 – Final Discussion

The overall aim of this study was to investigate the mechanisms underlying GLUT4 entry the insulin responsive compartment, which is one of the key questions remaining to be addressed in our understanding of GLUT4 traffic (Bryant *et al.*, 2002). More specifically I tested the hypothesis that ubiquitination of GLUT4 is required for the GGA-dependent sorting step from the *trans*-Golgi network (TGN) to the insulin responsive compartment, with subsequent deubiquitination stabilising GLUT4 and preventing its traffic to the lysosome.

6.1 Ubiquitination of GLUT4

Previous work in the Bryant group has shown that GLUT4 expressed in yeast traffics in a nitrogen-regulated manner similar to Gap1p (McCann R.K., 2007). Like Gap1p, GLUT4 expressed in yeast is ubiquitinated (Lamb *et al.*, 2010), and functional ubiquitin acceptor sites as well as the Ggas are required for its trafficking into the endosomal system (Lamb *et al.*, 2010). Given these data I decided to first test whether GLUT4 is ubiquitinated in 3T3-L1 adipocytes, and if so, whether ubiquitination is required for entry into the insulin responsive compartment.

Initial work on GLUT4 ubiquitination in 3T3-L1 cells had been carried out by a former member of the group (Dr. R.K. McCann), using a retroviral expression construct encoding GLUT4 with an HA-tag in the first exofacial loop (pHA-GLUT4) (Shewan *et al.*, 2000) and a construct expressing ubiquitin resistant HA-GLUT4 7K/R (pRM4; Table 2.3 (Lamb *et al.*, 2010)). However in these initial experiments, HA-GLUT4 was expressed at approximately twenty fold greater levels than HA-GLUT4 7K/R (McCann R.K., 2007), as pRM4 lacked sequences 5' of the GLUT4 open reading frame which seemed to raise expression of HA-GLUT4 (Fukumoto *et al.*, 1989;Quon *et al.*, 1994). Concerns were also raised about the structure of HA-GLUT4 7K/R. Five of the seven cytosolic lysines are located within the large intracellular loop of GLUT4, a region required for binding of factors involved in GLUT4 sorting – specifically, the lysine residue at position 245 is involved in recruitment of the ARF GAP ACAP1, required for clathrin coat nucleation (Li *et al.*, 2007). Therefore, mutation of the five lysines within the large intracellular loop could disrupt the structure of this region, altering binding of ACAP1 and consequently blocking entry into GSVs.

I addressed these concerns in Chapter 3 by making use of constructs already present in the lab encoding versions of HA-GLUT4 with single cytosolic lysines outwith the large intracellular loop (pRM35 and 36 encoding HA-GLUT4 6K/R 109 and 495 respectively ((Table 2.3)). These constructs were based on pRM4 and should thus express at the level seen for the 7K/R mutant. Firstly, in collaboration with Dr R.K. McCann, I subcloned a fragment of pHA-GLUT4 into simultaneously digested pRM36, generating a retroviral expression construct encoding the HA-GLUT4 ORF but lacking the 5' sequence (pRM55). When assayed by western blotting, levels of HA-GLUT4 (expressed from pRM55), HA-GLUT4 7K/R and the two 6K/R mutants were similar, which dealt with the issue of the overexpression of HA-GLUT4 previously observed (McCann R.K., 2007).

Also, in collaboration with Dr R.K. McCann I developed a pull-down assay, using a GST tagged UBA domain of the yeast protein Dsk2p (Ohno *et al.*, 2005) (GST-UBA), to enrich for ubiquitinated species. This approach showed that a small proportion of endogenous GLUT4 is ubiquitinated (Figure 3.6) – this was quantified by our group, showing approximately 0.1 % of total GLUT4 is ubiquitinated in 3T3-L1 adipocytes (Lamb *et al.*, 2010). I went on to use this approach to analyse the ubiquitination status of HA-GLUT4, HA-GLUT4 7K/R and the two 6K/R mutants, and found that HA-GLUT4 and both 6K/R mutants were ubiquitinated to a similar extent, whereas HA-GLUT4 7K/R was not (Figure 3.6)(Lamb *et al.*, 2010).

To address the issue of disruption of the structure of the large intracellular loop in HA-GLUT4 7K/R, I expressed HA-GLUT4, HA-GLUT4 7K/R and the two 6K/R mutants in 3T3-L1 adipocytes and studied their ability to translocate in response to insulin stimulation using labelling of the exofacial HA tag. This approach showed that HA-GLUT4 7K/R does not translocate in response to insulin, whereas HA-GLUT4 and the two HA-GLUT4 6K/R mutants all translocated to a similar extent (Figure 3.8) (Lamb *et al.*, 2010). These findings support the hypothesis that GLUT4 ubiquitination is required to enter GSVs, as only those versions of GLUT4 with functional ubiquitination sites translocate in response to insulin. Also, these data suggest that mutation of the lysine residues within the large intracellular loop does not alter the structure of this region sufficiently to affect recruitment of factors involved in GLUT4 translocation, such as ACAP1 (Li *et al.*, 2007). The mutations introduced into the large intracellular loop of GLUT4 by Li *et al* were alanine scanning mutations, so the bulky basic R-group of lysine was

being replaced by the much smaller, neutral alanine. In this study the lysines were being replaced by another residue with a bulky, basic R-group, arginine, and this would be expected to alter the charge and structure of the large intracellular loop much less.

To confirm that the defect in HA-GLUT4 7K/R sorting was at the level of entry into GSVs rather than translocation itself, I utilised two subcellular fractionation approaches. The first was to isolate light density microsomes (which include GSVs) from adipocytes and separate them on a self forming iodixanol gradients (Hashiramoto and James, 2000). This method proved too variable even with wild type HA-GLUT4 to give reliable results (Figure 3.9).

Instead, I utilised a differential centrifugation method that produces a fraction enriched in GSVs (Xu and Kandror, 2002;Kupriyanova *et al.*, 2002;Li and Kandror, 2005). Using this method, HA-GLUT4 7K/R was found to be depleted from the GSV enriched fraction, containing approximately 30 % of total GLUT4 (Figure 3.10) (Lamb *et al.*, 2010). This was significantly less than the approximately 55 % of total GLUT4 observed for HA-GLUT4 and the two 6K/R mutants (Lamb *et al.*, 2010).

The data presented in Chapter 3 support the hypothesis that GLUT4 ubiquitination is required to sort the transporter into the insulin responsive compartment. GLUT4 ubiquitination can be added to the C-terminal TELEY motif as a signal on GLUT4 required for its sorting into GSVs (Shewan *et al.*, 2000;Blot and McGraw, 2008).

Previously, ubiquitination of membrane proteins has been thought of as a signal for internalisation and subsequent degradation of membrane proteins, including MHCII (Shin *et al.*, 2006) and aquaporin 2 (Kamsteeg *et al.*, 2006). Sorting of Fas ligand into secretory lysosomes also requires ubiquitination, but likely has more in common with ESCRT dependent sorting into multivesicular bodies than sorting into classical secretory compartments (Zuccato *et al.*, 2007). The finding that GLUT4 ubiquitination is required for sorting into its secretory compartment is therefore novel in terms of protein sorting from the TGN.

6.2 The GGA3 GAT domain and GLUT4 traffic.

To further characterise how ubiquitin dependent sorting of GLUT4 occurs, I turned my attention to the GGA family of clathrin adaptors which, as mentioned earlier, have been implicated in sorting GLUT4 into GSVs (Watson *et al.*, 2004;Li and Kandror, 2005). The GAT domain of GGAs is responsible for ubiquitin binding (Scott *et al.*, 2004;Shiba *et al.*, 2004;Bilodeau *et al.*, 2004), and GGA3 GAT appears to have the highest avidity for ubiquitin (Puertollano and Bonifacino, 2004;Shiba *et al.*, 2004). With this in mind, in Chapter 4 I used a ubiquitin binding deficient mutant of GGA3 (E250N D284G) to study the interaction with GLUT4 *in vitro*, and effects on GLUT4 sorting *in vivo*. In an *in vitro* pull-down assay using immobilised GST-GGA3 VHS-GAT (GST-VHS-GAT) and a ubiquitin binding deficient mutant thereof (GST-VHS-GAT$_{mut}$) I demonstrated that GLUT4 expressed in yeast can bind to GST-VHS-GAT, however this interaction is reduced on mutation of the ubiquitin binding region of the GAT domain (Figure 4.6).

I attempted to use the pull-down approach to investigate the role of the GAT domain in binding endogenous GLUT4 from 3T3-L1 adipocytes. However it proved difficult to detect any interaction between recombinant GST-VHS-GAT and GLUT4 with this approach (Figure 4.7); possibly due to the relatively low affinity of the GAT domain for ubiquitin (Kawasaki *et al.*, 2005), and the small proportion (0.1 %) of ubiquitinated GLUT4 in 3T3-L1 cells (Lamb *et al.*, 2010).

What possible methods could be used to overcome these obstacles, to better study the interaction of endogenous GLUT4 and the GGAs? One possibility would be to enrich ubiquitinated species in 3T3-L1 cells, perhaps by lysosome inhibition (Chandler and Ballard, 1983) or knockdown of ESCRT subunits, which has been shown to result in an accumulation of ubiquitinated species at endosomes (Bishop *et al.*, 2002). A second possibility would be to take a more biochemical approach and use immobilised GST-UBA (described in Chapter 3) to purify ubiquitinated proteins from a large amount of adipocyte lysate – this would include GLUT4-Ub. The ubiquitinated proteins could be eluted from the GST-UBA column and passed over a GST-VHS-GAT or GST-VHS-GAT$_{mut}$ column, and interacting proteins detected by immunoblot. However this approach would be no small undertaking and would require significant optimisation.

It would also be interesting to study the effect of introducing yeast-expressed GLUT4-7K/R into the GST-VHS-GAT/GST-VHS-GAT$_{mut}$ pull-down assay. As this mutant is ubiquitin resistant, it would be expected to bind GST-VHS-GAT much less readily than the wild type transporter.

Further characterisation of the role of the GGA3 GAT domain in GLUT4 sorting in yeast *in vivo* would also be beneficial. As I have previously discussed (1.2.2), a chimaeric protein consisting of yeast Gga2p with the GAT domain of human GGA3 (Gga2p-GAT^{GGA3}) rescues Gap1p trafficking defects when expressed in a *gga1/2Δ* yeast strain (Bilodeau *et al.*, 2004). Our group has shown that GLUT4 expressed in yeast traffics in a nitrogen-responsive and ubiquitin-dependent manner similar to Gap1p (McCann R.K., 2007;Lamb *et al.*, 2010), and that GLUT4 sorting into the yeast endosomal system requires Ggas (Lamb *et al.*, 2010). Therefore if GLUT4 and Gga2p-GAT^{GGA3} were co-expressed in a *gga1/2Δ* yeast strain this system could be used to analyse the effect of mutations in the ubiquitin binding GAT of GGA3 domain on GLUT4 sorting.

Having established that GST-VHS-GAT$_{mut}$ is impaired in its ability to interact with ubiquitin, I went on to express full length myc-GGA3 (short isoform) and a mutant version harbouring the E250N D284G point mutations (myc-GGA3$_{mut}$) from retroviral constructs in 3T3-L1 adipocytes, to study the effects of expressing the mutant on GLUT4 loading into GSVs and glucose transport. My first observation on expression of these two proteins in 3T3-L1 cells was that myc-GGA3$_{mut}$ was expressed at much higher levels than the wild type protein, despite the expression cassettes being in identical vector backgrounds (pBABE puro; (Morgenstern and Land, 1990)). As I speculated in section 4.5, it may be that the reduced ubiquitin binding function of myc-GGA3$_{mut}$ results in a reduction in its ubiquitination, leading to increased stability. It already known that GAT mutation alters GGA3 ubiquitination (Shiba *et al.*, 2004) although the stability of GGA3 in this context was not measured. Use of pulse-chase to radiolabel newly synthesised myc-GGA3 and myc-GGA3$_{mut}$ could allow the stability of both proteins to be measured. Despite the observed difference in expression there was no obvious effect on the subcellular localisation of myc-GGA3$_{mut}$ compared to the wild-type protein (Figure 4.9).

With the differing expression of myc-GGA3 and myc-GGA3$_{mut}$ in mind, I went on to analyse the effects of expressing these two proteins on the loading of GLUT4

into the GSV enriched 16,000 xg supernatant, as had been done previously in cells expressing a dominant negative GGA (Li and Kandror, 2005). Expression of myc-GGA3$_{mut}$ resulted in 10 % less total GLUT4 being loaded into the GSV enriched fraction (Figure 4.10). This result was interesting in that it replicated the decreased loading of GLUT4 into the 16,000 xg supernatant observed by Li and Kandror (2005), albeit to a lesser extent, and indicated that the ubiquitin binding function of the GAT domain is at least partly required for sorting GLUT4 into GSVs. There was no significant effect of myc-GGA3 expression on GLUT4 loading into the 16,000 xg supernatant, which might be expected due to the low expression of the wild type protein. It is also important to note that the 2005 study (Li and Kandror) did not use a wild-type GGA protein as a control, instead comparing empty vector transfected cells with cells expressing dominant negative GGA (EGFP-VHS-GAT).

Although there is a significant effect on GLUT4 loading into the 16,000 xg supernatant on expression of myc-GGA3$_{mut}$, this did not translate into a significant effect on GLUT4 translocation as measure indirectly by [^{3}H] 2-deoxyglucose uptake (Figure 4.11). The variability of the measured uptake rates (as detailed in Appendix I) likely contributed to this.

Although more technically challenging, the effect of myc-GGA3/myc-GGA3$_{mut}$ expression on GLUT4 translocation could be measured more directly by using the HA-GLUT4 translocation assay detailed in chapter 3. 3T3-L1 cells could be stably infected with a retroviral construct with a particular antibiotic resistance, for example hygromycin, encoding HA-GLUT4. This stable cell line could then subsequently be infected with the pBABE puro based GGA3 constructs, and their effects on HA-GLUT4 translocation measured by analysing the levels of HA immunoreactivity in the plasma membrane of insulin stimulated adipocytes.

In summary, my work on the role of the GGA3 GAT domain in GLUT4 traffic has shown that the ubiquitin binding function of this domain is at least partially required for the sorting of GLUT4 into the insulin responsive compartment, perhaps working in concert with other GSV cargoes such as sortilin to sort GLUT4 into GSVs from the TGN. My data, when considered with previous studies from our lab, indicate that GGA3 facilitates ubiquitin dependent GLUT4 sorting into GSVs.

6.3 The deubiquitinase USP25 and GLUT4 traffic.

Although my work in chapters 3 and 4, and previous studies from our group (McCann R.K., 2007;Lamb *et al.*, 2010) have implicated GLUT4 ubiquitination in its sorting into GSVs, there is a caveat in that ubiquitination of membrane proteins directs them into the ESCRT dependent MVB sorting pathway, eventually leading to degradation at the lysosome (Hicke and Dunn, 2003;Piper and Luzio, 2007). Our group has previously shown that only 0.1 % of endogenous GLUT4 is ubiquitinated in 3T3-L1 adipocytes (Lamb *et al.*, 2010), suggesting that the modification is transient. A requirement for deubiquitination has previously been demonstrated for the recycling of several cell surface proteins, including Frizzled (Mukai *et al.*, 2010) and β2-AR (Berthouze *et al.*, 2009). Given these data, I reasoned that the ubiquitin modification on GLUT4 may be a transient one, and that there may be a deubiquitination step involved in GLUT4 traffic.

A link between GLUT4 traffic and a deubiquitinase has been provided by several studies from the laboratory of Nai-Wen Chi (UCSD). Work from his laboratory identified a role for the GSV cargo IRAP and its binding partner tankyrase in the trafficking of GLUT4 (Chi and Lodish, 2000;Yeh *et al.*, 2007). Yeast two hybrid studies by the same group identified that the deubiquitinase USP25 can interact with tankyrase and contains a putative tankyrase binding motif (RTPADG) near the C-terminus (Sbodio and Chi, 2002).

To extend these data, I used a GST pull-down approach to investigate the interaction between tankyrase and recombinant USP25. I found that GST-USP25 could pull detectable levels of tankyrase 1 out of an adipocyte lysate (Figure 5.4), and that mutation of the conserved arginine residue within the putative tankyrase binding motif prevented this interaction (Figure 5.6). These findings substantiate the yeast-2-hybrid data (Sbodio and Chi, 2002) and more recently generated *in vivo* co-immunoprecipitation data (N-W Chi, unpublished) that USP25 and tankyrase interact, and moreover show that the interaction is direct and depends on the integrity of the USP25 RTPADG motif. This supports my hypothesis that tankyrase and IRAP form a platform to recruit the DUB USP25 to GSVs.

Although the pull-down data are conclusive, it would be interesting to extend the investigation of the USP25-tankyrase interaction further. For instance, an epitope tagged version of USP25 R1049A and its wild type counterpart could be

expressed in 3T3-L1 adipocytes, immunoprecipitated and co-precipitated proteins blotted for tankyrase. If tankyrase 1 was not co-immunoprecipitated with USP25 R1049A this would lend further weight to my hypothesis that the two proteins interact directly and form part of a complex in 3T3-L1 adipocytes.

Another possibility would be to attempt to reconstitute the putative IRAP-tankrase-USP25 complex *in vitro*. It has previously been demonstrated that the IRAP RQSPDG tankyrase binding motif alone readily binds tankyrase 1 from a 3T3-L1 lysate when expressed as a GST fusion protein (GST-RQSPDG) (Sbodio *et al.*, 2002). This recombinant protein could be immobilised on glutathione-Sepharose beads and recombinant USP25 and tankyrase added to the beads individually and in combination with appropriate controls, for example, non-tankyrase binding versions of GST-RQSPDG and USP25, or adding recombinant USP28 in place of USP25, as it is a homologue of USP25 (Valero *et al.*, 2001). If the three proteins formed a complex, I would anticipate recombinant USP25 to be pulled down by the GST-RQSPDG, with tankyrase 1 acting as a scaffold linking the two molecules. This method would however require some optimisation, especially regarding expression of recombinant tankyrase 1.

I went on to deplete USP25 in 3T3-L1 adipocytes using siRNA (Figure 5.7) and found that depletion of USP25 resulted in a reduction in the amount of GLUT4 in 3T3-L1 adipocytes (Figure 5.7), suggesting that USP25 is involved in maintaining GLUT4 stability. My initial attempt to ascertain whether the lysosome was responsible for this reduction in GLUT4 levels was hampered by the transfection method used and the lysosome inhibitors available; however further investigation of this would be valuable, as discussed in section 5.6. I went on to analyse the effect of the observed GLUT4 depletion on insulin responsive glucose uptake, and found that the fold change in [3^{H}] 2-deoxyglucose uptake was reduced on USP25 knockdown. These data suggest that the proportion of GLUT4 lost on USP25 knockdown may represent an insulin responsive pool of the protein. Further analysis of USP25 depleted cells is important, for example the subcellular fractionation approach applied in chapters 3 and 4 (Li and Kandror, 2005;Lamb *et al.*, 2010) could shed light on whether the observed GLUT4 depletion is actually from GSVs.

Overall, my investigation of knockdown of USP25 in 3T3-L1 adipocytes supports my hypothesis that USP25 is recruited to GSVs by IRAP and tankyrase, and acts to

deubiquitinate GLUT4, “trapping” it in GSVs and preventing its traffic to the lysosome. These findings are interesting in the context of studies highlighting the importance of deubiquitinases in stabilising cell surface proteins (McCullough *et al.*, 2004;Berthouze *et al.*, 2009;Mukai *et al.*, 2010).

6.4 Future directions

The work I have presented in this thesis implicates ubiquitination of GLUT4 in the sorting of the transporter into GSVs. I have also begun to characterise the roles of GGA3 and USP25 in the ubiquitin dependent sorting of GLUT4. What other directions could the study of GLUT4 ubiquitination take?

One issue to address is which E3 ligase ubiquitinates GLUT4 in 3T3-L1 cells. Of the three enzyme families in the ubiquitination cascade, the E3 ligases are the most numerous (with approximately 600 ligases encoded by the human genome (Li *et al.*, 2008)) and give the reaction its substrate specificity (Hicke and Dunn, 2003;Ciechanover, 2005). Two possible approaches could be taken to identify which of the many ligases ubiquitinated GLUT4. A screen approach using a fluorescent GLUT4 reporter (HA-GLUT4-GFP for example (Blot and McGraw, 2008)) expressed in a readily transfected cell line, such as HEK-293, would be one option. If USP25 was stably depleted in these cells, for example using a retroviral shRNA construct, this would deplete GLUT4 and reduce GFP fluorescence in these cells to a minimal level. An siRNA library of E3 ligases (Stagg *et al.*, 2009) could be used in this background and the cells assayed for fluorescence. The prediction would be that depletion of the ligase that ubiquitinates GLUT4 would result in an increase in GFP fluorescence in these cells, as the transporter would be diverted from lysosomal degradation.

A second possibility would be to look for ligases which can interact with GLUT4, or indeed other GSV components, and characterise whether their depletion or overexpression affects GLUT4 sorting. One candidate is βTrCP (β transducing repeat containing protein), which is the substrate recognition component of the SCF (Skip-Cullin-F box) ligase complex, shown to be required for growth hormone receptor degradation (Govers *et al.*, 1999;van Kerkhof *et al.*, 2007). βTrCP recognises motifs related to the sequence DDSWVEFIELD on substrates (Govers *et al.*, 1999). GLUT4 contains a variant of this motif (G. Gould, I. Adamson and N.

Bryant, unpublished) and has previously been proposed as a candidate for βTrCP directed ubiquitination (Govers *et al.*, 1999). Mutagenesis of this motif in the context of HA-GLUT4, and subsequent analysis of the ubiquitination status, insulin responsiveness and subcellular localisation of the mutant would test whether this ligase is responsible for ubiquitin dependent GLUT4 traffic.

GLUT4 has been shown to be SUMOlated (Lalioti *et al.*, 2002). Levels of GLUT4 are raised in 3T3-L1 cells by overexpression of the SUMO conjugating enzyme Ubc9 and decreased by depletion of the enzyme (Giorgino *et al.*, 2000;Liu *et al.*, 2007). However it seems that the scaffolding role of Ubc9 is more important than its enzymatic activity in maintaining GLUT4 stability, as overexpression of a catalytically inactive version of Ubc9 has the same effect on GLUT4 stability as overexpressing the wild type enzyme (Liu *et al.*, 2007). Further study of the interplay between GLUT4 SUMOlation and ubiquitination would be of interest, especially in light of data implicating SUMOlation as a tag for protein ubiquitination (Mullen and Brill, 2008).

Finally, as the overall aim of this thesis is to better understand the biology of insulin responsive tissues and consequently type 2 diabetes, it would be interesting to extend these studies into tissue samples from type 2 diabetic patients. One study has demonstrated that adipose tissue from a cohort of type 2 diabetic patients, while displaying normal expression of IRAP, exhibits markedly altered localisation of the peptidase, with the protein redistributed from the GSV enriched LDM (low density microsome) compartment to the HDM (high density microsome) and plasma membrane (Maianu *et al.*, 2001). This IRAP redistribution was associated with a depletion of GLUT4 from all membrane subfractions (Maianu *et al.*, 2001). When taken together with the data I have generated in this thesis, these findings suggest that the IRAP-tankyrase-USP25 complex may be being trafficked away from the GSV compartment in this cohort of type 2 diabetes patients, resulting in increased ubiquitination and thus lysosomal degradation of GLUT4.

Chapter 7 – Appendices

7.1 Appendix I – Glucose transport assay data for Figure 4.11

Basal

	pBABE	myc-GGA3	myc-GGA3$_{mut}$
	0.00114	0.00466	0.00234
	0.00444	0.00307	0.00356
	0.00119	0.00305	0.003112
	0.00431	0.00646	0.00571
Mean	0.00273	0.00431	0.00368
Standard Deviation	0.00181	0.00162	0.00145

Insulin

	pBABE	myc-GGA3	myc-GGA3$_{mut}$
	0.0162	0.0118	0.0117
	0.0565	0.0334	0.0322
	0.0271	0.0324	0.0220
	0.0546	0.0713	0.0398
Mean	0.0386	0.0372	0.0264
Standard Deviation	0.0200	0.0248	0.0122

Table 7.1 [^{3}H] 2-deoxyglucose uptake data for Figure 4.11.

Data are expressed as nmoles [^{3}H] 2-deoxyglucose per minute per well.

7.2 Appendix II – Glucose transport assay data for Figure 5.9

Basal

Scrambled	siRNA25	siRNA27
376.6667	562.5567	482.78
205.2233	508.7833	437.8933
131.3333	325.3367	346.56

Insulin

Scrambled	siRNA25	siRNA27
1773.34	761.5567	722.7867
1207.333	1704.123	1013.94
609.78	1168.45	1278.237

Table 7.2 Glucose transport assay data for Figure 5.9

Data are expressed as total counts in 5 minutes.

7.3 Appendix III – publications arising from this work

Lamb,C.A., McCann,R.K., Stockli,J., James,D.E., Bryant,N.J. (2010). Insulin-Regulated Trafficking of GLUT4 Requires Ubiquitination. Traffic *11* 1445-145

Bibliography

Agromayor,M., Martin-Serrano,J. (2006). Interaction of AMSH with ESCRT-III and deubiquitination of endosomal cargo. J.Biol.Chem. *281*, 23083-23091.

Alwan,H.A., van Leeuwen,J.E. (2007). UBPY-mediated epidermal growth factor receptor (EGFR) de-ubiquitination promotes EGFR degradation. J.Biol.Chem. *282*, 1658-1669.

Amenta,J.S., Brocher,S.C. (1980). Role of lysosomes in protein turnover: catch-up proteolysis after release from NH4Cl inhibition. J.Cell Physiol *102*, 259-266.

Bache,K.G., Stuffers,S., Malerod,L., Slagsvold,T., Raiborg,C., Lechardeur,D., Walchli,S., Lukacs,G.L., Brech,A., Stenmark,H. (2006). The ESCRT-III subunit hVps24 is required for degradation but not silencing of the epidermal growth factor receptor. Mol.Biol.Cell *17*, 2513-2523.

Barlowe,C., d'Enfert,C., Schekman,R. (1993). Purification and characterization of SAR1p, a small GTP-binding protein required for transport vesicle formation from the endoplasmic reticulum. J.Biol.Chem. *268*, 873-879.

Barlowe,C., Orci,L., Yeung,T., Hosobuchi,M., Hamamoto,S., Salama,N., Rexach,M.F., Ravazzola,M., Amherdt,M., Schekman,R. (1994). COPII: a membrane coat formed by Sec proteins that drive vesicle budding from the endoplasmic reticulum. Cell *77*, 895-907.

Barlowe,C., Schekman,R. (1993). SEC12 encodes a guanine-nucleotide-exchange factor essential for transport vesicle budding from the ER. Nature *365*, 347-349.

Berthouze,M., Venkataramanan,V., Li,Y., Shenoy,S.K. (2009). The deubiquitinases USP33 and USP20 coordinate beta2 adrenergic receptor recycling and resensitization. EMBO J. *28*, 1684-1696.

Bilodeau,P.S., Urbanowski,J.L., Winistorfer,S.C., Piper,R.C. (2002). The Vps27p Hse1p complex binds ubiquitin and mediates endosomal protein sorting. Nat.Cell Biol. *4*, 534-539.

Bilodeau,P.S., Winistorfer,S.C., Allaman,M.M., Surendhran,K., Kearney,W.R., Robertson,A.D., Piper,R.C. (2004). The GAT domains of clathrin-associated GGA proteins have two ubiquitin binding motifs. J.Biol.Chem. *279*, 54808-54816.

Birnbaum,M.J. (1989). Identification of a novel gene encoding an insulin-responsive glucose transporter protein. Cell *57*, 305-315.

Bishop,N., Horman,A., Woodman,P. (2002). Mammalian class E vps proteins recognize ubiquitin and act in the removal of endosomal protein-ubiquitin conjugates. J.Cell Biol. *157*, 91-101.

Blot,V., McGraw,T.E. (2008). Molecular mechanisms controlling GLUT4 intracellular retention. Mol.Biol.Cell *19*, 3477-3487.

Blott,E.J., Griffiths,G.M. (2002). Secretory lysosomes. Nat.Rev.Mol.Cell Biol. *3*, 122-131.

Boeke,J.D., LaCroute,F., Fink,G.R. (1984). A positive selection for mutants lacking orotidine-5'-phosphate decarboxylase activity in yeast: 5-fluoro-orotic acid resistance. Mol.Gen.Genet. *197*, 345-346.

Bogan,J.S., Hendon,N., McKee,A.E., Tsao,T.S., Lodish,H.F. (2003). Functional cloning of TUG as a regulator of GLUT4 glucose transporter trafficking. Nature *425*, 727-733.

Boman,A.L., Zhang,C., Zhu,X., Kahn,R.A. (2000). A family of ADP-ribosylation factor effectors that can alter membrane transport through the trans-Golgi. Mol.Biol.Cell *11*, 1241-1255.

Bonifacino,J.S. (2004). The GGA proteins: adaptors on the move. Nat.Rev.Mol.Cell Biol. *5*, 23-32.

Bosch-Comas,A., Lindsten,K., Gonzalez-Duarte,R., Masucci,M.G., Marfany,G. (2006). The ubiquitin-specific protease USP25 interacts with three sarcomeric proteins. Cell Mol.Life Sci. *63*, 723-734.

Brant,A.M., McCoid,S., Thomas,H.M., Baldwin,S.A., Davies,A., Parker,J.C., Gibbs,E.M., Gould,G.W. (1992). Analysis of the glucose transporter content of islet cell lines: implications for glucose-stimulated insulin release. Cell Signal. *4*, 641-650.

Braulke,T., Bonifacino,J.S. (2009). Sorting of lysosomal proteins. Biochim.Biophys.Acta *1793*, 605-614.

Brodsky,F.M., Chen,C.Y., Knuehl,C., Towler,M.C., Wakeham,D.E. (2001). Biological basket weaving: formation and function of clathrin-coated vesicles. Annu.Rev.Cell Dev.Biol. *17*, 517-568.

Bryant,N.J., Govers,R., James,D.E. (2002). Regulated transport of the glucose transporter GLUT4. Nat.Rev.Mol.Cell Biol. *3*, 267-277.

Bryant,N.J., Stevens,T.H. (1997). Two separate signals act independently to localize a yeast late Golgi membrane protein through a combination of retrieval and retention. J.Cell Biol. *136*, 287-297.

Cain,C.C., Trimble,W.S., Lienhard,G.E. (1992). Members of the VAMP family of synaptic vesicle proteins are components of glucose transporter-containing vesicles from rat adipocytes. J.Biol.Chem. *267*, 11681-11684.

Capilla,E., Suzuki,N., Pessin,J.E., Hou,J.C. (2007). The glucose transporter 4 FQQI motif is necessary for Akt substrate of 160-kilodalton-dependent plasma membrane translocation but not Golgi-localized (gamma)-ear-containing Arf-binding protein-dependent entry into the insulin-responsive storage compartment. Mol.Endocrinol. *21*, 3087-3099.

Chandler,C.S., Ballard,F.J. (1983). Inhibition of pyruvate carboxylase degradation and total protein breakdown by lysosomotropic agents in 3T3-L1 cells. Biochem.J. *210*, 845-853.

Chen,H.J., Yuan,J., Lobel,P. (1997). Systematic mutational analysis of the cation-independent mannose 6-phosphate/insulin-like growth factor II receptor

cytoplasmic domain. An acidic cluster containing a key aspartate is important for function in lysosomal enzyme sorting. J.Biol.Chem. *272*, 7003-7012.

Chi,N.W., Lodish,H.F. (2000). Tankyrase is a golgi-associated mitogen-activated protein kinase substrate that interacts with IRAP in GLUT4 vesicles. J.Biol.Chem. *275*, 38437-38444.

Chiang,Y.J., Hsiao,S.J., Yver,D., Cushman,S.W., Tessarollo,L., Smith,S., Hodes,R.J. (2008). Tankyrase 1 and tankyrase 2 are essential but redundant for mouse embryonic development. PLoS.One. *3*, e2639.

Cholay,M., Reverdy,C., Benarous,R., Colland,F., Daviet,L. (2010). Functional interaction between the ubiquitin-specific protease 25 and the SYK tyrosine kinase. Exp.Cell Res. *316*, 667-675.

Ciechanover,A. (2005). Intracellular protein degradation: from a vague idea, through the lysosome and the ubiquitin-proteasome system, and onto human diseases and drug targeting (Nobel lecture). Angew.Chem.Int.Ed Engl. *44*, 5944-5967.

Clague,M.J., Urbe,S. (2006). Endocytosis: the DUB version. Trends Cell Biol. *16*, 551-559.

Coster,A.C., Govers,R., James,D.E. (2004). Insulin stimulates the entry of GLUT4 into the endosomal recycling pathway by a quantal mechanism. Traffic. *5*, 763-771.

Coulombe,P., Rodier,G., Bonneil,E., Thibault,P., Meloche,S. (2004). N-Terminal ubiquitination of extracellular signal-regulated kinase 3 and p21 directs their degradation by the proteasome. Mol.Cell Biol. *24*, 6140-6150.

Cushman,S.W., Wardzala,L.J. (1980). Potential mechanism of insulin action on glucose transport in the isolated rat adipose cell. Apparent translocation of intracellular transport systems to the plasma membrane. J.Biol.Chem. *255*, 4758-4762.

Dacks,J.B., Field,M.C. (2007). Evolution of the eukaryotic membrane-trafficking system: origin, tempo and mode. J.Cell Sci. *120*, 2977-2985.

Dell'Angelica,E.C., Puertollano,R., Mullins,C., Aguilar,R.C., Vargas,J.D., Hartnell,L.M., Bonifacino,J.S. (2000). GGAs: a family of ADP ribosylation factor-binding proteins related to adaptors and associated with the Golgi complex. J.Cell Biol. *149*, 81-94.

Denuc,A., Bosch-Comas,A., Gonzalez-Duarte,R., Marfany,G. (2009). The UBA-UIM domains of the USP25 regulate the enzyme ubiquitination state and modulate substrate recognition. PLoS.One. *4*, e5571.

Dobson,S.P., Livingstone,C., Gould,G.W., Tavare,J.M. (1996). Dynamics of insulin-stimulated translocation of GLUT4 in single living cells visualised using green fluorescent protein. FEBS Lett. *393*, 179-184.

Doray,B., Knisely,J.M., Wartman,L., Bu,G., Kornfeld,S. (2008). Identification of Acidic Dileucine Signals in LRP9 that Interact with Both GGAs and AP-1/AP-2. Traffic.

Efe,J.A., Plattner,F., Hulo,N., Kressler,D., Emr,S.D., Deloche,O. (2005). Yeast Mon2p is a highly conserved protein that functions in the cytoplasm-to-vacuole transport pathway and is required for Golgi homeostasis. J.Cell Sci. *118*, 4751-4764.

Elbashir,S.M., Harborth,J., Lendeckel,W., Yalcin,A., Weber,K., Tuschl,T. (2001). Duplexes of 21-nucleotide RNAs mediate RNA interference in cultured mammalian cells. Nature *411*, 494-498.

Eliasson,L., Abdulkader,F., Braun,M., Galvanovskis,J., Hoppa,M.B., Rorsman,P. (2008). Novel aspects of the molecular mechanisms controlling insulin secretion. J.Physiol *586*, 3313-3324.

Fasshauer,D., Sutton,R.B., Brunger,A.T., Jahn,R. (1998). Conserved structural features of the synaptic fusion complex: SNARE proteins reclassified as Q- and R-SNAREs. Proc.Natl.Acad.Sci.U.S.A *95*, 15781-15786.

Fernando,R.N., Albiston,A.L., Chai,S.Y. (2008). The insulin-regulated aminopeptidase IRAP is colocalised with GLUT4 in the mouse hippocampus--potential role in modulation of glucose uptake in neurones? Eur.J.Neurosci. *28*, 588-598.

Fernando,R.N., Luff,S.E., Albiston,A.L., Chai,S.Y. (2007). Sub-cellular localization of insulin-regulated membrane aminopeptidase, IRAP to vesicles in neurons. J.Neurochem. *102*, 967-976.

Fukumoto,H., Kayano,T., Buse,J.B., Edwards,Y., Pilch,P.F., Bell,G.I., Seino,S. (1989). Cloning and characterization of the major insulin-responsive glucose transporter expressed in human skeletal muscle and other insulin-responsive tissues. J.Biol.Chem. *264*, 7776-7779.

Funakoshi,M., Sasaki,T., Nishimoto,T., Kobayashi,H. (2002). Budding yeast Dsk2p is a polyubiquitin-binding protein that can interact with the proteasome. Proc.Natl.Acad.Sci.U.S.A *99*, 745-750.

Gary,D.J., Puri,N., Won,Y.Y. (2007). Polymer-based siRNA delivery: perspectives on the fundamental and phenomenological distinctions from polymer-based DNA delivery. J.Control Release *121*, 64-73.

Geetha,T., Jiang,J., Wooten,M.W. (2005). Lysine 63 polyubiquitination of the nerve growth factor receptor TrkA directs internalization and signaling. Mol.Cell *20*, 301-312.

Geoffroy,M.C., Hay,R.T. (2009). An additional role for SUMO in ubiquitin-mediated proteolysis. Nat.Rev.Mol.Cell Biol. *10*, 564-568.

Ghosh,P., Dahms,N.M., Kornfeld,S. (2003). Mannose 6-phosphate receptors: new twists in the tale. Nat.Rev.Mol.Cell Biol. *4*, 202-212.

Gillingham,A.K., Whyte,J.R., Panic,B., Munro,S. (2006). Mon2, a relative of large Arf exchange factors, recruits Dop1 to the Golgi apparatus. J.Biol.Chem. *281*, 2273-2280.

Giorgino,F., de Robertis,O., Laviola,L., Montrone,C., Perrini,S., McCowen,K.C., Smith,R.J. (2000). The sentrin-conjugating enzyme mUbc9 interacts with GLUT4 and GLUT1 glucose transporters and regulates transporter levels in skeletal muscle cells. Proc.Natl.Acad.Sci.U.S.A *97*, 1125-1130.

Goldstein,G., Scheid,M., Hammerling,U., Schlesinger,D.H., Niall,H.D., Boyse,E.A. (1975). Isolation of a polypeptide that has lymphocyte-differentiating properties and is probably represented universally in living cells. Proc.Natl.Acad.Sci.U.S.A *72*, 11-15.

Govers,R., Coster,A.C., James,D.E. (2004). Insulin increases cell surface GLUT4 levels by dose dependently discharging GLUT4 into a cell surface recycling pathway. Mol.Cell Biol. *24*, 6456-6466.

Govers,R., ten Broeke,T., van Kerkhof,P., Schwartz,A.L., Strous,G.J. (1999). Identification of a novel ubiquitin conjugation motif, required for ligand-induced internalization of the growth hormone receptor. EMBO J. *18*, 28-36.

Haglund,K., Sigismund,S., Polo,S., Szymkiewicz,I., Di Fiore,P.P., Dikic,I. (2003). Multiple monoubiquitination of RTKs is sufficient for their endocytosis and degradation. Nat.Cell Biol. *5*, 461-466.

Harter,C., Pavel,J., Coccia,F., Draken,E., Wegehingel,S., Tschochner,H., Wieland,F. (1996). Nonclathrin coat protein gamma, a subunit of coatomer, binds to the cytoplasmic dilysine motif of membrane proteins of the early secretory pathway. Proc.Natl.Acad.Sci.U.S.A *93*, 1902-1906.

Hashiramoto,M., James,D.E. (2000). Characterization of insulin-responsive GLUT4 storage vesicles isolated from 3T3-L1 adipocytes. Mol.Cell Biol. *20*, 416-427.

Hassink,G.C., Zhao,B., Sompallae,R., Altun,M., Gastaldello,S., Zinin,N.V., Masucci,M.G., Lindsten,K. (2009). The ER-resident ubiquitin-specific protease 19 participates in the UPR and rescues ERAD substrates. EMBO Rep. *10*, 755-761.

Helliwell,S.B., Losko,S., Kaiser,C.A. (2001). Components of a ubiquitin ligase complex specify polyubiquitination and intracellular trafficking of the general amino acid permease. J.Cell Biol. *153*, 649-662.

Hicke,L., Dunn,R. (2003). Regulation of membrane protein transport by ubiquitin and ubiquitin-binding proteins. Annu.Rev.Cell Dev.Biol. *19*, 141-172.

Hida,T., Ikeda,H., Kametaka,S., Akazawa,C., Kohsaka,S., Ebisu,S., Uchiyama,Y., Waguri,S. (2007). Specific depletion of GGA2 causes cathepsin D missorting in HeLa cells. Arch.Histol.Cytol. *70*, 303-312.

Hirst,J., Lindsay,M.R., Robinson,M.S. (2001). GGAs: roles of the different domains and comparison with AP-1 and clathrin. Mol.Biol.Cell *12*, 3573-3588.

Hirst,J., Lui,W.W., Bright,N.A., Totty,N., Seaman,M.N., Robinson,M.S. (2000). A family of proteins with gamma-adaptin and VHS domains that facilitate trafficking between the trans-Golgi network and the vacuole/lysosome. J.Cell Biol. *149*, 67-80.

Hirst,J., Sahlender,D.A., Choma,M., Sinka,R., Harbour,M.E., Parkinson,M., Robinson,M.S. (2009). Spatial and functional relationship of GGAs and AP-1 in Drosophila and HeLa cells. Traffic. *10*, 1696-1710.

Hirst,J., Seaman,M.N., Buschow,S.I., Robinson,M.S. (2007). The role of cargo proteins in GGA recruitment. Traffic. *8*, 594-604.

Hong,W. (2005). SNAREs and traffic. Biochim.Biophys.Acta *1744*, 493-517.

Honing,S., Griffith,J., Geuze,H.J., Hunziker,W. (1996). The tyrosine-based lysosomal targeting signal in lamp-1 mediates sorting into Golgi-derived clathrin-coated vesicles. EMBO J. *15*, 5230-5239.

Hou,D., Cenciarelli,C., Jensen,J.P., Nguygen,H.B., Weissman,A.M. (1994). Activation-dependent ubiquitination of a T cell antigen receptor subunit on multiple intracellular lysines. J.Biol.Chem. *269*, 14244-14247.

Hou,J.C., Suzuki,N., Pessin,J.E., Watson,R.T. (2006). A specific dileucine motif is required for the GGA-dependent entry of newly synthesized insulin-responsive aminopeptidase into the insulin-responsive compartment. J.Biol.Chem. *281*, 33457-33466.

Hsiao,S.J., Smith,S. (2008). Tankyrase function at telomeres, spindle poles, and beyond. Biochimie *90*, 83-92.

Huh,W.K., Falvo,J.V., Gerke,L.C., Carroll,A.S., Howson,R.W., Weissman,J.S., O'Shea,E.K. (2003). Global analysis of protein localization in budding yeast. Nature *425*, 686-691.

Ishikura,S., Weissman,A.M., Bonifacino,J.S. (2010). Serine residues in the cytosolic tail of the T-cell antigen receptor alpha-chain mediate ubiquitination and endoplasmic reticulum-associated degradation of the unassembled protein. J.Biol.Chem. *285*, 23916-23924.

Ito,H., Fukuda,Y., Murata,K., Kimura,A. (1983). Transformation of intact yeast cells treated with alkali cations. J.Bacteriol. *153*, 163-168.

Jahn,R., Scheller,R.H. (2006). SNAREs--engines for membrane fusion. Nat.Rev.Mol.Cell Biol. *7*, 631-643.

James,D.E., Strube,M., Mueckler,M. (1989). Molecular cloning and characterization of an insulin-regulatable glucose transporter. Nature *338*, 83-87.

Jedrychowski,M.P., Gartner,C.A., Gygi,S.P., Zhou,L., Herz,J., Kandror,K.V., Pilch,P.F. (2010). Proteomic analysis of GLUT4 storage vesicles reveals LRP1 to be an important vesicle component and target of insulin signaling. J.Biol.Chem. *285*, 104-114.

Jordens,I., Molle,D., Xiong,W., Keller,S.R., McGraw,T.E. (2010). Insulin-regulated aminopeptidase is a key regulator of GLUT4 trafficking by controlling the sorting of GLUT4 from endosomes to specialized insulin-regulated vesicles. Mol.Biol.Cell *21*, 2034-2044.

Kakhlon,O., Sakya,P., Larijani,B., Watson,R., Tooze,S.A. (2006). GGA function is required for maturation of neuroendocrine secretory granules. EMBO J. *25*, 1590-1602.

Kaminker,P.G., Kim,S.H., Taylor,R.D., Zebarjadian,Y., Funk,W.D., Morin,G.B., Yaswen,P., Campisi,J. (2001). TANK2, a new TRF1-associated poly(ADP-ribose) polymerase, causes rapid induction of cell death upon overexpression. J.Biol.Chem. *276*, 35891-35899.

Kamsteeg,E.J., Hendriks,G., Boone,M., Konings,I.B., Oorschot,V., van der,S.P., Klumperman,J., Deen,P.M. (2006). Short-chain ubiquitination mediates the regulated endocytosis of the aquaporin-2 water channel. Proc.Natl.Acad.Sci.U.S.A *103*, 18344-18349.

Kanayama,A., Seth,R.B., Sun,L., Ea,C.K., Hong,M., Shaito,A., Chiu,Y.H., Deng,L., Chen,Z.J. (2004). TAB2 and TAB3 activate the NF-kappaB pathway through binding to polyubiquitin chains. Mol.Cell *15*, 535-548.

Kang,E.L., Cameron,A.N., Piazza,F., Walker,K.R., Tesco,G. (2010). Ubiquitin regulates GGA3-mediated degradation of BACE1. J.Biol.Chem.

Karylowski,O., Zeigerer,A., Cohen,A., McGraw,T.E. (2004). GLUT4 is retained by an intracellular cycle of vesicle formation and fusion with endosomes. Mol.Biol.Cell *15*, 870-882.

Kasahara,T., Kasahara,M. (1997). Characterization of rat Glut4 glucose transporter expressed in the yeast Saccharomyces cerevisiae: comparison with Glut1 glucose transporter. Biochim.Biophys.Acta *1324*, 111-119.

Kato,M., Miyazawa,K., Kitamura,N. (2000). A deubiquitinating enzyme UBPY interacts with the Src homology 3 domain of Hrs-binding protein via a novel binding motif PX(V/I)(D/N)RXXKP. J.Biol.Chem. *275*, 37481-37487.

Kawasaki,M., Shiba,T., Shiba,Y., Yamaguchi,Y., Matsugaki,N., Igarashi,N., Suzuki,M., Kato,R., Kato,K., Nakayama,K., Wakatsuki,S. (2005). Molecular mechanism of ubiquitin recognition by GGA3 GAT domain. Genes Cells *10*, 639-654.

Keen,J.H. (1987). Clathrin assembly proteins: affinity purification and a model for coat assembly. J.Cell Biol. *105*, 1989-1998.

Keller,S.R., Davis,A.C., Clairmont,K.B. (2002). Mice deficient in the insulin-regulated membrane aminopeptidase show substantial decreases in glucose transporter GLUT4 levels but maintain normal glucose homeostasis. J.Biol.Chem. *277*, 17677-17686.

Kirchhausen,T. (2000). Three ways to make a vesicle. Nat.Rev.Mol.Cell Biol. *1*, 187-198.

Knuehl,C., Chen,C.Y., Manalo,V., Hwang,P.K., Ota,N., Brodsky,F.M. (2006). Novel binding sites on clathrin and adaptors regulate distinct aspects of coat assembly. Traffic. *7*, 1688-1700.

Komander,D., Clague,M.J., Urbe,S. (2009). Breaking the chains: structure and function of the deubiquitinases. Nat.Rev.Mol.Cell Biol. *10*, 550-563.

Kupriyanova,T.A., Kandror,K.V. (2000). Cellugyrin is a marker for a distinct population of intracellular Glut4-containing vesicles. J.Biol.Chem. *275*, 36263-36268.

Kupriyanova,T.A., Kandror,V., Kandror,K.V. (2002). Isolation and characterization of the two major intracellular Glut4 storage compartments. J.Biol.Chem. *277*, 9133-9138.

Lalioti,V.S., Vergarajauregui,S., Pulido,D., Sandoval,I.V. (2002). The insulin-sensitive glucose transporter, GLUT4, interacts physically with Daxx. Two proteins with capacity to bind Ubc9 and conjugated to SUMO1. J.Biol.Chem. *277*, 19783-19791.

Lamb,C.A., McCann,R.K., Stockli,J., James,D.E., Bryant,N.J. (2010). Insulin-Regulated Trafficking of GLUT4 Requires Ubiquitination. Traffic.

Lampson,M.A., Racz,A., Cushman,S.W., McGraw,T.E. (2000). Demonstration of insulin-responsive trafficking of GLUT4 and vpTR in fibroblasts. J.Cell Sci. *113 (Pt 22)*, 4065-4076.

Lawson,D., Fewtrell,C., Raff,M.C. (1978). Localized mast cell degranulation induced by concanavalin A-sepharose beads. Implications for the Ca2+ hypothesis of stimulus-secretion coupling. J.Cell Biol. *79*, 394-400.

Li,J., Peters,P.J., Bai,M., Dai,J., Bos,E., Kirchhausen,T., Kandror,K.V., Hsu,V.W. (2007). An ACAP1-containing clathrin coat complex for endocytic recycling. J.Cell Biol. *178*, 453-464.

Li,L.V., Kandror,K.V. (2005). Golgi-localized, gamma-ear-containing, Arf-binding protein adaptors mediate insulin-responsive trafficking of glucose transporter 4 in 3T3-L1 adipocytes. Mol.Endocrinol. *19*, 2145-2153.

Li,W., Bengtson,M.H., Ulbrich,A., Matsuda,A., Reddy,V.A., Orth,A., Chanda,S.K., Batalov,S., Joazeiro,C.A.P. (2008). Genome-Wide and Functional Annotation of Human E3 Ubiquitin Ligases Identifies MULAN, a Mitochondrial E3 that Regulates the Organelle's Dynamics and Signaling. PLoS ONE *3*, e1487.

Lin,B.Z., Pilch,P.F., Kandror,K.V. (1997). Sortilin is a major protein component of Glut4-containing vesicles. J.Biol.Chem. *272*, 24145-24147.

Lin,Y., Sun,Z. (2010). Current views on type 2 diabetes. J.Endocrinol. *204*, 1-11.

Liu,L.B., Omata,W., Kojima,I., Shibata,H. (2007). The SUMO conjugating enzyme Ubc9 is a regulator of GLUT4 turnover and targeting to the insulin-responsive storage compartment in 3T3-L1 adipocytes. Diabetes *56*, 1977-1985.

Livingstone,C., James,D.E., Rice,J.E., Hanpeter,D., Gould,G.W. (1996). Compartment ablation analysis of the insulin-responsive glucose transporter (GLUT4) in 3T3-L1 adipocytes. Biochem.J. *315 (Pt 2)*, 487-495.

Losko,S., Kopp,F., Kranz,A., Kolling,R. (2001). Uptake of the ATP-binding cassette (ABC) transporter Ste6 into the yeast vacuole is blocked in the doa4 Mutant. Mol.Biol.Cell *12*, 1047-1059.

Mackall,J.C., Student,A.K., Polakis,S.E., Lane,M.D. (1976). Induction of lipogenesis during differentiation in a "preadipocyte" cell line. J.Biol.Chem. *251*, 6462-6464.

Maeda,K., Kawamura,K., Kondo,S., Aoyagi,T., Takeuchi,T. (1971). The structure and activity of leupeptins and related analogs. J.Antibiot.(Tokyo) *24*, 402-404.

Magasanik,B., Kaiser,C.A. (2002). Nitrogen regulation in Saccharomyces cerevisiae. Gene *290*, 1-18.

Maianu,L., Keller,S.R., Garvey,W.T. (2001). Adipocytes exhibit abnormal subcellular distribution and translocation of vesicles containing glucose transporter 4 and insulin-regulated aminopeptidase in type 2 diabetes mellitus: implications regarding defects in vesicle trafficking. J.Clin.Endocrinol.Metab *86*, 5450-5456.

Malerod,L., Stuffers,S., Brech,A., Stenmark,H. (2007). Vps22/EAP30 in ESCRT-II mediates endosomal sorting of growth factor and chemokine receptors destined for lysosomal degradation. Traffic. *8*, 1617-1629.

Martin,O.J., Lee,A., McGraw,T.E. (2006). GLUT4 distribution between the plasma membrane and the intracellular compartments is maintained by an insulin-modulated bipartite dynamic mechanism. J.Biol.Chem. *281*, 484-490.

Martin,S., Millar,C.A., Lyttle,C.T., Meerloo,T., Marsh,B.J., Gould,G.W., James,D.E. (2000). Effects of insulin on intracellular GLUT4 vesicles in adipocytes: evidence for a secretory mode of regulation. J.Cell Sci. *113 Pt 19*, 3427-3438.

Martin,S., Tellam,J., Livingstone,C., Slot,J.W., Gould,G.W., James,D.E. (1996). The glucose transporter (GLUT-4) and vesicle-associated membrane protein-2 (VAMP-2) are segregated from recycling endosomes in insulin-sensitive cells. J.Cell Biol. *134*, 625-635.

Martin,T.F. (1997). Stages of regulated exocytosis. Trends Cell Biol. *7*, 271-276.

Mascorro-Gallardo,J.O., Covarrubias,A.A., Gaxiola,R. (1996). Construction of a CUP1 promoter-based vector to modulate gene expression in Saccharomyces cerevisiae. Gene *172*, 169-170.

Mattera,R., Puertollano,R., Smith,W.J., Bonifacino,J.S. (2004). The trihelical bundle subdomain of the GGA proteins interacts with multiple partners through overlapping but distinct sites. J.Biol.Chem. *279*, 31409-31418.

McCann R.K. The role of ubiquitination in the regulated trafficking of GLUT4: A study with yeast and adipocytes. 2007.

Ref Type: Thesis/Dissertation

McCullough,J., Clague,M.J., Urbe,S. (2004). AMSH is an endosome-associated ubiquitin isopeptidase. J.Cell Biol. *166*, 487-492.

McNew,J.A., Parlati,F., Fukuda,R., Johnston,R.J., Paz,K., Paumet,F., Sollner,T.H., Rothman,J.E. (2000). Compartmental specificity of cellular membrane fusion encoded in SNARE proteins. Nature *407*, 153-159.

Meulmeester,E., Kunze,M., Hsiao,H.H., Urlaub,H., Melchior,F. (2008). Mechanism and consequences for paralog-specific sumoylation of ubiquitin-specific protease 25. Mol.Cell *30*, 610-619.

Millar,C.A., Shewan,A., Hickson,G.R., James,D.E., Gould,G.W. (1999). Differential regulation of secretory compartments containing the insulin-responsive glucose transporter 4 in 3T3-L1 adipocytes. Mol.Biol.Cell *10*, 3675-3688.

Mills,I.G., Praefcke,G.J., Vallis,Y., Peter,B.J., Olesen,L.E., Gallop,J.L., Butler,P.J., Evans,P.R., McMahon,H.T. (2003). EpsinR: an AP1/clathrin interacting protein involved in vesicle trafficking. J.Cell Biol. *160*, 213-222.

Mishra,S.K., Keyel,P.A., Hawryluk,M.J., Agostinelli,N.R., Watkins,S.C., Traub,L.M. (2002). Disabled-2 exhibits the properties of a cargo-selective endocytic clathrin adaptor. EMBO J. *21*, 4915-4926.

Morgenstern,J.P., Land,H. (1990). Advanced mammalian gene transfer: high titre retroviral vectors with multiple drug selection markers and a complementary helper-free packaging cell line. Nucleic Acids Res. *18*, 3587-3596.

Morita,S., Kojima,T., Kitamura,T. (2000). Plat-E: an efficient and stable system for transient packaging of retroviruses. Gene Ther. *7*, 1063-1066.

Morris,N.J., Ross,S.A., Lane,W.S., Moestrup,S.K., Petersen,C.M., Keller,S.R., Lienhard,G.E. (1998). Sortilin is the major 110-kDa protein in GLUT4 vesicles from adipocytes. J.Biol.Chem. *273*, 3582-3587.

Mukai,A., Yamamoto-Hino,M., Awano,W., Watanabe,W., Komada,M., Goto,S. (2010). Balanced ubiquitylation and deubiquitylation of Frizzled regulate cellular responsiveness to Wg/Wnt. EMBO J. *29*, 2114-2125.

Mullen,J.R., Brill,S.J. (2008). Activation of the Slx5-Slx8 ubiquitin ligase by poly-small ubiquitin-like modifier conjugates. J.Biol.Chem. *283*, 19912-19921.

Muretta,J.M., Romenskaia,I., Mastick,C.C. (2008). Insulin releases Glut4 from static storage compartments into cycling endosomes and increases the rate constant for Glut4 exocytosis. J.Biol.Chem. *283*, 311-323.

Nielsen,M.S., Madsen,P., Christensen,E.I., Nykjaer,A., Gliemann,J., Kasper,D., Pohlmann,R., Petersen,C.M. (2001). The sortilin cytoplasmic tail conveys Golgi-endosome transport and binds the VHS domain of the GGA2 sorting protein. EMBO J. *20*, 2180-2190.

Nikko,E., Andre,B. (2007). Evidence for a direct role of the Doa4 deubiquitinating enzyme in protein sorting into the MVB pathway. Traffic. *8*, 566-581.

Nothwehr,S.F., Conibear,E., Stevens,T.H. (1995). Golgi and vacuolar membrane proteins reach the vacuole in vps1 mutant yeast cells via the plasma membrane. J.Cell Biol. *129*, 35-46.

Odorizzi,G., Babst,M., Emr,S.D. (1998). Fab1p PtdIns(3)P 5-kinase function essential for protein sorting in the multivesicular body. Cell *95*, 847-858.

Ohno,A., Jee,J., Fujiwara,K., Tenno,T., Goda,N., Tochio,H., Kobayashi,H., Hiroaki,H., Shirakawa,M. (2005). Structure of the UBA domain of Dsk2p in complex with ubiquitin molecular determinants for ubiquitin recognition. Structure. *13*, 521-532.

Pak,Y., Glowacka,W.K., Bruce,M.C., Pham,N., Rotin,D. (2006). Transport of LAPTM5 to lysosomes requires association with the ubiquitin ligase Nedd4, but not LAPTM5 ubiquitination. J.Cell Biol. *175*, 631-645.

Pelham,H.R. (2004). Membrane traffic: GGAs sort ubiquitin. Curr.Biol. *14*, R357-R359.

Peng,J., Schwartz,D., Elias,J.E., Thoreen,C.C., Cheng,D., Marsischky,G., Roelofs,J., Finley,D., Gygi,S.P. (2003). A proteomics approach to understanding protein ubiquitination. Nat.Biotechnol. *21*, 921-926.

Pickart,C.M. (2001). Mechanisms underlying ubiquitination. Annu.Rev.Biochem. *70*, 503-533.

Pickart,C.M., Fushman,D. (2004). Polyubiquitin chains: polymeric protein signals. Curr.Opin.Chem.Biol. *8*, 610-616.

Piper,R.C., Bryant,N.J., Stevens,T.H. (1997). The membrane protein alkaline phosphatase is delivered to the vacuole by a route that is distinct from the VPS-dependent pathway. J.Cell Biol. *138*, 531-545.

Piper,R.C., Cooper,A.A., Yang,H., Stevens,T.H. (1995). VPS27 controls vacuolar and endocytic traffic through a prevacuolar compartment in Saccharomyces cerevisiae. J.Cell Biol. *131*, 603-617.

Piper,R.C., Luzio,J.P. (2007). Ubiquitin-dependent sorting of integral membrane proteins for degradation in lysosomes. Curr.Opin.Cell Biol. *19*, 459-465.

Puertollano,R., Bonifacino,J.S. (2004). Interactions of GGA3 with the ubiquitin sorting machinery. Nat.Cell Biol. *6*, 244-251.

Quon,M.J., Guerre-Millo,M., Zarnowski,M.J., Butte,A.J., Em,M., Cushman,S.W., Taylor,S.I. (1994). Tyrosine kinase-deficient mutant human insulin receptors (Met1153-->Ile) overexpressed in transfected rat adipose cells fail to mediate translocation of epitope-tagged GLUT4. Proc.Natl.Acad.Sci.U.S.A *91*, 5587-5591.

Raasi,S., Varadan,R., Fushman,D., Pickart,C.M. (2005). Diverse polyubiquitin interaction properties of ubiquitin-associated domains. Nat.Struct.Mol.Biol. *12*, 708-714.

Raiborg,C., Stenmark,H. (2009). The ESCRT machinery in endosomal sorting of ubiquitylated membrane proteins. Nature *458*, 445-452.

Raiborg,C., Wesche,J., Malerod,L., Stenmark,H. (2006). Flat clathrin coats on endosomes mediate degradative protein sorting by scaffolding Hrs in dynamic microdomains. J.Cell Sci. *119*, 2414-2424.

Raymond,C.K., Howald-Stevenson,I., Vater,C.A., Stevens,T.H. (1992). Morphological classification of the yeast vacuolar protein sorting mutants: evidence for a prevacuolar compartment in class E vps mutants. Mol.Biol.Cell *3*, 1389-1402.

Ren,X., Hurley,J.H. (2010). VHS domains of ESCRT-0 cooperate in high-avidity binding to polyubiquitinated cargo. EMBO J. *29*, 1045-1054.

Reyes-Turcu,F.E., Ventii,K.H., Wilkinson,K.D. (2009). Regulation and cellular roles of ubiquitin-specific deubiquitinating enzymes. Annu.Rev.Biochem. *78*, 363-397.

Risinger,A.L., Kaiser,C.A. (2008). Different ubiquitin signals act at the Golgi and plasma membrane to direct GAP1 trafficking. Mol.Biol.Cell *19*, 2962-2972.

Roberg,K.J., Rowley,N., Kaiser,C.A. (1997). Physiological regulation of membrane protein sorting late in the secretory pathway of Saccharomyces cerevisiae. J.Cell Biol. *137*, 1469-1482.

Robinson,M.S. (2004). Adaptable adaptors for coated vesicles. Trends Cell Biol. *14*, 167-174.

Rosen,E.D., Spiegelman,B.M. (2006). Adipocytes as regulators of energy balance and glucose homeostasis. Nature *444*, 847-853.

Ross,S.A., Herbst,J.J., Keller,S.R., Lienhard,G.E. (1997). Trafficking kinetics of the insulin-regulated membrane aminopeptidase in 3T3-L1 adipocytes. Biochem.Biophys.Res.Commun. *239*, 247-251.

Ross,S.A., Keller,S.R., Lienhard,G.E. (1998). Increased intracellular sequestration of the insulin-regulated aminopeptidase upon differentiation of 3T3-L1 cells. Biochem.J. *330 (Pt 2)*, 1003-1008.

Ross,S.A., Scott,H.M., Morris,N.J., Leung,W.Y., Mao,F., Lienhard,G.E., Keller,S.R. (1996). Characterization of the insulin-regulated membrane aminopeptidase in 3T3-L1 adipocytes. J.Biol.Chem. *271*, 3328-3332.

Rothman,J.H., Howald,I., Stevens,T.H. (1989). Characterization of genes required for protein sorting and vacuolar function in the yeast Saccharomyces cerevisiae. EMBO J. *8*, 2057-2065.

Row,P.E., Prior,I.A., McCullough,J., Clague,M.J., Urbe,S. (2006). The ubiquitin isopeptidase UBPY regulates endosomal ubiquitin dynamics and is essential for receptor down-regulation. J.Biol.Chem. *281*, 12618-12624.

Rubio-Texeira,M., Kaiser,C.A. (2006). Amino acids regulate retrieval of the yeast general amino acid permease from the vacuolar targeting pathway. Mol.Biol.Cell *17*, 3031-3050.

Saltiel,A.R., Kahn,C.R. (2001). Insulin signalling and the regulation of glucose and lipid metabolism. Nature *414*, 799-806.

Sambrook,J., Fritsch,E.F., Maniatis,T. (1989). Molecular Cloning: A Laboratory Manual. Cold Springs Harbour: Cold Springs Harbour Press.

Sandoval,I.V., Martinez-Arca,S., Valdueza,J., Palacios,S., Holman,G.D. (2000). Distinct reading of different structural determinants modulates the dileucine-mediated transport steps of the lysosomal membrane protein LIMPII and the insulin-sensitive glucose transporter GLUT4. J.Biol.Chem. *275*, 39874-39885.

Sano,H., Kane,S., Sano,E., Miinea,C.P., Asara,J.M., Lane,W.S., Garner,C.W., Lienhard,G.E. (2003). Insulin-stimulated phosphorylation of a Rab GTPase-activating protein regulates GLUT4 translocation. J.Biol.Chem. *278*, 14599-14602.

Sassenfeld,H.M. (1990). Engineering proteins for purification. Trends Biotechnol. *8*, 88-93.

Saveanu,L., Carroll,O., Weimershaus,M., Guermonprez,P., Firat,E., Lindo,V., Greer,F., Davoust,J., Kratzer,R., Keller,S.R., Niedermann,G., van Endert,P. (2009). IRAP identifies an endosomal compartment required for MHC class I cross-presentation. Science *325*, 213-217.

Sbodio,J.I., Chi,N.W. (2002). Identification of a tankyrase-binding motif shared by IRAP, TAB182, and human TRF1 but not mouse TRF1. NuMA contains this RXXPDG motif and is a novel tankyrase partner. J.Biol.Chem. *277*, 31887-31892.

Sbodio,J.I., Lodish,H.F., Chi,N.W. (2002). Tankyrase-2 oligomerizes with tankyrase-1 and binds to both TRF1 (telomere-repeat-binding factor 1) and IRAP (insulin-responsive aminopeptidase). Biochem.J. *361*, 451-459.

Scott,P.M., Bilodeau,P.S., Zhdankina,O., Winistorfer,S.C., Hauglund,M.J., Allaman,M.M., Kearney,W.R., Robertson,A.D., Boman,A.L., Piper,R.C. (2004). GGA proteins bind ubiquitin to facilitate sorting at the trans-Golgi network. Nat.Cell Biol. *6*, 252-259.

Seimiya,H., Smith,S. (2002). The telomeric poly(ADP-ribose) polymerase, tankyrase 1, contains multiple binding sites for telomeric repeat binding factor 1 (TRF1) and a novel acceptor, 182-kDa tankyrase-binding protein (TAB182). J.Biol.Chem. *277*, 14116-14126.

Serafini,T., Orci,L., Amherdt,M., Brunner,M., Kahn,R.A., Rothman,J.E. (1991). ADP-ribosylation factor is a subunit of the coat of Golgi-derived COP-coated vesicles: a novel role for a GTP-binding protein. Cell *67*, 239-253.

Shenoy,S.K. (2007). Seven-transmembrane receptors and ubiquitination. Circ.Res. *100*, 1142-1154.

Shenoy,S.K., Modi,A.S., Shukla,A.K., Xiao,K., Berthouze,M., Ahn,S., Wilkinson,K.D., Miller,W.E., Lefkowitz,R.J. (2009). Beta-arrestin-dependent signaling and trafficking of 7-transmembrane receptors is reciprocally regulated by the deubiquitinase USP33 and the E3 ligase Mdm2. Proc.Natl.Acad.Sci.U.S.A *106*, 6650-6655.

Shewan,A.M., Marsh,B.J., Melvin,D.R., Martin,S., Gould,G.W., James,D.E. (2000). The cytosolic C-terminus of the glucose transporter GLUT4 contains an acidic cluster endosomal targeting motif distal to the dileucine signal. Biochem.J. *350 Pt 1*, 99-107.

Shewan,A.M., van Dam,E.M., Martin,S., Luen,T.B., Hong,W., Bryant,N.J., James,D.E. (2003). GLUT4 recycles via a trans-Golgi network (TGN) subdomain enriched in Syntaxins 6 and 16 but not TGN38: involvement of an acidic targeting motif. Mol.Biol.Cell *14*, 973-986.

Shi,J., Huang,G., Kandror,K.V. (2008). Self-assembly of Glut4 storage vesicles during differentiation of 3T3-L1 adipocytes. J.Biol.Chem. *283*, 30311-30321.

Shi,J., Kandror,K.V. (2005). Sortilin is essential and sufficient for the formation of Glut4 storage vesicles in 3T3-L1 adipocytes. Dev.Cell *9*, 99-108.

Shi,J., Kandror,K.V. (2007). The luminal Vps10p domain of sortilin plays the predominant role in targeting to insulin-responsive Glut4-containing vesicles. J.Biol.Chem. *282*, 9008-9016.

Shiba,T., Takatsu,H., Nogi,T., Matsugaki,N., Kawasaki,M., Igarashi,N., Suzuki,M., Kato,R., Earnest,T., Nakayama,K., Wakatsuki,S. (2002). Structural basis for recognition of acidic-cluster dileucine sequence by GGA1. Nature *415*, 937-941.

Shiba,Y., Katoh,Y., Shiba,T., Yoshino,K., Takatsu,H., Kobayashi,H., Shin,H.W., Wakatsuki,S., Nakayama,K. (2004). GAT (GGA and Tom1) domain responsible for ubiquitin binding and ubiquitination. J.Biol.Chem. *279*, 7105-7111.

Shin,J.S., Ebersold,M., Pypaert,M., Delamarre,L., Hartley,A., Mellman,I. (2006). Surface expression of MHC class II in dendritic cells is controlled by regulated ubiquitination. Nature *444*, 115-118.

Singer-Kruger,B., Lasic,M., Burger,A.M., Hausser,A., Pipkorn,R., Wang,Y. (2008). Yeast and human Ysl2p/hMon2 interact with Gga adaptors and mediate their subcellular distribution. EMBO J. *27*, 1423-1435.

Smith,S., Giriat,I., Schmitt,A., de Lange,T. (1998). Tankyrase, a poly(ADP-ribose) polymerase at human telomeres. Science *282*, 1484-1487.

Soetens,O., De Craene,J.O., Andre,B. (2001). Ubiquitin is required for sorting to the vacuole of the yeast general amino acid permease, Gap1. J.Biol.Chem. *276*, 43949-43957.

Sollner,T., Bennett,M.K., Whiteheart,S.W., Scheller,R.H., Rothman,J.E. (1993). A protein assembly-disassembly pathway in vitro that may correspond to sequential steps of synaptic vesicle docking, activation, and fusion. Cell *75*, 409-418.

Stagg,H.R., Thomas,M., van den,B.D., Wiertz,E.J., Drabkin,H.A., Gemmill,R.M., Lehner,P.J. (2009). The TRC8 E3 ligase ubiquitinates MHC class I molecules before dislocation from the ER. J.Cell Biol. *186*, 685-692.

Stang,E., Johannessen,L.E., Knardal,S.L., Madshus,I.H. (2000). Polyubiquitination of the epidermal growth factor receptor occurs at the plasma membrane upon ligand-induced activation. J.Biol.Chem. *275*, 13940-13947.

Struthers,M.S., Shanks,S.G., MacDonald,C., Carpp,L.N., Drozdowska,A.M., Kioumourtzoglou,D., Furgason,M.L., Munson,M., Bryant,N.J. (2009). Functional homology of mammalian syntaxin 16 and yeast Tlg2p reveals a conserved regulatory mechanism. J.Cell Sci. *122*, 2292-2299.

Sun,S.C. (2010). CYLD: a tumor suppressor deubiquitinase regulating NF-kappaB activation and diverse biological processes. Cell Death.Differ. *17*, 25-34.

Sutton,R.B., Fasshauer,D., Jahn,R., Brunger,A.T. (1998). Crystal structure of a SNARE complex involved in synaptic exocytosis at 2.4 A resolution. Nature *395*, 347-353.

Suzuki,K., Kono,T. (1980). Evidence that insulin causes translocation of glucose transport activity to the plasma membrane from an intracellular storage site. Proc.Natl.Acad.Sci.U.S.A *77*, 2542-2545.

Swaminathan,S., Amerik,A.Y., Hochstrasser,M. (1999). The Doa4 deubiquitinating enzyme is required for ubiquitin homeostasis in yeast. Mol.Biol.Cell *10*, 2583-2594.

Tesco,G., Koh,Y.H., Kang,E.L., Cameron,A.N., Das,S., Sena-Esteves,M., Hiltunen,M., Yang,S.H., Zhong,Z., Shen,Y., Simpkins,J.W., Tanzi,R.E. (2007). Depletion of GGA3 stabilizes BACE and enhances beta-secretase activity. Neuron *54*, 721-737.

Tettamanzi,M.C., Yu,C., Bogan,J.S., Hodsdon,M.E. (2006). Solution structure and backbone dynamics of an N-terminal ubiquitin-like domain in the GLUT4-regulating protein, TUG. Protein Sci. *15*, 498-508.

Tortorella,L.L., Schapiro,F.B., Maxfield,F.R. (2007). Role of an acidic cluster/dileucine motif in cation-independent mannose 6-phosphate receptor traffic. Traffic. *8*, 402-413.

Treier,M., Staszewski,L.M., Bohmann,D. (1994). Ubiquitin-dependent c-Jun degradation in vivo is mediated by the delta domain. Cell *78*, 787-798.

Urbe,S. (2005). Ubiquitin and endocytic protein sorting. Essays Biochem. *41*, 81-98.

Valero,R., Bayes,M., Francisca Sanchez-Font,M., Gonzalez-Angulo,O., Gonzalez-Duarte,R., Marfany,G. (2001). Characterization of alternatively spliced products and tissue-specific isoforms of USP28 and USP25. Genome Biol. *2*, RESEARCH0043.

Valero,R., Marfany,G., Gonzalez-Angulo,O., Gonzalez-Gonzalez,G., Puelles,L., Gonzalez-Duarte,R. (1999). USP25, a novel gene encoding a deubiquitinating enzyme, is located in the gene-poor region 21q11.2. Genomics *62*, 395-405.

van den Hazel,H.B., Kielland-Brandt,M.C., Winther,J.R. (1992). Autoactivation of proteinase A initiates activation of yeast vacuolar zymogens. Eur.J.Biochem. *207*, 277-283.

van Kerkhof,P., Putters,J., Strous,G.J. (2007). The ubiquitin ligase SCF(betaTrCP) regulates the degradation of the growth hormone receptor. J.Biol.Chem. *282*, 20475-20483.

Vellai,T., Vida,G. (1999). The origin of eukaryotes: the difference between prokaryotic and eukaryotic cells. Proc.Biol.Sci. *266*, 1571-1577.

Venables,M.C., Jeukendrup,A.E. (2009). Physical inactivity and obesity: links with insulin resistance and type 2 diabetes mellitus. Diabetes Metab Res.Rev. *25 Suppl 1*, S18-S23.

Verhey,K.J., Birnbaum,M.J. (1994). A Leu-Leu sequence is essential for COOH-terminal targeting signal of GLUT4 glucose transporter in fibroblasts. J.Biol.Chem. *269*, 2353-2356.

Verhey,K.J., Yeh,J.I., Birnbaum,M.J. (1995). Distinct signals in the GLUT4 glucose transporter for internalization and for targeting to an insulin-responsive compartment. J.Cell Biol. *130*, 1071-1079.

Wakasugi,M., Waguri,S., Kametaka,S., Tomiyama,Y., Kanamori,S., Shiba,Y., Nakayama,K., Uchiyama,Y. (2003). Predominant expression of the short form of GGA3 in human cell lines and tissues. Biochem.Biophys.Res.Commun. *306*, 687-692.

Watson,R.T., Khan,A.H., Furukawa,M., Hou,J.C., Li,L., Kanzaki,M., Okada,S., Kandror,K.V., Pessin,J.E. (2004). Entry of newly synthesized GLUT4 into the insulin-responsive storage compartment is GGA dependent. EMBO J. *23*, 2059-2070.

Weber,T., Zemelman,B.V., McNew,J.A., Westermann,B., Gmachl,M., Parlati,F., Sollner,T.H., Rothman,J.E. (1998). SNAREpins: minimal machinery for membrane fusion. Cell *92*, 759-772.

Wilkinson,K.D., Urban,M.K., Haas,A.L. (1980). Ubiquitin is the ATP-dependent proteolysis factor I of rabbit reticulocytes. J.Biol.Chem. *255*, 7529-7532.

Williams,R.L., Urbe,S. (2007). The emerging shape of the ESCRT machinery. Nat.Rev.Mol.Cell Biol. *8*, 355-368.

Winge,D.R., Nielson,K.B., Gray,W.R., Hamer,D.H. (1985). Yeast metallothionein. Sequence and metal-binding properties. J.Biol.Chem. *260*, 14464-14470.

Wolf,D.H., Fink,G.R. (1975). Proteinase C (carboxypeptidase Y) mutant of yeast. J.Bacteriol. *123*, 1150-1156.

Wollert,T., Hurley,J.H. (2010). Molecular mechanism of multivesicular body biogenesis by ESCRT complexes. Nature *464*, 864-869.

Wollert,T., Yang,D., Ren,X., Lee,H.H., Im,Y.J., Hurley,J.H. (2009). The ESCRT machinery at a glance. J.Cell Sci. *122*, 2163-2166.

Wood,I.S., Trayhurn,P. (2003). Glucose transporters (GLUT and SGLT): expanded families of sugar transport proteins. Br.J.Nutr. *89*, 3-9.

Woodman,P.G., Futter,C.E. (2008). Multivesicular bodies: co-ordinated progression to maturity. Curr.Opin.Cell Biol. *20*, 408-414.

Wooten,M.W., Geetha,T. (2006). The role of ubiquitin in neurotrophin receptor signalling and sorting. Biochem.Soc.Trans. *34*, 757-760.

Wu-Baer,F., Lagrazon,K., Yuan,W., Baer,R. (2003). The BRCA1/BARD1 heterodimer assembles polyubiquitin chains through an unconventional linkage involving lysine residue K6 of ubiquitin. J.Biol.Chem. *278*, 34743-34746.

Xu,Z., Kandror,K.V. (2002). Translocation of small preformed vesicles is responsible for the insulin activation of glucose transport in adipose cells. Evidence from the in vitro reconstitution assay. J.Biol.Chem. *277*, 47972-47975.

Yang,J., Clark,A.E., Kozka,I.J., Cushman,S.W., Holman,G.D. (1992). Development of an intracellular pool of glucose transporters in 3T3-L1 cells. J.Biol.Chem. *267*, 10393-10399.

Yeh,T.Y., Beiswenger,K.K., Li,P., Bolin,K.E., Lee,R.M., Tsao,T.S., Murphy,A.N., Hevener,A.L., Chi,N.W. (2009). Hypermetabolism, hyperphagia, and reduced adiposity in tankyrase-deficient mice. Diabetes.

Yeh,T.Y., Sbodio,J.I., Tsun,Z.Y., Luo,B., Chi,N.W. (2007). Insulin-stimulated exocytosis of GLUT4 is enhanced by IRAP and its partner tankyrase. Biochem.J. *402*, 279-290.

Yu,C., Cresswell,J., Loffler,M.G., Bogan,J.S. (2007). The glucose transporter 4-regulating protein TUG is essential for highly insulin-responsive glucose uptake in 3T3-L1 adipocytes. J.Biol.Chem. *282*, 7710-7722.

Zhande,R., Mitchell,J.J., Wu,J., Sun,X.J. (2002). Molecular mechanism of insulin-induced degradation of insulin receptor substrate 1. Mol.Cell Biol. *22*, 1016-1026.

Zhu,P., Zhou,W., Wang,J., Puc,J., Ohgi,K.A., Erdjument-Bromage,H., Tempst,P., Glass,C.K., Rosenfeld,M.G. (2007). A histone H2A deubiquitinase complex coordinating histone acetylation and H1 dissociation in transcriptional regulation. Mol.Cell *27*, 609-621.

Zimmet,P., Alberti,K.G., Shaw,J. (2001). Global and societal implications of the diabetes epidemic. Nature *414*, 782-787.

Zuccato,E., Blott,E.J., Holt,O., Sigismund,S., Shaw,M., Bossi,G., Griffiths,G.M. (2007). Sorting of Fas ligand to secretory lysosomes is regulated by mono-ubiquitylation and phosphorylation. J.Cell Sci. *120*, 191-199.